2010

Secretion and activity of a novel cysteine-rich protein from Helicobacter pylori, HcpE

Sari Kichler
Western University

Secretion and activity of a novel cysteine-rich protein from *Helicobacter pylori*, HcpE

(Spine title: Secretion and activity of a novel *H. pylori* protein, HcpE)

(Thesis format: Monograph)

By:

Sari Kichler

Graduate program

in

Microbiology and Immunology

A thesis submitted in partial fulfillment

of the requirements for the degree of

Master of Science

School of Graduate and Postdoctoral Studies

The University of Western Ontario

London, Ontario, Canada

THE UNIVERSITY OF WESTERN ONTARIO
SCHOOL OF GRADUATE AND POSTDOCTORAL STUDIES

CERTIFICATE OF EXAMINATION

Supervisor	Examiners
Dr. Carole Creuzenet	Dr. David Heinrich
Supervisory Committee	Dr. Vincent Morris
Dr. John McCormick	Dr. Robert Cumming
Dr. Susan Koval	

The thesis by

Sari Beth Kichler

entitled:

Secretion and activity of a novel cysteine-rich protein from *Helicobacter pylori*, HcpE

is accepted in partial fulfillment of the
requirements for the degree of
Master of Science

Date _____

_____
Dr. Sung Kim
Chair of the Thesis Examination Board

ABSTRACT

HcpE (HP0235) is a cysteine-rich protein that is specific to and highly conserved in Helicobacters. HcpE elicits strong antibody production in patients infected with *H. pylori*. We demonstrated that HcpE is secreted by *H. pylori*. Structural modeling demonstrated that HcpE is a solenoid protein that requires the formation of many disulphide bonds prior to secretion. Moreover, the presence of Sel1-like repeat (SLR) motifs implies that protein-protein interactions are necessary for function of HcpE. Two experimental approaches were implemented to identify interacting partners for HcpE. Using mature folded HcpE, an interaction with HP0184, a protein of unknown function was identified. Using unfolded HcpE, a specific folding factor, DsbG was identified. The interaction with DsbG was confirmed biochemically. DsbG not only interacts with unfolded HcpE, but this interaction could solubilize unfolded HcpE probably via disulfide bond formation between the many cysteines of HcpE. A tissue culture model using gastric cells and an *hcpE* knockout mutant was used to investigate the role of HcpE during infection. Difficulties with viability and differential expression of surface carbohydrates by the *hcpE* mutant, which altered its surface properties, complicated the analysis. Identifying interactions with host cells and with other *H. pylori* proteins will contribute to our understanding of the biological role of HcpE in *H. pylori* pathogenesis.

KEY WORDS: *Helicobacter pylori*, secretion, folding, protein-protein interactions, Dsb proteins, disulfide bonds

DEDICATION

To my family, and especially my *mom*;

Because without your love, support, and encouragement this would not have been possible. *Thank-you!*

ACKNOWLEDGEMENTS

First and foremost I would like to thank my supervisor, Dr. Carole Creuzenet for all her guidance, support and encouragement throughout the past two years. I came here with minimal lab experience and she took the time to not only teach me technical laboratory skills, but helped cultivate my critical thinking and taught me how to approach science, and research in a new way. Her passion and enthusiasm motivated me every step of the way, and I could not have achieved this without her.

I would like to thank my advisory committee members, Dr. John McCormick and Dr. Susan Koval, for all their positive feedback and suggestions throughout the course of my graduate work.

I would also like to thank all the members of the Creuzenet lab, both past and present. Your patience and assistance over the past two years was greatly appreciated. You helped make the lab a more enjoyable place to work. For their help generating the constructs used in this study, special mention goes to Dr. Dinath Ratnayake (*hcpE::kan* mutant), Dr. Alexandea Merkx-Jacques (pET23-TsaA), Jaspreet Chahal (pET30-HcpE) and Lesley J-Y Meng (pET30-DsbG). All the hard work that went into producing them was greatly appreciated.

I would also like to acknowledge and thank everyone in the Microbiology and Immunology departmental office for all their help throughout my master's work. The open-door policy and welcoming atmosphere made this entire process much easier at times.

Thank-you!!!

Table of Contents

List of Figures

List of Tables

List of Abbreviations

AA	Amino acids
AD	Activation domain
AGS	Gastric adenocarcinoma
BD	Binding domain
BHI	Brain heart infusion
bp	Base-pairs
BSA	Bovine serum albumin
CagA	Cytotoxin associated gene A
CFU	Colony forming unit
CV	Column volume
Dsb	Disulfide bond
ELISA	Enzyme-linked immunosorbent assay
FBS	Fetal bovine serum
FPLC	Fast performance liquid chromatography
Hcp	Helicobacter cysteine rich protein
HS	Horse serum
IL-8	Interleukin-8
IM	Inner membrane
IPTG	Isopropyl β-D-1-thiogalactopyranoside
kDa	Kilodalton
LB	Luria Bertani
LPS	Lipopolysaccharide
MOI	Multiplicity of infection
MS	Mass spectrometry
OD	Optical density
OM	Outer membrane
O/N	Over-night
ORF	Open reading fram
PAI	Pathogenicity Island
PBP	Penicillin Binding Proteins
PCR	Polymerase chain reaction
PG	Peptidoglycan
PIC	Protease inhibitor cocktail
PPI	Peptidyl-propyl isomerases
PPR	Pentatricopeptide repeat
PR	Ponceau red
PVDF	Polyvinylidene fluoride
qRT-PCR	Quantitative real time polymerase chain reaction
SDS-PAGE	Sodium dodecyl sulfate polyacrylamide gel electrophoresis
SLR	Sel1-like repeat
TAP-tag	Tandem affinity purification tag
Tat	Twin arginine transport
TBS	Tris buffered saline
TCA	Trichloroacetic acid
TEV	Tobacco etch virus
Th1	T-helper 1
TLR	Toll-like receptor
TPR	Tetratricopeptide repeats
TsaA	Cytoplasmic alkyl hydroperoxide reductase (control protein; HP1563)
WB	Western blot
VacA	Vacuolating cytotxin

CHAPTER 1: INTRODUCTION

1.1 A human gastric pathogen: *Helicobacter pylori*

Helicobacter pylori is a Gram-negative, spiral shaped microaerophilic bacterium, that chronically infects the human gastric mucosa. It is the main etiological agent of peptic ulceration, gastric adenocarcinoma and gastric lymphoma (67). Infected individuals often have histological evidence of gastritis, but the vast majority of infections remain asymptomatic (89). The bacterium was first discovered in 1982 by Barry Marshall and Robin Warren (79). Together they revolutionized scientific thinking implicating a bacterium as the cause of peptic ulcers, challenging the existing dogma. Their radical theory was met with much skepticism and criticism. It was not until Marshall performed a self-ingestion experiment, fulfilling Koch's postulates, that they were able to undeniably establish that it was a bacterium that lead to the inflammation and stomach pains associated with peptic ulcers. With this experiment, they successfully de-bunked a long standing myth, that ulcers were the result of eating spicy food and irrefutably implicated *H. pylori* as the primary cause. Since its discovery, *H. pylori* has become the focus of extensive scientific research. More recently, the World Health Organization recognized *H. pylori* as a Group-1 carcinogen causing gastric cancer, the second most common cancer in the world (1). In 2005 after years of dedicated research, Marshall and Warren were finally acknowledged for their discovery and were awarded the Nobel Prize in physiology and medicine.

H. pylori was first identified as a member of the campylobacter species, called *Campylobacter pylori*; however, continued analysis of its flagellar morphology, fatty acid

profile and 16S RNA sequence lead to re-classification as the first member of a new genus called Helicobacter (67). In 1989 the bacteria was officially renamed *Helicobacter pylori*.

H. pylori is believed to infect ~ 50% of the world's population. Infection rates are more pronounced and wide spread in developing countries, reaching nearly 70% of the population and 20-30% of the population in industrialized countries (20). *H. pylori* infections show no preference for age, or immune status of its target, causing infections in young and old, as well as healthy and immune compromised individuals equally. Most infections are contracted in childhood and persist into adulthood where symptoms begin to manifest. In the tropics, infections often occur before the age of ten, especially in high-density populations with low socio-economical status. Transmission is from person-to-person, presumably via the oral-oral, or oral-faecal route (48). Transmission is most common with poor sanitary conditions, overcrowded living arrangements and unclean water. The different outcomes of *H. pylori* infections are predominantly influenced by the host's reaction to the bacterium as well as by environmental factors (137) and the accessibility to treatment.

Infection with *H. pylori* results in a typical sequence of events, ultimately resulting in the development of gastric diseases. Colonization of the gastric mucosa by the bacterium initially results in the induction of an inflammatory response that is predominantly of the T-helper 1 (Th1) Type (14). This inflammation typically goes unnoticed as there are no clinical symptoms associated with it (67). The inflammatory response in the host is characterized by an influx of neutrophils, mononuclear cells and Th1 cells (82). This response is typically aimed at clearing intracellular infections, and

since *H. pylori* is not an intracellular pathogen it results in epithelial damage as opposed to removal of the bacterium. Thus, persistent *H. pylori* infections trigger a permanent pro-inflammatory response resulting in cellular damage and the histological cascade associated with gastric diseases (27).

In the absence of treatment, *H. pylori* infections are potentially life-long. Current treatment options are often complex to administer and poorly tolerated by patients. They include the use of several antibiotics, proton pump inhibitors and stomach lining protectors to safeguard the stomach from acid (137). Moreover, these treatments are threatened by the emergence of antibiotic resistant *H. pylori* strains (46). The emergence of antibiotic resistance warrants the search for new therapeutic strategies and novel targets to eliminate the pathogen.

1.2 *H. pylori* virulence mechanisms

Successful life-long colonization of the human stomach by *H. pylori* is achieved through a combination of bacterial virulence factors that specifically address the various challenges presented by this harsh environment. These include structural features like the bacterial flagella and lipopolysaccharide (LPS), the synthesis of urease to buffer the pH of the stomach, and the production and secretion of toxins, adhesins and proteins to alter epithelial integrity and induce an inflammatory response. Together these factors enable the bacteria to establish chronic infections making it one of the most successful human bacterial pathogens (89).

1.2.1 Flagella

H. pylori uses multiple flagella to propel itself through the mucus lining of the stomach to reach the epithelium where it establishes infection. Flagellar mediated motility is absolutely essential for the bacteria to cross the mucous barrier and establish infections, as non-motile mutants are unable to colonize the stomach (62). *H. pylori* has 2 to 6 unipolar sheathed flagella (49) made up of two flagellins, flagellin A (FlaA) and flagellin B (FlaB). Disruption of *flaA* results in a non-motile phenotype, whereas disruption of *flaB* does not abrogate motility (131). The membranous sheath surrounding the flagella is thought to play a role in protecting the filaments from the acidity of the gastric lumen, thereby conferring protection from degradation in this harsh environment.

The bacterial flagellum consists of a basal body containing the flagellar motor, the hook structure, the central filament, and a membranous sheath that envelops each filament (45, 49). Flagella assembly is a complex process involving more than 40 different proteins (76). The filament, made of the individual flagellin subunits, is assembled using a type III-like secretion system, in which the partially folded flagellins A and B pass through the base structures, the central pore in the basal body, the hook and the growing filament, until they reach their end position where they polymerize.

It was recently established that the flagellin proteins of *H. pylori* are glycosylated by pseudaminic acid (115). The exact role of protein glycosylation in flagellar function has yet to be determined; however, glycosylation has been shown to be necessary for the complete assembly of the *H. pylori* flagella (62), thereby establishing a relationship between protein glycosylation, motility and bacterial virulence.

1.2.2 LPS

Lipopolysaccharide (LPS) is a major component of the Gram-negative bacterial outer membrane composed of phosphorylated glyco-lipids (106). Bacterial LPS is indispensable, playing a pivotal role in maintaining the integrity of the outer membrane, immuno-modulation, and immuno-stimulation. As a surface molecule, LPS directly contributes to interactions between the bacterial cell surface and the host cell environment. The LPS of different bacterial species share a common architecture consisting of three conserved structural elements (106). Lipid-A tethers the LPS molecule to the bacterial outer membrane and is typically the source of much of the toxicity associated with Gram-negative bacteria (91). Bound directly to the lipid-A moiety is the core-oligosaccharide, which comprises 10-15 sugars. The outermost portion of the LPS molecule is the O-specific antigen, or O-polysaccharide. This repetitive glycan polymer shows high strain to strain variability. The O-antigen is a target for recognition by host antibodies, since it is exposed at the outer-most surface of the bacterial cell.

The LPS structure of *H. pylori* has been well characterized (91). A number of structural differences, compared to other bacterial LPS molecules, have been identified that are thought to contribute to *H. pylori* pathogenicity and survival in the gastric lumen. Clinical isolates of *H. pylori* produce smooth-form LPS with O-polysaccharide chains of relatively constant length (90, 92, 95). The lipid-A portion of the *H. pylori* LPS molecule has low endotoxic and immunological activities compared to other enterobacterial LPS molecules (91). Detailed structural studies have been carried out to explain this phenomenon. *H. pylori* lipid-A is underphosphorylated, underacylated and contains substitutions by long chain fatty acids (127). Together these modifications are believed to

contribute to the low immunological reactivity of the *H. pylori* lipid-A molecule. Recognition of microorganisms by the innate immune system involves Toll-like receptors (TLRs) that discriminate pathogen-associated molecular patterns (PAMPs) (14). In the innate immune system, the lipid-A moiety of LPS is detected by the TLR4/MD2 receptor (105), resulting in a potent immune response. Due to inherent differences in its structure, the lipid-A of *H. pylori* is anergic compared to that of other enteric bacteria, capable of stimulating macrophage TLR4, but not gastric epithelial cell TLR4 (11).

The O-antigen chains of *H. pylori* mimic human blood group antigen Lewis x , y, a and b. Typical O-antigen chains have a poly(*N*-acetyl-β-lactosamine) chain decorated with multiple α-L-fucose residues which form the internal Le^x determinants with terminal Le^x or Le^y determinants (91). Expression of Le^x or Le^y determinants is very common, occurring in 80-90% of serologically screened *H. pylori* strains (80). Biologically, expression of human blood group antigens by *H. pylori* has been implicated in evasion of the immune response upon initial infection and in influencing bacterial colonization and adhesion (93). Molecular mimicry essentially provides *H. pylori* with an escape from the humoral response by decorating itself with structures that the host organism is tolerant to and will not be perceived as being foreign and, consequently, will not be targeted.

Aside from its role in molecular mimicry and evasion of the immune response, the *H. pylori* O-antigen has been shown to contribute to colonization, adhesion and global pathogenicity. Both O-antigen and Le^x expression were shown to be essential for *in vivo* colonization in a mouse model (94). Additionally, O-antigen chains have been shown to mediate adhesion (40), and strains with high expression of Le^x display an increase in colonization density compared to those with weaker expression (54).

1.2.3 Urease

The stomach is an inhospitable environment that prevents the growth of most bacterial organisms. This is generally attributed to its high acidity. *H. pylori* is unique as it has adapted to this harsh environment, making it suitable for its growth and replication. A gene cluster containing seven genes is responsible for the biosynthesis of the enzyme urease (59, 68). These genes encode UreA, UreB, and five other proteins required for the enzymatic activity. Urease hydrolyses urea, generating ammonia (NH_3) and carbon dioxide (CO_2). The ammonia helps buffer the cytosol, forming a neutral environment for the bacteria (89). The uptake of urea by *H. pylori* takes place through a proton-gated channel which is open only at low pH (142), as in the stomach. Urease activity is believed to be essential for colonization by *H. pylori*, as urease deficient mutants are unable to colonize the stomachs of gnotobiotic piglets (38). Urease has also been shown to activate monocytes, inducing the production of pro-inflammatory cytokines. The local production of cytokines in response to urease may play a role in the development of gastroduodenal inflammation associated with *H. pylori* infections (53).

Urease activity may be considered a double-edged sword for the bacteria, as hydrolysis of urea produces ammonia, which is in itself toxic to cells. Moreover, ammonia is thought to react with reactive intermediates generated by neutrophil myeloperoxidase to form carcinogenic agents responsible for *H. pylori*-associated stomach adenocarcinoma (132). Ammonia is only toxic at high concentrations, and the level of toxicity varies considerably with cell type and culture conditions; thus, it is not exactly known if the amount of ammonia produced by *H. pylori in vivo* is toxic. Urease is present in the bacterial cytosol and at the bacterial surface (32). It is nevertheless

considered an intracellular enzyme, released to the extracellular space only following bacterial autolysis (102).

1.2.4 Toxins

H. pylori makes two main toxins that are implicated in the development of gastroduodenal ulcers; Vacuolating cytotoxin (VacA) and Cytotoxin associated gene A (CagA) (6). Strains expressing CagA and VacA have been classified as *type I* strains, associated with a poor prognosis characterized by peptic ulceration (28). The *vacA* gene is present in virtually all stains of *H. pylori*, but has been shown to be polymorphic in nature (8). VacA is a high-molecular weight multimeric pore-forming protein that causes massive vacuolation in epithelial cells. VacA is associated with membrane channel formation, disruption of endosomal and lysosomal activity, having effects on integrin receptor-induced cell signaling, interference with cytoskeleton-dependent functions, induction of apoptosis, and immune modulation (67).

The cytotoxin-associated gene pathogenicity island (*cag*PAI) is comprised of 27-31 genes (22) encoding a type IV secretion system. Translocation of CagA into gastric epithelial cells causes inflammation by activation of NF-κB and the secretion of cytokines and chemokines such as interleukin 8 (IL-8) (136), the pro-inflammatory cytokine characteristic of *H. pylori* infections. Eighteen of the *cag*PAI-encoded proteins serve as building blocks for a type IV secretion apparatus, which forms a syringe-like structure that penetrates gastric epithelial cells and facilitates the direct transport of CagA, peptidoglycan and possibly other factors into host cells. Once inside eukaryotic cells, CagA is phosphorylated at tyrosine residues by Src family kinases. Phosphorylated CagA interacts with a range of host signaling molecules, resulting primarily in

morphological changes to the epithelial cells called the hummingbird phenotype. This is characterized by a dramatic elongation and spreading of host cells, including the production of filapodia and lamellipodia (118).

1.2.5 Adhesins

H. pylori colonizes the human gastric mucosa by strongly adhering to epithelial cells and the mucous layer lining the gastric epithelium. The properties of adherence protect the bacterium from the extreme acidity of the gastric lumen, as the local pH at the surface of the epithelium is known to be close to neutral, as well as from displacement from the stomach by forces such as those generated by peristalsis (60). Adherence is mediated by a number of bacterial adhesins, binding proteins and glycolipids. Blood group antigen-binding adhesion BabA, is one of the best characterized adhesin proteins of *H. pylori*. BabA mediates binding to fucosylated Lewis b (Le^b) blood group antigens on human cells (97). The BabA adhesin was found to be localized to the bacterial outer membrane by electron microscopy (60). Animal studies have shown that BabA-mediated adhesion is necessary for colonization and pathogenesis of *H. pylori* (103). It has also been suggested that recognition of the Le^b antigen by BabA plays a central role in site-specific colonization, and BabA mediated adherence to the gastric epithelium contributes to the efficient delivery of bacterial virulence factors that damage host tissue resulting in inflammation.

The sialic acid-binding adhesin (SabA) binds to sialylated Lewis a (Le^a) antigens expressed during chronic inflammation. *H. pylori* induced gastric inflammation and gastric carcinoma are associated with the replacement of non-sialylated Lewis antigens by sialylated Le^x and sialylated Le^a, implicating a role for SabA in the chronic

inflammatory stages of disease (77). Human granulocytes carry sialylated carbohydrates on their surface and high levels of sialylated glycoconjugates are associated with severe gastric disease including dysplasia and cancer (3). In fact, the binding of SabA to sialyl-Lewis glycoconjugates exemplifies the adaptive nature of *H. pylori* infections. It has been proposed that *H. pylori* infections trigger host tissue to up regulate the inflammation-associated sialyl-Lewis x antigens. In response, surface located SabA, binds sialylated Le^x and Le^a antigens facilitating membrane attachment and contributing to the inflammatory response (77).

Other well established adhesins include the *H. pylori* protein HpaA that binds to glycoconjugates (41), and two closely related outer membrane proteins AlpA and AlpB, that were shown to be necessary for adherence to gastric epithelial cells (32). Efficient adhesion of *H. pylori* to gastric epithelial cells is crucial for the bacterium to inject toxins and other virulence effector proteins into host cells, which trigger tissue damage, cytokine release, and subsequently lead to the development of gastric inflammation and persistent infections.

1.2.6 Secreted proteins

Secreted proteins collectively play an important role in bacterial pathogenesis. They possess diverse biological functions like contributing to host cell toxicity to more subtle alterations of the host cell for the benefit of the pathogen. The importance of secreted proteins in bacterial pathogenesis is exemplified by the array of mechanisms that have evolved to facilitate secretion. Identification and characterization of secreted proteins is valuable as these proteins come in direct contact with host compartments, and thus play a fundamental role in host-pathogen interactions.

In *H. pylori*, the comprehensive analysis of secreted proteins has for the most part been prevented due to inherent technical difficulties associated with studying the bacterial secretome. *H. pylori* is commonly cultivated in rich media supplemented with serum. The abundance of serum proteins makes it difficult to analyze secreted bacterial proteins (16). Growth in protein-free media has been implemented (138), but growth is generally much slower under these conditions. *H. pylori* is also prone to spontaneous autolysis (102), resulting in the non-specific release of numerous proteins, making the analysis of the secretome from culture supernatants difficult. Nonetheless, serum-free culture conditions minimizing autolysis have been optimized to facilitate the study of *H. pylori* secreted proteins, but they too have their limitations. In a comprehensive analysis of the *H. pylori* secretome 26 secreted proteins were identified using optimized growth conditions (16). Of these, 16 were identified to have putative signal peptides for Sec-dependent secretion across the plasma membrane into the periplasm. Four of the secreted proteins identified (TrxA, TrxC, DsbC and FldA) are homologous to oxidoreductases involved in the modification of disulfide bonds in the periplasm. These proteins are only functional within the periplasmic space and serve no purpose in the extracellular environment. They appear to have not been secreted, but rather released as result of cell lysis, thereby demonstrating the difficulty in studying the bacterial secretome. Nevertheless, these findings draw attention to the diversity of secreted proteins and their influence on host-pathogen interactions.

1.3 Protein secretion systems of *H. pylori* relevant to this research

1.3.1 Generalities about protein secretion in bacteria

Protein secretion systems in bacteria have been shown to be important to organelle biogenesis, secretion of virulence factors and release of effector proteins. Gram-negative bacteria are faced with an even more difficult challenge for transport, as proteins must transit across two membranes to reach the exterior environment. Secretion can therefore occur in a single step providing direct exit from the cell, or in a two-step process first crossing the inner membrane into the periplasm and then crossing the outer membrane to reach the exterior of the cell. Six secretory pathways have been well characterized in Gram-negative bacteria illustrating the different mechanisms by which proteins are secreted from bacterial cells (Figure 1). These secretion systems can be relatively simple structures that translocate one substrate protein, or complex machines that export a number of proteins or protein complexes either outside the bacteria, or directly into target host cells. The main structural and functional features of the secretion systems that have functional relevance to *H. pylori* pathogenesis and to this work are outlined below.

1.3.2 Sec-secretion for transport across the inner membrane

The Sec secretion system exports proteins from the bacterial cytoplasm to the periplasm for post-translational folding. In the classic *Escherichia coli* Sec system, nine proteins are involved in the secretion process (78). The Sec pathway is divided into three distinct but sequential stages: (i) targeting, (ii) translocation, and (iii) release. In the first stage proteins with the Sec signal peptide are targeted to the membrane. Recognition and targeting of substrate proteins to the secretion apparatus is facilitated by the SecB

Figure 1: Summary of the main features of bacterial protein secretion systems. In Gram-negative bacteria, secreted proteins have a double membrane barrier to cross to reach the exterior of the cell. Protein transport across the inner membrane to the periplasm occurs via the Sec- or Tat- pathways. From the periplasm, most proteins are transported across the outer membrane using the general type II secretion system, or type V autotransporter system. Many proteins are secreted directly from the cytoplasm to the extracellular milieu, or directly into host cells via specialized secretion systems such as the type III, type IV, type VI and type I secretion systems. Gram-positive bacteria share some of the same secretion systems, but do not have to deal with the double membrane barrier to secretion. They also display one unique system, the type VII system. Of relevance to this study is the Sec secretion system and general secretory (type II) pathway. HM: host membrane; OM: outer membrane, IM: inner membrane. ATPases and chaperones are shown in yellow. *Adapted from Tseng et al., 2009* (138).

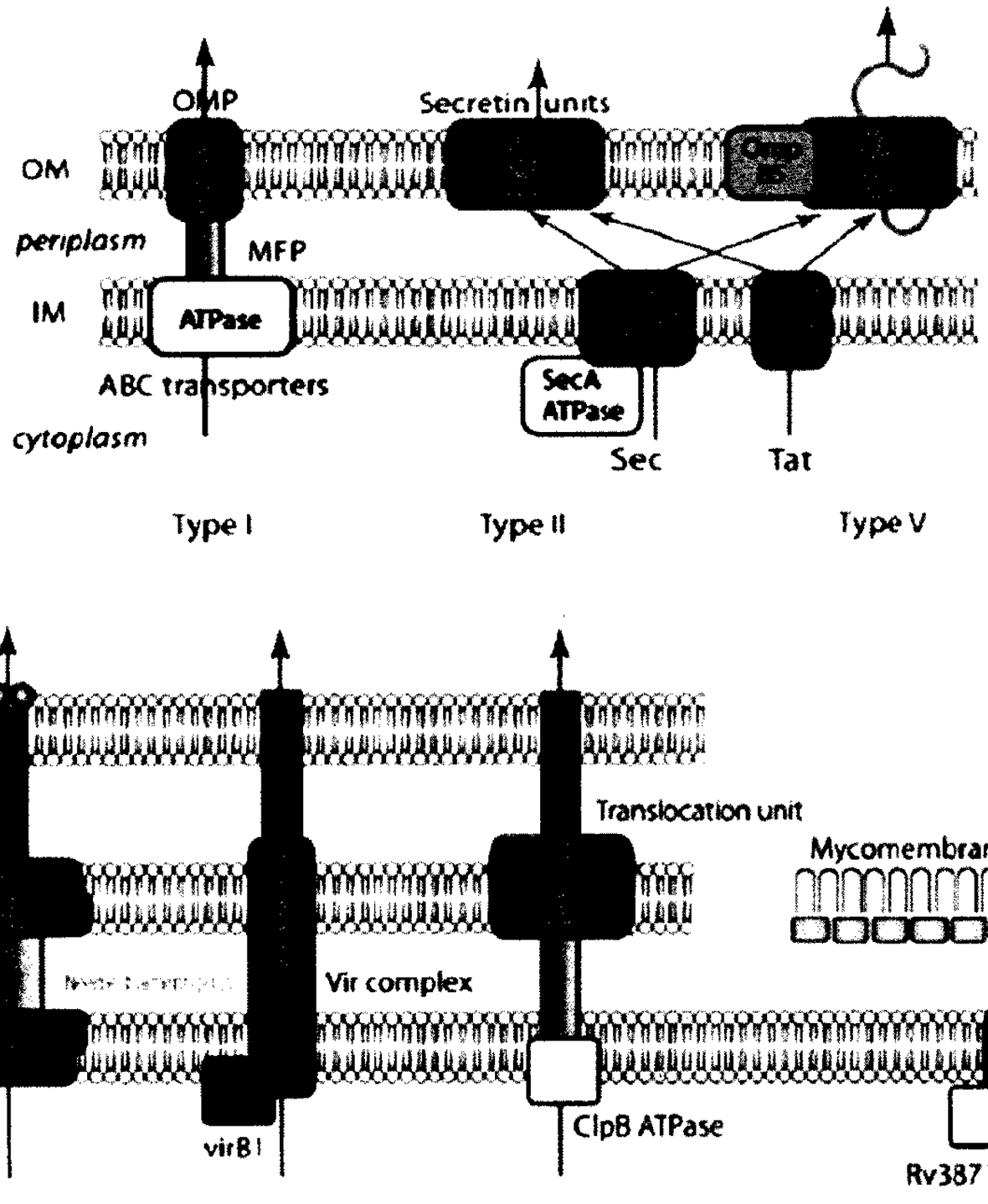
OMP
Secretin units
OM
periplasm
MFP
IM
ATPase
ABC transporters
cytoplasm
SecA ATPase
Sec
Tat
Type I
Type II
Type V
HM
Translocation unit
Mycomembrane
MM
Vir complex
Rv3877
IM
ATPase
virB1
ClpB ATPase
Rv3871
Rv3868
Type III
Type IV
Type VI
Type VII

chaperone. Substrate proteins secreted by the Sec system are very diverse and found all across bacterial species. They share no sequence similarity, yet are all targeted by the same secretion apparatus. This phenomenon is explained by the presence of a signal sequence or leader peptide. All proteins secreted via this system have a N-terminal signal peptide 20-30 amino acids in length (39). The signal peptides contain three conserved domains: (i) a basic N-terminus with a net positive charge, (ii) a hydrophobic core, and (iii) a hydrophilic C-terminus with a consensus signal and cleavage site. Once target proteins are recognized and localized to the inner membrane secretion apparatus, the second stage is initiated. This stage requires a protein translocase that is embedded in the membrane to serve as the transport channel. The translocase has a membrane spanning domain containing heterotrimers of the membrane proteins SecY, SecE and SecG. In addition to the SecYEG structural component, an energy source is absolutely required to fuel the secretion process (78). The SecA-ATPase provides the energy that drives the secretion of proteins across the inner membrane. In the third stage the translocated protein is released into the periplasm where it is processed for its final folding by periplasmic folding catalysts. Before being released into the periplasm, the signal sequence is cleaved by signal-peptidases. From here, the protein may reside in the periplasm, or may be targeted to the outer membrane for final secretion, or may integrate into the membrane (39).

To date, putative homologues of Sec components except SecB, YajC and YidC have been identified in the *H. pylori* genome (42). Moreover, a number of known secreted proteins, and putative secreted proteins contain the classical Sec N-terminal signal sequences, including the well characterized VacA toxin, implying that this system

is functional in *H. pylori* and involved in the secretion of virulence associated proteins (8).

1.3.3 Protein folding in the periplasm

Proteins translocated via the Sec system carry an amino-terminal signal sequence that is cleaved by signal peptidases when the protein is released into the periplasmic space. Protein stability in the periplasm is an extremely important aspect of secretion via the general secretory pathway. A number of periplasmic enzymes have been identified that catalyze folding and turnover of these proteins. Formation of disulfide bonds can be vital for the stability of proteins in the periplasm. In *E. coli,* formation of disulfide bonds in the periplasm is catalyzed by the Dsb protein system, which will be discussed in detail in section 1.5. Periplasmic proteins containing proline residues may require isomerization of peptidyl-proline bonds to fold correctly (39). This is facilitated by the peptidyl-proline isomerases or PPIs (126). The periplasm also contains factors that assist proteins in folding correctly. This is typically mediated by molecular chaperones and is essential for the secretion of extracellular proteins which must acquire a properly folded state before transit across the outer membrane. Chaperones recognize hydrophobic domains that are surface exposed in the unfolded or mis-folded protein and bind preventing aggregation or proteolysis. Chaperones can also target secreted proteins from the inner membrane to their secretion apparatus in the outer membrane, functioning as shuttles that facilitate movement across the periplasm, as in the case of pilin. The periplasm also contains several proteases that play an important role in the physiology of the bacterial cell by activating turnover of damaged or mis-folded proteins. The final step of the general secretory pathway is translocation of the folded protein across the outer membrane.

1.3.4 General secretory pathway for transport from the periplasm to the exterior of cells

The general secretory pathway or type II secretion system (T2SS) of Gram-negative bacteria is a universal secretion system that translocates proteins from the periplasm across the bacterial outer membrane to the external environment. The T2SS is believed to be a specialized system that promotes interactions between a species and its environment (19), and it is required for virulence in a number of human pathogens. The components of the T2SS and their functions have been well characterized (24). The translocation pore in the outer membrane is composed of 12-15 secretin subunits and is large enough to accommodate fully folded proteins. The remaining 11-14 conserved components are likely involved in anchoring of the pore and regulating its opening and closing (24). The process by which proteins are transported across the periplasm to the outer membrane pore remains somewhat elusive and is likely species-specific as well as specific to the protein being secreted. The mechanisms governing type II secretion in *H. pylori* are not well understood, but it is reasonable to assume that the bacterium uses the general type II secretion pathway as no *H. pylori* specific systems have been identified to facilitate transport across the outer membrane.

1.3.5 Direct transport from the cytoplasm to the exterior of the cell

(a) Type III secretion system: The type III secretion system (T3SS) is a single step contact-dependent secretion system used by many pathogens. The T3SS transports proteins into the eukaryotic host cell cytoplasm in a Sec-independent manner (112). The secretion machinery is a large structure composed of more than 20 different proteins reaching over the bacterial inner and outer membranes and possibly into the eukaryotic

host cell membrane. Components of the type III secretion machinery implicated in transfer across the inner membrane show homology to components of the flagella export apparatus. As a result, the system has been genetically, structurally and functionally related to the bacterial flagella assembly system (113). The mechanism by which substrate proteins are recognized and targeted by this system is not completely understood. The process likely involves cytoplasmic chaperones that bind the proteins to be secreted and specifically targets them to the type III secretion machinery for translocation. To date, no T3SS or homologues of its protein components have been identified in the genome of *H. pylori* (108, 133). Despite its absence in *H. pylori*, the methods used to study type III chaperones and their substrate proteins were implemented to study our protein of interest.

(b) Type IV secretion: The type IV secretion system (T4SS) is homologous to the conjugation machinery of bacteria, capable of translocating both DNA and proteins that alter various eukaryotic cell processes. The T4SS is composed of approximately 12 proteins that form an inner membrane complex, a core complex that spans the periplasm, and a pilus, or pilus-like surface structure, that extends beyond the outer membrane (21). The pilus ultimately serves as the secretion tube through which translocated proteins travel. The T4SS facilitates direct secretion of complex proteins and nucleoproteins across both membranes into the extracellular milieu or directly into the eukaryotic host cell cytosol. A T4SS, the *cag* pathogenicity island, plays a major role in *H. pylori* pathogenesis. Virulent *H. pylori* strains secrete the CagA protein into gastric epithelial cells following attachment (10). For the purposes of this work, secretion via the type IV

secretion system is relevant to the *in vivo* functional studies done with human gastric cells.

1.4 Helicobacter cysteine-rich proteins (Hcps)

The availability of complete genome data for *H. pylori* (2, 133) has facilitated the study of a large number of proteins and has improved our knowledge and understanding of bacterial virulence and pathogenicity. Although *H. pylori* has a small genome, encoding approximately 1600 proteins, the function of many of these proteins remains unknown. Deciphering their function will contribute to our understanding of bacterial virulence mechanisms and could have major implications for the development of alternative treatments. The helicobacter cysteine rich protein (Hcp) family is a family of seven proteins (HcpA-G). It is one of the largest protein families specific for proteobacteria from the delta/epsilon subgroup (87). First identified by Cao and co-workers (18) and named for their high cysteine content, these proteins are well conserved among all sequenced *H. pylori* strains (2, 133). Moreover, patients infected with *H. pylori* have been shown to produce a massive antibody response to these proteins (87) demonstrating that they are not only expressed under native conditions, but that they are recognized by the host immune system. This suggests that Hcps are secreted by the bacterium and potentially play an important role in host-pathogen interactions. Understanding the function of Hcp family members will be important in assessing their role in the pathogenesis of *H. pylori* infections.

1.4.1 Hcp structural motifs: Sel1-Like Repeats (SLR)

Hcps are solenoid proteins. Solenoid proteins are distinguished from globular proteins by the presence of intra-molecular sequence similarities, or repeat units. Most repeats consist of 5-40 amino acids that fold into two to four secondary structural elements (98). Individual repeats in solenoid proteins are typically stacked on top of each other forming an extended superhelical macromolecule with a hydrophobic core.

Structural repeat units have been divided into three groups based on the number of amino acids within each repeat unit: (i) tetratricopeptide repeats (TPR) were identified in the yeast *cdc23* gene product and were designated tetratricopeptides because they have 34 amino acids (AA) in each repeat (121), (ii) pentatricopeptide repeats (PPR) were identified following analysis of the *Arabidopsis* genome (9, 123), and were designated *penta-* as each repeat contains of 35 AA, (iii) the third structural motif was identified following a cross genome analysis of organisms representing the three divisions of cellular life (archaea, bacteria and eukaryote), which revealed an α/α-repeat consisting of 36-44 AA, designated Sel1-like repeat (SLR) (104, 117); as it is present in the *C. elegans* *sel*-1 gene (50).

The three-dimensional architecture of the TPR motif was characterized following crystallography of the TPR domain of the protein phosphatase, PP5 (30). From this work it was established that each TPR motif consists of a pair of anti-parallel α-helices, helices A and B, of equivalent length evenly spaced by a series of AA designated the loop. Within a single TPR helix A and B are attached by loop 1, and helix B and A of neighbouring TPRs are attached by a second loop, designated loop 2. Structurally, PPRs differ from TPRs by a single amino acid insertion in loop 2, and SLRs differ from TPRs

by the presence of a 4-12 amino acid insertion in loop 1 and a deletion of 2 amino acids in loop 2 (88).

SLRs have been identified in approximately 858 protein sequences (104), yet TPR proteins have been shown to be much more abundant than SLR proteins. The SLR motif is postulated to establish a link between signal transduction pathways from eukaryotes and bacteria, suggesting that proteins containing these motifs are functionally important in host pathogen interactions. The prototypical structure for the SLR family was established by the crystal structure of HcpB. With this structure, the spatial differences between TPR and SLR motifs was established (75). Structural studies of HcpB recognized the Hcp family as a unique subset of SLR proteins with a repetitive pattern of paired cysteine residues in which two cysteine residues are spaced by 7 AA, with 36 AA between adjacent pairs. Additionally, the two α-helices of each motif are cross-linked and stabilized by the presence of disulfide bridges between cysteine residues. Hcp family members contain between 4 and 9 SLRs, and sequence conservation within the family is between 22 to 66% (75).

1.4.2 Helicobacter-cysteine rich protein E (HcpE)

Helicobacter-cysteine rich protein E (HcpE) is a 355 amino acid protein encoded by the open reading frame (ORF) HP0235 of the *H. pylori* strain 26695. The protein is annotated in the *H. pylori* genome as a hypothetical secreted protein, with no functional designation to date. Recent work by Mittl *et al.*, established that patients infected with *H. pylori* have high antibody titers to HcpE, indicating that it is well expressed *in vivo* and induces an immune response in the host (87). The sequence of HcpE contains a predicted signal peptide at its N-terminus, identified by SignalP 3.0 signal prediction software that

is larger than the archetypical Sec secretion peptide (Figure 2A). HcpE contains a total of 19 cysteine residues, one within its signal sequence, and the 18 others occurring in the mature protein. With 19 cysteine residues, HcpE has the highest cysteine content (5.4%) of all Hcp family members. The mature protein contains nine SLR motifs. Each SLR contains a pair of cysteine residues, with one cysteine belonging to each of the predicted α-helices of the SLR. The cysteines of each SLR are evenly spaced by 7 AA residues in all of the 9 SLRs of HcpE. Furthermore, the pair of cysteine residues in each SLR is predicted to participate in the formation of a disulfide bridge (Figure 2B), stabilizing the structure of each SLR by cross linking neighbouring α-helices. In the predicted model of HcpE, the 9 SLRs are believed to come together to form a superhelical structure characteristic of the Hcp family of proteins (Figure 2C).

1.4.3 Putative function of Hcp proteins

A screen for *H. pylori* penicillin-binding proteins (PBPs) identified HcpA as a novel PBP based on its ability to bind fluorescein-C_6-aminopenicillic acid (Flu-6-APA) (66). This finding was supported by later work that confirmed this result using purified HcpA (86). Similarly, HcpB was found to bind and hydrolyze 6-amino penicillic acid and 7-amino cephalosporanic acids derivatives, suggesting the presence of similar enzymatic β-lactamase activity. This was ultimately attributed to its distinct penicillin binding fold. However, the availability of crystal structures for HcpB (75) and HcpC (74) revealed no significant sequence or structural similarity between Hcp family members and known β-lactamases or PBPs, finding that these proteins lack the well known sequence motifs ubiquitously found in PBPs (81). The most probable biological function attributed to this penicillin-binding activity is biosynthesis of peptidoglycan and maintenance of cellular

Figure 2: Schematic representation and structural model of the HcpE protein. Panel A: The sequence of HcpE contains 19 cysteine residues. Their position along the entire sequence is marked by a C. The sequence includes a predicted 23 AA long signal peptide that is predicted to be cleaved upon secretion of HcpE. The mature portion of the protein is predicted to contain 9 SLR repeats (depicted as red and black cylinders). Each SLR repeat is made of 2 α-helices (labeled a and b for each SLR). A pair of cysteine residues is found in each SLR. **Panel B:** Structural modeling done using SwissProt illustrating that the two helices of each SLR are held together in a V-shape in the 3D structure of the protein. An example is shown here for the first SLR of HcpE. The cysteines from each helix (highlighted in red) are involved in stabilizing the position of the two helices of the SLR via formation of a disulfide bridge. **Panel C:** Predicted super-helical structure of HcpE with 9 SLRs super-imposed using PyMol software. *Modeling and figure courtesy of Dr. Creuzenet.*

A-

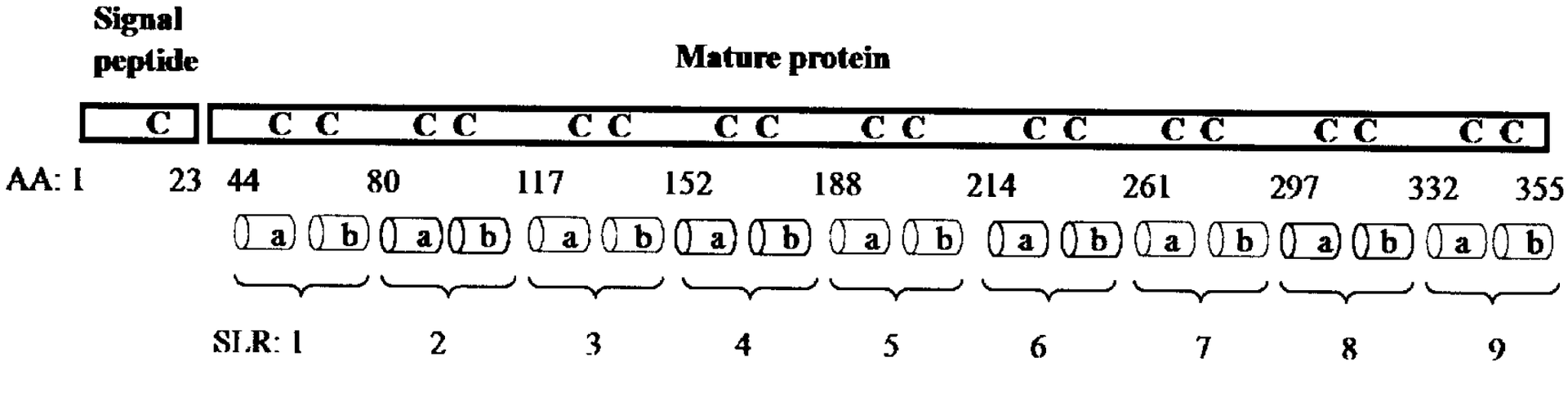
Signal peptide
Mature protein
C
C C C C C C C C C C C C C C C C C C C C
AA: 1 23 44 80 117 152 188 214 261 297 332 355
a b a b a b a b a b a b a b a b a b
SLR: 1 2 3 4 5 6 7 8 9

B-

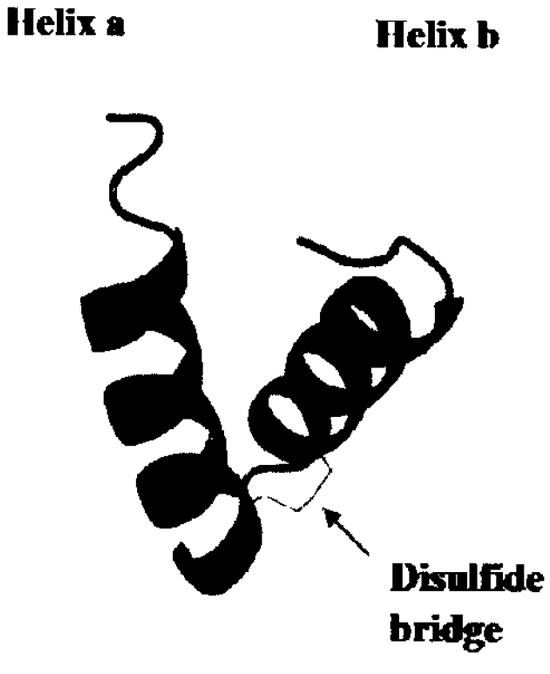
Helix a
Helix b
Disulfide bridge

C-

morphology. *H. pylori* posses a characteristic spiral-shaped morphology and as a result, it is thought that biosynthesis of its peptidoglycan occurs in a unique way; however, a functional association between enzymatic activity and cellular morphology has yet to be established.

More recently a role for HcpA in adherence to and differentiation of human monocytes was described (31). HcpA was identified as a novel pro-inflammatory and Th1-promoting protein stimulating the release of high concentrations of IL-6 and IFN-γ, in addition to significant levels of IL-12, TNF-α, and IL-10. The cytokine profile elicited by HcpA was comparable to that induced by LPS. From this, HcpA was thought to represent a novel bacterial virulence factor triggering the release of cytokines that instructs the adaptive immune system to initiate a pro-inflammatory Th1 response. This role as a modulator of the immune response was supported by more recent work that recognized the ability of HcpA to trigger the differentiation of human monocytes into macrophages (36). This functional ability would not help clear *H. pylori* infections; rather it is thought to promote the persistence of the bacterium in the gastric mucosa (36).

1.5 Disulfide bond proteins and pathogenesis

Disulfide bond (Dsb) formation is crucial for proper folding and for maintaining stability in many proteins. In Gram-negative bacteria disulfide bond formation occurs in the periplasm with the help of a number of accessory and/or chaperone proteins. Disulfide bond formation has been well characterized in *E. coli*, serving as a model for understanding the process in other bacterial systems. In *E. coli* the Dsb protein system is composed of a number of proteins localized to the bacterial periplasm and inner membrane (109). Each of these proteins contains a pair of cysteine residues that form

mixed disulfides with the polypeptide that requires processing, or with a partner Dsb protein. Two metabolic pathways have been proposed to explain the process of disulfide bond formation; (i) the oxidative pathway which is responsible for the formation of disulfide bonds and (ii) the isomerization pathway which is responsible for correcting erroneous cysteine bonds therefore allowing for the proper folding of proteins.

1.5.1 Pathways of disulfide bond formation

(i) Oxidative pathway: Disulfide bond formation involves the protein DsbA. DsbA is a small periplasmic protein that contains two active site cysteine residues in a CXXC motif. To be active, the two cysteines of DsbA need to be in the oxidized state, making the protein extremely unstable (13). Oxidized DsbA reacts rapidly with unfolded proteins in the periplasm. Upon contact, a transient mixed disulfide forms between the substrate and the first cysteine of the CXXC motif, the disulfide bond is transferred onto the folding protein and reduced DsbA is released. To begin a new round of catalytic oxidation, DsbA must be re-oxidized. Re-oxidation is accomplished with the help of its partner DsbB, an inner membrane protein that generates disulfides *de novo* from oxidized quinones (25) (Figure 3A). DsbA and DsbB have been shown to interact directly (51) and re-oxidation of DsbA involves two pairs of cysteines presented by DsbB in the characteristic CXXC motif.

(ii) Isomerization pathway: The isomerization pathway is critical for proteins that contain more than two cysteines. As the number of cysteine residues increases in a protein, the possibility that incorrect disulfide bonds will form also increases. In *E. coli*, isomerization of non-native disulfides is catalyzed by the thiol-sulphide oxidoreductases DsbC and DsbG, which are maintained in a reduced state by the membrane protein DsbD.

Figure 3: Pathways of disulfide bond formation and isomerization in *E. coli*. The paradigm for disulfide bond formation in the periplasm is best characterized in *E. coli*. **Panel A: The oxidative pathway:** DsbA reacts with a newly translocated protein. Free thiol groups are oxidized to form a disulfide bond between cysteine residues. After donating its disulfide bond to a target protein, DsbA is released in its reduced form. To start a new catalytic oxidation cycle, DsbA must be re-oxidized by its partner enzyme DsbB. Electrons flow from DsbB to ubiquinones and to terminal oxidases of the electron transport chain. **Panel B: The isomerization pathway:** Disulfide bond rearrangement is catalyzed by the thiol-disulfide oxidoreductases DsbC and DsbG, which are maintained in a reduced state by the membrane protein DsbD. DsbD is reduced by cytoplasmic thioredoxin, which is recycled by thioredoxin reductase in a NADPH-dependent manner. Bioinformatics studies have revealed that the paradigm is not conserved in all bacteria.

Adapted from Messens and Collet, 2006 (88).

A- Oxidative pathway

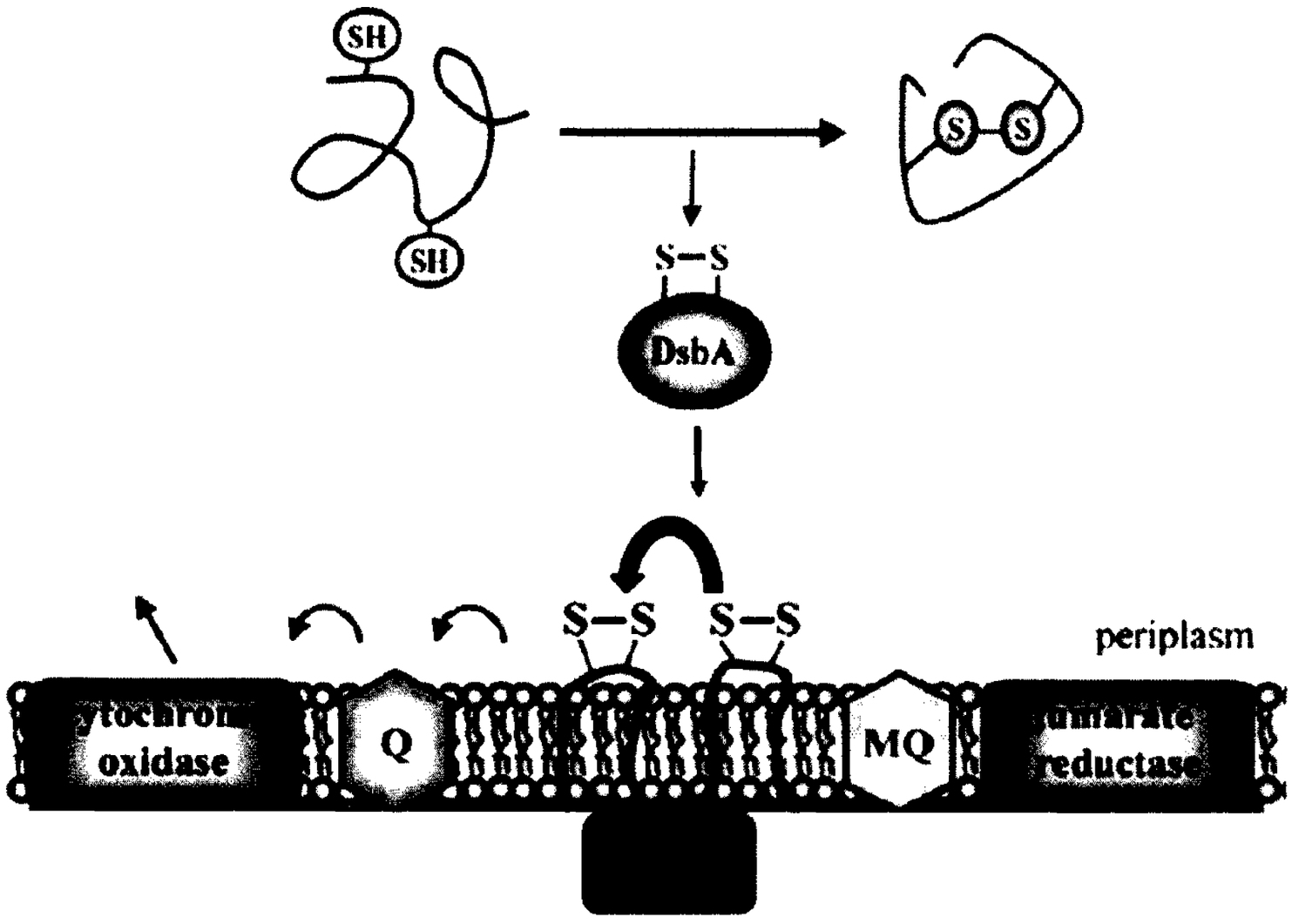

B- Isomerization pathway

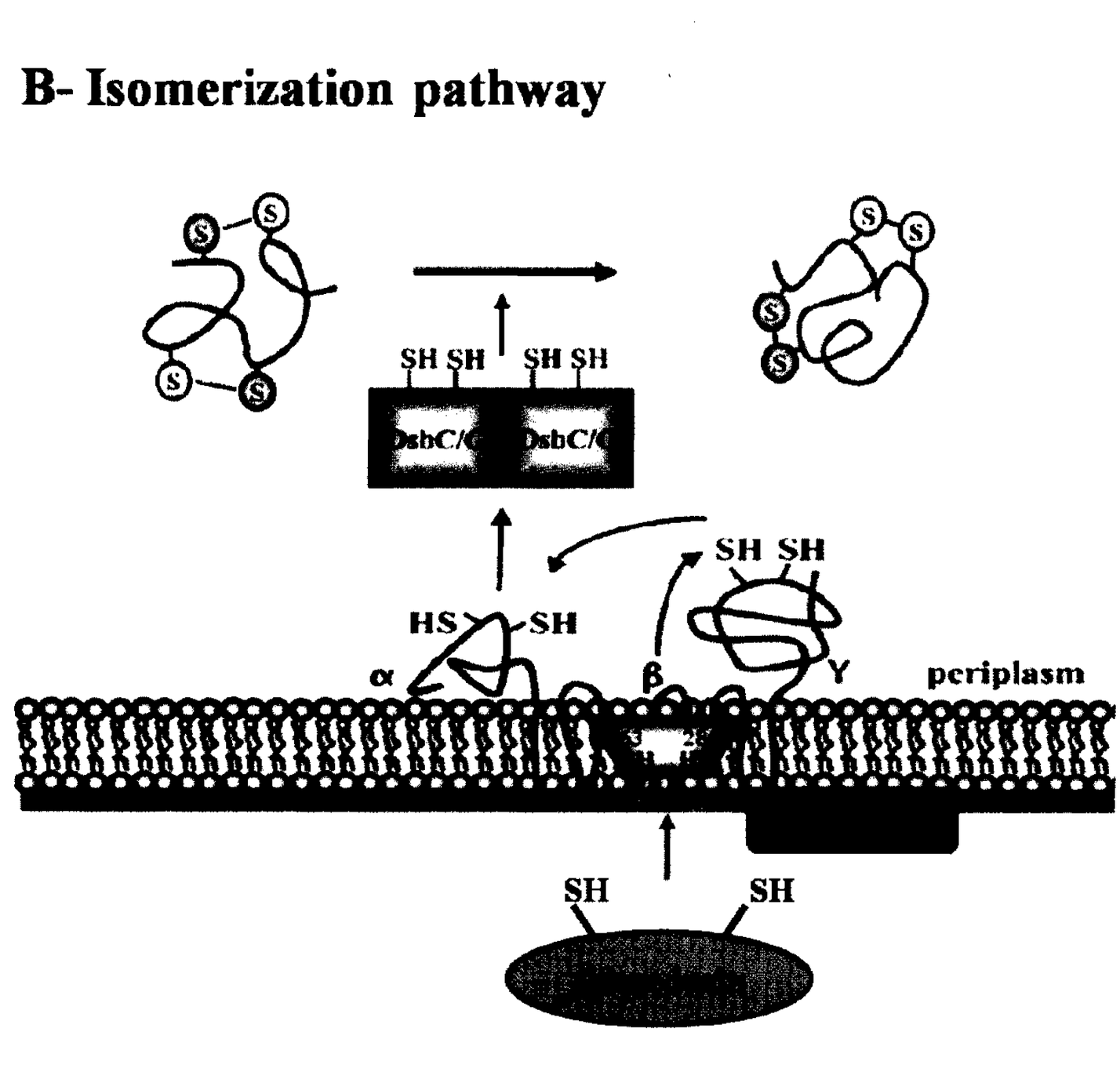

DsbD is reduced by cytoplasmic thioredoxin, which is recycled by thioredoxin reductase in a NADPH-dependent manner (25) (Figure 3B).

Of relevance to this study, DsbG was first identified in 1997 by Anderson *et al.*, who found that when present in multiple copies, this gene could confer resistance to elevated concentrations of dithiothreitol (4). DsbG shows 28% sequence identity and 56% sequence similarity with DsbC. DsbG was identified as a non-essential disulfide isomerase similar to DsbC, but it is presumed to have different substrate specificity. To date, no known *in vivo* substrate for DsbG has been identified (56).

The coordination between oxidation and reduction systems within the same periplasmic compartment implies the existence of barriers to prevent cross-talk between the two systems. In the absence of such barriers, an ineffective cycle would arise in which DsbB would oxidize DsbC. DsbB has been shown to oxidize DsbC 500-fold times more slowly than DsbA, and the dimeric structure of DsbC (120) has been implicated in contributing to its ability to evade DsbB activity (25). When dimerized the active site cysteine residues of DsbC are believed to be protected from catalytic oxidation by DsbB. As a result, the two pathways are able to coexist side by side in the same periplasmic environment yet remain functionally distinct.

1.5.2 Dsb protein impairments and bacterial virulence

Inactivation of genes encoding for Dsb systems in the cells of many pathogenic bacterial species has been shown to reduce their virulence. This impairment affects virulence by either disturbing bacterial protein secretion or by affecting the secreted proteins and virulence factors directly. Defects in various Dsb proteins have been shown

to affect the secretion of virulence related proteins secreted by the general secretory pathway and by a type III secretion system (70). The type III system, as previously explained, translocates effector proteins directly to the cytosol of eukaryotic cells where they modulate the metabolism of infected cells. Disruption of specific components of this secretion system due to the impairment of the Dsb protein system results in avirulence in a number of species including *Salmonella enterica* sv. Typhimurium, *Yersinia pestis*, *Shigella flexneri*, and others (70). Dsb proteins have also been shown to play a role in regulating secretion of the *Bordetella pertussis* PTX toxin. Dsb mutants impart different phenotypes on the functionality of the PTX toxin which include degradation of its subunits and inhibition of toxin transport (128). In uropathogenic *E. coli*, Dsb proteins affect the activity and synthesis of type P pili, which are responsible for adhesion to the epithelium of the urinary tract (85). Dsb proteins also affect the periplasmic chaperonin PapD, which binds pili subunits and transports them to the PapC protein in the outer membrane. Inhibition has been linked to the tertiary structure of PapD, which contains one disulfide bond, catalyzed by the DsbA-DsbB protein system. In the absence of DsbA, PapD adopts an incorrect conformation, targeting it for proteolytic degradation by the DegP protease. This results in an overall reduction in strain virulence due to a lack of adhesion structures (70).

Dsb proteins also influence secreted virulence factors that transit through the periplasm before being secreted across the outer membrane. This has the greatest influence on virulence factors secreted by the general secretory pathway. A hallmark of this pathway is that many of the secreted proteins adopt their active conformation in the periplasm following the formation of disulfide bonds, which are absolutely essential for

their final secretion (56). Dsb proteins promote maturation of a number of toxins in the periplasm belonging to the AB_5 toxin group, which include the toxins of *Vibrio cholera*, *E. coli* and *B. pertusis*. In *V. cholera* a mutation in DsbA results in defective folding of the B subunits, each of which contain a disulfide bridge (146). In *E. coli*, assembly of the mature toxin depends on the activity of DsbA, and mutation in *dsbA*-gene results in instability, degradation, and incorrect toxin assembly (99). DsbA is also responsible for introducing a disulfide bond essential to the virulence of *Pseudomonas aeruginosa*, resulting in reduced colonization potential and an avirulent phenotype (107).

1.5.3 Dsb proteins in *H. pylori*

Recent bioinformatics studies have revealed that the well established paradigm of disulfide bond formation is not conserved in all bacteria, as some bacteria are missing certain homologues, and others seem to have extra Dsb proteins, such as DsbI (37). In *H. pylori* extensive bioinformatics studies have been unable to identify a DsbA homologue; but DsbB, DsbG, and DsbI orthologs have been identified (37, 47, 56, 133). DsbI is believed to function similar to DsbB in campylobacter species, but due to the absence of DsbA in helicobacter species, the process of oxidative folding is thought to occur via different mechanisms that have yet to be elucidated. Nonetheless, DsbI has been implicated in playing an important role in oxidative folding in the periplasm. It was recently shown, using a mouse model of *H. pylori* infection, that *dsbI* mutants display reduced colonization of the stomach (47).

Of relevance to this work, our protein of interest, HcpE contains 19 cysteine residues, 18 of which are predicted to participate in disulfide bonds. If the severity of a

folding defect increases with the number of disulfide bonds formed in a protein, this protein would be significantly impacted in the absence of its folding factor.

1.6 Experimental methods for studying protein-protein interactions

Protein-protein interactions are central to many biological processes ranging from basic cellular functions such as DNA replication, gene transcription, and protein synthesis to more specialized processes involved in cell-to-cell signaling and coordination of immune responses (69). Protein-protein interactions are also involved in catalytic reactions, transport, formation of regulatory channels, transmission of information from DNA to RNA, and are responsible for degradation of unnecessary proteins and nucleic acids. They may act as vehicles of the immune response and are responsible for viral entry into cells. Given their importance in basic cellular processes, identification of these interactions and characterization of their physiological significance constitutes one of the main goals of current research in different biological fields. Over the years, a number of different techniques have been developed to identify protein-protein interactions in different biological systems. Some of the methods relevant to this research are discussed below.

(a) Yeast two-hybrid: Twenty years ago, Fields and colleagues introduced a powerful *in vivo* genetic tool that facilitates detection of interactions between two polypeptides known as the yeast two-hybrid system (23, 125). The technique relies on the co-expression of two-hybrid proteins in a given cell that upon interaction lead to the transcriptional activation of a reporter gene. A classical eukaryotic activator of transcription has two conserved domains; one that specifically binds the DNA sequence, known as the binding domain (BD), and one that recruits the transcription machinery,

known as the activation domain (AD). In the yeast two-hybrid system, these two domains are distinct polypeptides each fused to a protein of interest, X and Y (Figure 4) (71). The rationale for the assay is that transcription will occur only if proteins X and Y interact with one another, bringing the BD and AD in close proximity of one another.

The yeast two-hybrid system was initially designed to detect associations between two known proteins, and has since its discovery become the most rapid and widely used system to screen gene libraries (71). This approach for screening complete libraries has been adapted to many organisms other than yeast. An exhaustive proteome-wide approach was recently adopted to construct a protein-protein interaction map in *H. pylori* (108). A total of 261 *H. pylori* proteins were screened against a highly complex library of genome-encoded polypeptides. From this, over 1200 interactions were identified between *H. pylori* proteins, linking an overwhelming 46.6% of the proteome. Due to the large proportion of false positive results associated with yeast two-hybrid screens, this number is likely exaggerated and all interactions need to be confirmed by other methods. Nonetheless, this work serves as an excellent reference and starting point for identifying protein-protein interactions in *H. pylori*.

(b) Bacterial two-hybrid: Development of the bacterial two-hybrid system was prompted by the success associated with identifying protein-protein interactions using yeast two-hybrid technology. Bacterial two-hybrid systems present the advantage of assaying protein interactions under conditions that match their native environment more closely (111). Bacterial two-hybrid systems can be placed in two categories; those based on transcriptional activation or repression of reporter genes, and those based on the

Figure 4: General overview of the yeast two-hybrid system. Yeast two-hybrid systems have been used to detect interactions between two known proteins, or polypeptides as well as for searching for unknown (prey) proteins of a given (bait) protein. The concept relies on the transcriptional activation of one or several reporter genes. A typical eukaryotic transcriptional activator contains two fundamental domains: a domain that specifically binds DNA (binding domain; BD) and a domain that recruits the transcription machinery (activation domain; AD). Transcription can only be activated if these two domains are in close proximity. When these two domains are fused to two proteins, X and Y, transcriptional activation will only occur if X and Y interact.

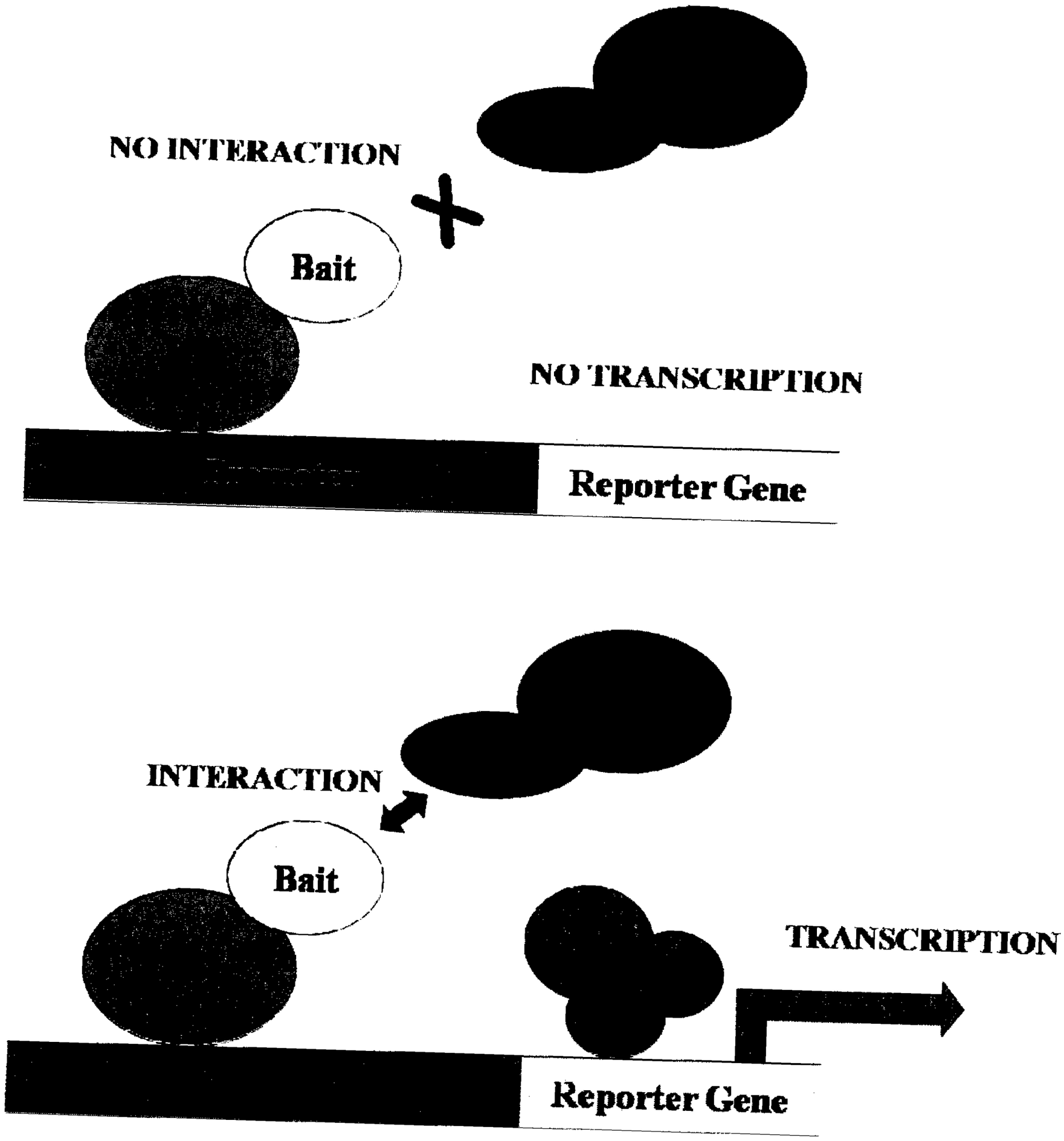
NO INTERACTION
Bait
NO TRANSCRIPTION
Reporter Gene
INTERACTION
Bait
TRANSCRIPTION
Reporter Gene

reconstitution of an enzyme. The first category takes advantage of the dimerization properties of the λ-phage cI repressor (33) or the bacterial transcription repressor LexA (125). Repressor proteins cI and LexA can be divided into two functionally distinct domains; (i) N-terminal DNA BD unable to dimerize and (ii) a C-terminal domain that is strictly required for dimerization and thus, for the functional activity of the repressor. Only the dimeric form of λ-cI or LexA is capable of acting as a transcriptional repressor. The DNA BD alone, without dimerization capability is unable to repress transcription. When this domain is genetically fused to a protein or polypeptide that can dimerize, or two proteins that interact with one another, a functional chimeric repressor can be restored (Figure 5). This activity can be assayed by measuring the repression of transcription of the reporter gene fused to the λ-promoter-operator, which is usually *E. coli lacZ* encoding β-galactosidase.

The second category was first described by Karimova *et al.*, and is based on the reconstitution of a signal transduction pathway mediated by cAMP (64). The system takes advantage of the fact that the catalytic domain of the adenylate cyclase from *Bordetella pertussis* consists of two complementary fragments, T18 and T25, which are only active when in contact with one another. If these fragments are fused to interacting proteins or polypeptides, heterodimerization of the hybrid proteins will result in functional complementation between T18 and T25 fragments, and cAMP synthesis. In cells, cAMP binds to the catabolite activator protein, CAP, which turns on expression of several genes, including genes involved in lactose and maltose catabolism. In the presence of cAMP, bacteria are able to utilize lactose or maltose as a unique carbon source, which can easily be identified using selective media (71).

Figure 5: Bacterial two-hybrid systems based on transcriptional repressors. Lambda cI is the transcriptional repressor that controls the lytic/lysogenic cycle of bacteriophage-λ. The λ repressor is a dimer of two identical polypeptides chains. Each contains an N-terminal DNA binding domain (DBD) and a C-terminal dimerization domain (DD). The λ cI is only functional as a transcriptional repressor in its dimeric form. Thus the DBD alone is unable to repress transcription. The system is used to study protein-protein interactions by fusing DBDs to different proteins and measuring transcriptional activation of a reporter gene. If the bound proteins interact, a functional chimeric repressor can be restored and transcription will be shut off. If the proteins do not interact, the reporter gene will be transcribed.

A- λ cI repressor

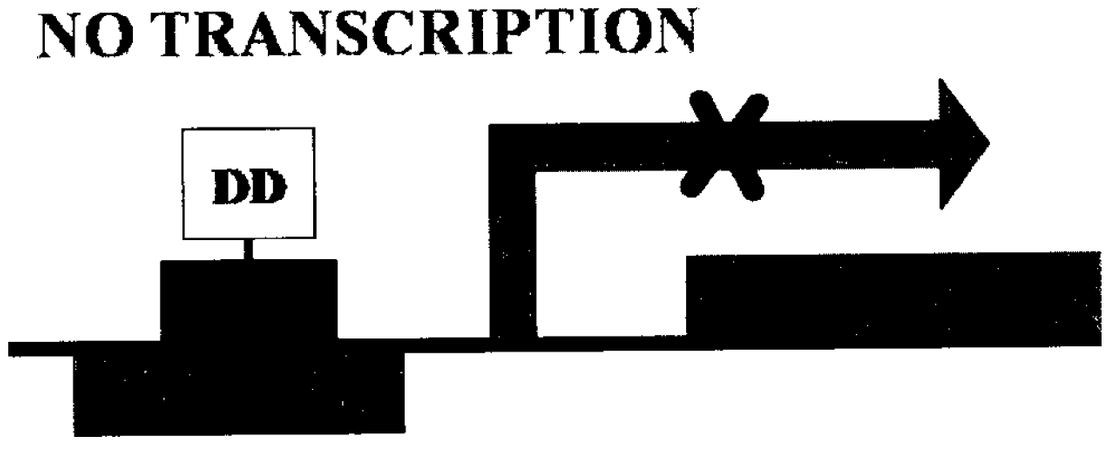

B- repression by fusion proteins

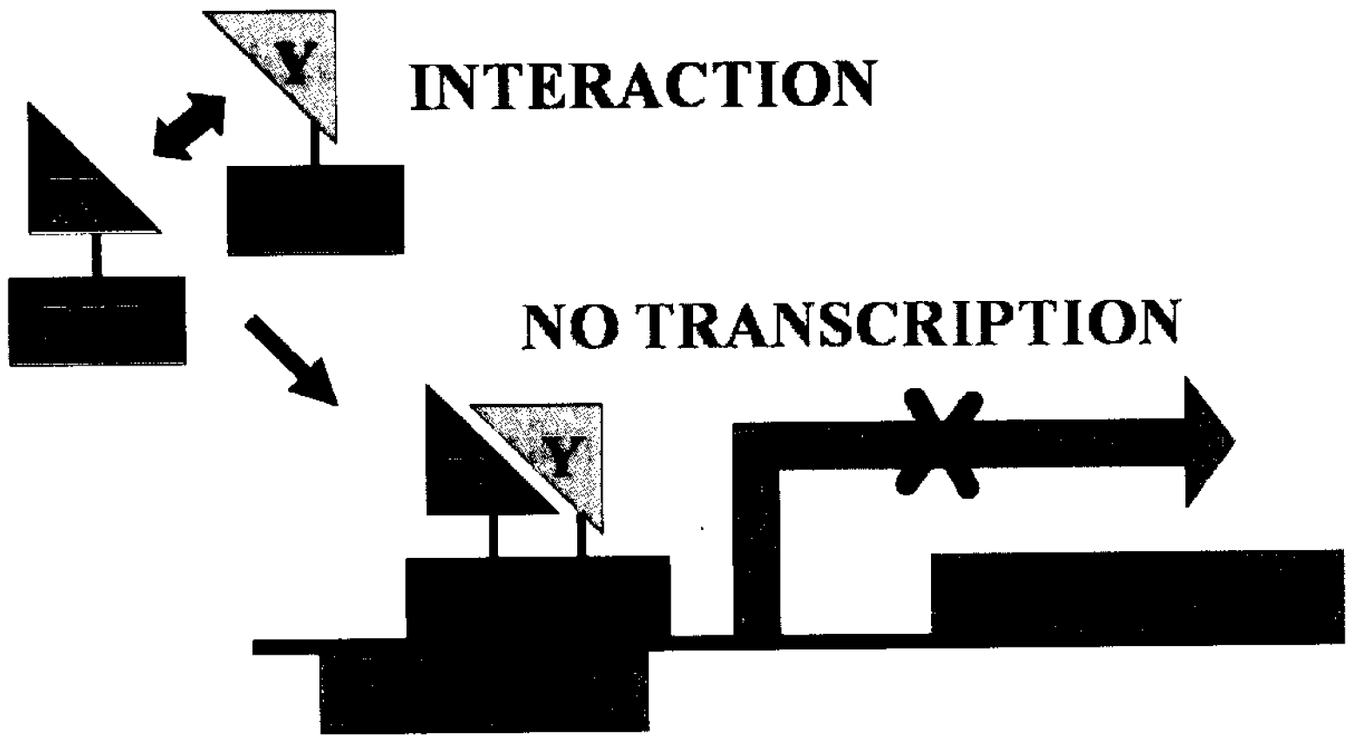

The latter system's efficacy in identifying and screening interacting proteins using selective media was tested in *H. pylori*. A screening experiment was performed using a protein identified using the yeast two-hybrid system to validate the system in *H. pylori*. Among the candidate colonies selected in this screen, two distinct families of preys were identified, one of which corresponded to a known interacting partner (71).

(c) Tandem Affinity Purification (TAP): The TAP method allows for rapid and high yield purification of protein complexes under native conditions. It involves fusion of the TAP-tag to a target protein and introduction of the construct into the host cell. Cell extracts are prepared and the fusion protein and its interacting partners are recovered by two sequential and specific affinity purification steps. The TAP-tag contains the IgG binding domain of *Staphylococcus aureus* protein A (ProtA) and a calmodulin binding peptide (CBP) separated by a Tobacco etch virus (TEV) protease cleavage site. The presence of these two sites allows for the two-step affinity purification. The first step requires an IgG affinity matrix for which ProtA will bind strongly. The TEV protease is used to elute the bound material under native conditions. In the second step, the eluate is incubated with calmodulin-coated beads in the presence of calcium, which facilitates binding. Afterwards, unbound material is washed away and bound proteins, or protein complexes are released following mild treatment with EGTA (Figure 6).

The TAP-tag purification method has not yet been established in a fastidious organism like *H. pylori*. Because of the appeal and promise of this purification method, a previous member of the Creuzenet lab undertook the task of TAP-tagging various *H. pylori* bait proteins to identify their interacting partners from whole cell extracts. Application of this method in *H. pylori* was unsuccessful for a number of reasons. First,

Figure 6: Schematic representation of the Tandem Affinity Purification (TAP) method. The TAP-tag consists of three essential components: a calmodulin-binding peptide, a tobacco etch virus (TEV) protease cleavage site and Protein A as an immunoglobulin (IgG)-binding domain. Purification using TAP-tag methodology requires a known protein, the bait, which is fused to the TAP-tag. Cell extracts are incubated with the recombinant TAP-tagged protein. The extracts are then loaded onto an affinity column. The first column contains IgG beads, which bind specifically to Protein A of the TAP-tag. TEV protease cleaves the immobilized multi-protein complexes. The second step in the purification is carried out on calmodulin beads. The calmodulin-binding peptide of the TAP-tag will bind, and native complexes are eluted using mild EGTA treatment.

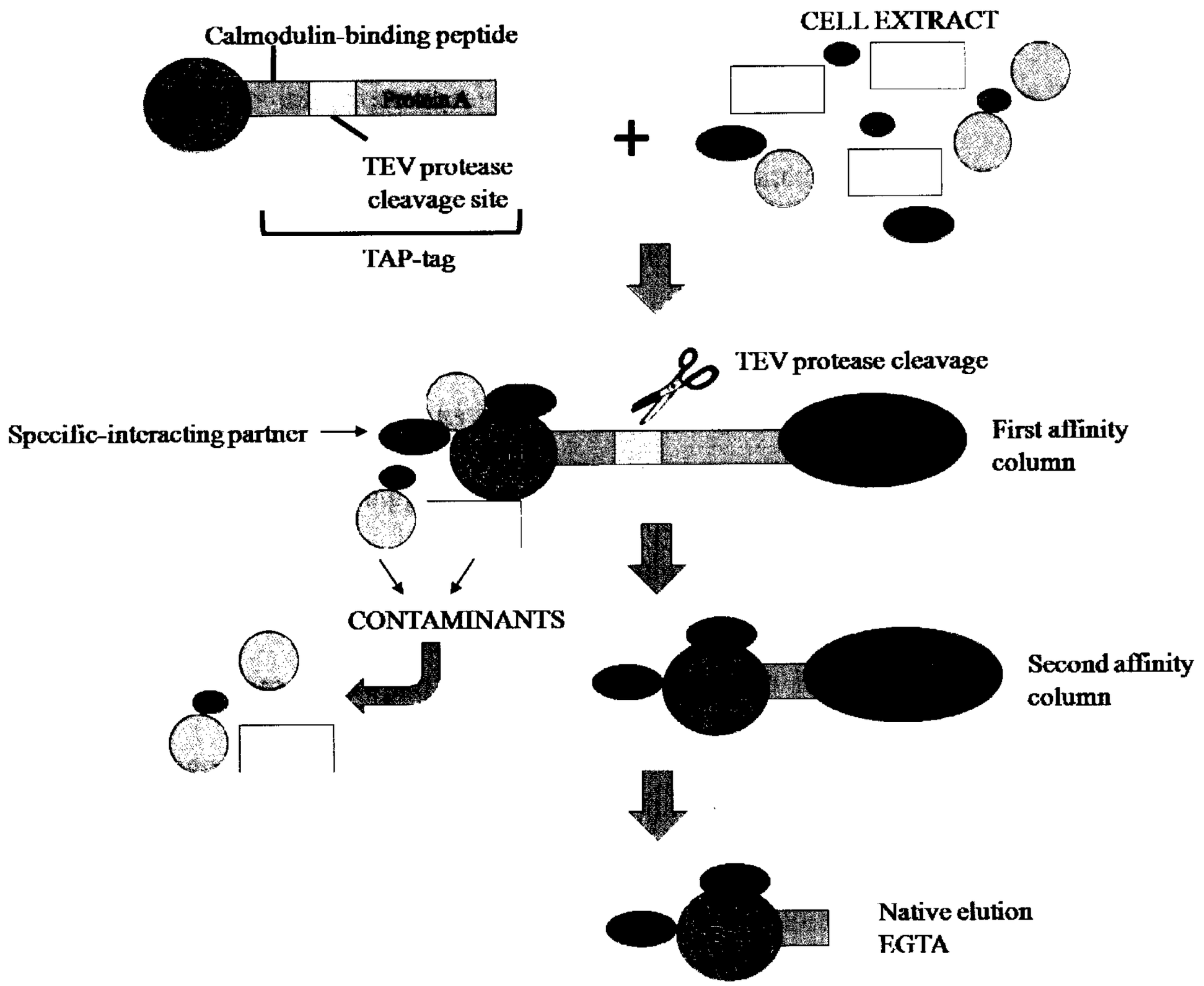
Calmodulin-binding peptide
Protein A
TEV protease cleavage site
TAP-tag
CELL EXTRACT
TEV protease cleavage
Specific-interacting partner
First affinity column
CONTAMINANTS
Second affinity column
Native elution EGTA

H. pylori is not hospitable to the uptake of foreign DNA (5), and as a result, it proved to be very difficult to introduce foreign DNA into *H. pylori,* so only a few bait proteins could be investigated. Second, a relatively large amount of starting material is required for purification of complexes and *H. pylori* is a slow growing organism that is not easily cultured (67). Therefore, growing large amounts of *H. pylori* to assess protein interactions was unfeasible and as a result, only a small amount of protein could be used. Third, elution of the TAP-tagged proteins by TEV cleavage was ineffective for the baits tested. Due of these limitations the strategy was abandoned.

(d) Affinity chromatography interaction assay: To identify interactions that occur between a tagged recombinant protein and other proteins within the cell, the presence of an affinity tag can be exploited to purify protein complexes. The purified tagged protein can be incubated with whole cell extracts so that interactions can occur and after incubation, the protein complexes can be purified using affinity chromatography.

This method was adopted to identify interacting partners for HcpE, the hypothetical virulence-associated protein. HcpE was tagged with a hexahistidine (His_6) tag and over-expressed in the pET expression system in *E. coli* BL21(DE3)pLys cells and nickel chromatography was used to purify HcpE and its potential interacting partner (Figure 7). The detailed methods are explained in section 2.4 and reviewed in section 3.3.1.

(e) Affinity blotting: Affinity blotting, or filter binding, as it is also commonly called (139), of putative chaperones to immobilized substrates has been used to demonstrate *in vitro* associations between type III secretion chaperones and secreted virulence factors in a number of bacterial species (44, 139, 141, 143). The method was pioneered in 1994 in

Figure 7: Detecting protein-protein interactions by affinity chromatography with a histidine-tagged protein. Panel A: Purification of histidine-tagged HcpE by nickel chelation chromatography. HcpE was over-expressed in *E. coli* with a C-terminal histidine-tag and was purified by affinity chromatography with a nickel charged column. Bound proteins were eluted with an imidazole gradient, and eluted fractions were separated and visualized by SDS-PAGE. The purified protein (circled in red) was isolated and used for the second step of the interaction assay. **Panel B: Interaction assay based on affinity chromatography.** The purified histidine-tagged protein was incubated with a total *H. pylori* cell lysates, to allow interactions to occur between the pure proteins and endogenous *H. pylori* proteins. The mixture was then subjected to a second round of affinity chromatography using a nickel charged column. Protein complexes were eluted with an imidazole gradient, followed by visualization by SDS-PAGE. Proteins eluting before, or at the same time as the pure protein (red box) represent potential interacting partners (blue box), which can be identified by MS.

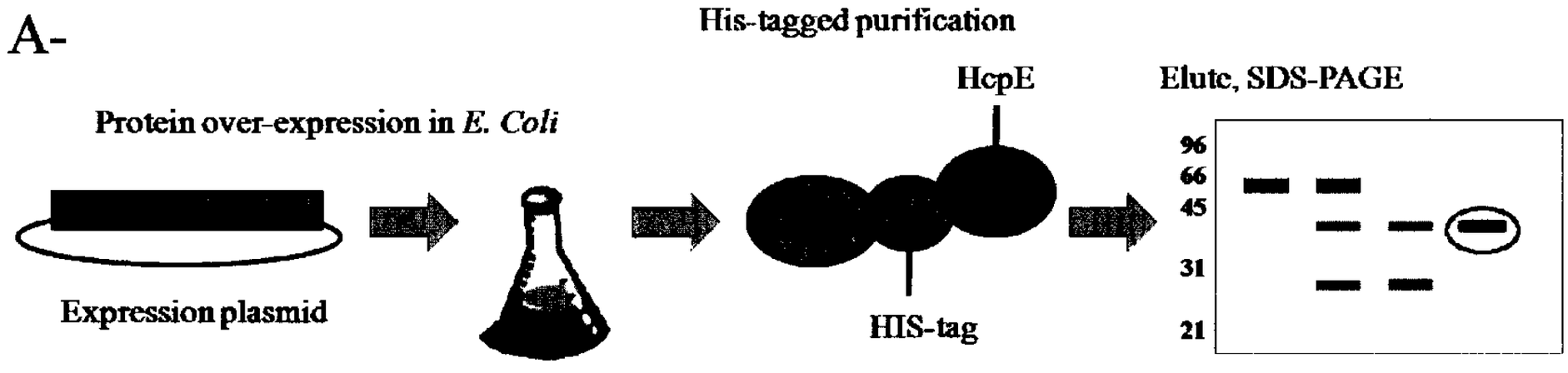
A-
His-tagged purification
HcpE
Elute, SDS-PAGE
Protein over-expression in E. Coli
96
66
45
31
21
Expression plasmid
HIS-tag

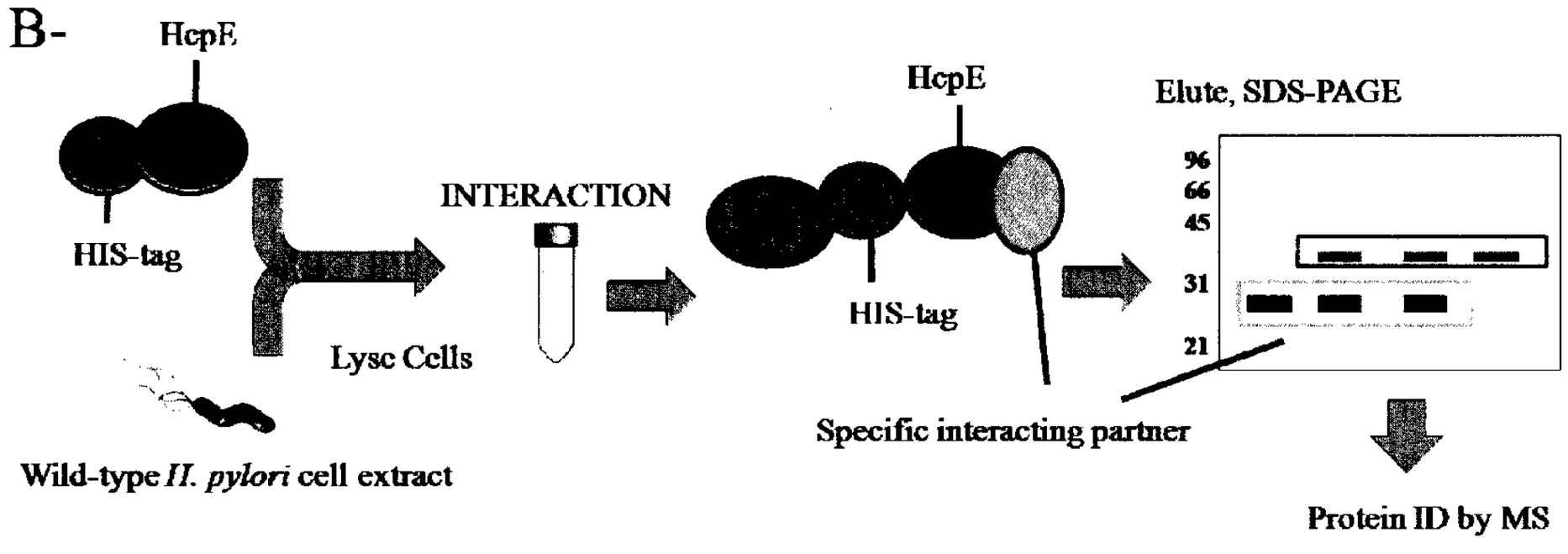
B-
HcpE
HcpE
Elute, SDS-PAGE
INTERACTION
96
66
45
31
21
HIS-tag
HIS-tag
Lysc Cells
Specific interacting partner
Wild-type H. pylori cell extract
Protein ID by MS

Yersinia spp. identifying interactions between chaperones and secreted Yops proteins (141). Similar methodology was adopted to identify chaperone-substrate interactions in enteropathogenic *E. coli* (EPEC) (139). In *S. typhimurium*, the affinity blotting technique was utilized to study interactions between flagellar proteins and the chaperones that facilitate their secretion through the flagellum (44).

This method is specific for chaperone proteins or folding factors that react with unfolded, denatured proteins. The fundamental feature of this method is that one of the proteins involved in the interaction is immobilized in its denatured form on a membrane while the other is in its mature and active form. Therefore this method is not applicable to identify all protein-protein interactions and applies to only a small subset of interactions. For interactions that result in re-folding, bond formation, or secretion, this method is effective and high throughput.

In practice, one of the proteins (the substrate) participating in the proposed interaction is separated by SDS-PAGE gel electrophoresis and electro-transferred to nitrocellulose or PVDF membrane. The membranes are then incubated with cell lysates containing the folding factor, or purified proteins. Binding of the chaperone/ folding factor to its substrate can be visualized by immunoblotting (139), autoradiography (44) if one of the proteins is radiolabeled, or by mass spectrometry if antibodies are not available, or if the interacting protein is unknown.

Affinity blotting of the immobilized substrate has not been attempted in *H. pylori* to date. However, its efficacy in identifying interactions between chaperones and their denatured substrates in other bacterial species, coupled with the fact that very small

amounts of sample are necessary, render it appealing to identify protein-protein interactions in *H. pylori*.

In this study, the affinity blotting method was adapted and modified to identify a folding factor for a known substrate protein HcpE. In all of the aforementioned applications of the technique, the substrate protein was unknown and the chaperone protein was tagged or provided in the cell extract. In this adaptation, the substrate protein (HcpE) was known and its folding factor was to be identified. Substrate proteins (HcpE and control TsaA, see Figure 8 below) were expressed as recombinant histidine-tagged proteins. These proteins were over-expressed and purified using Ni-chelation affinity chromatography. The purified proteins were separated, and denatured by SDS-PAGE gel electrophoresis and transferred to PVDF, or nitrocellulose membrane. The membranes were incubated with whole cell extracts containing endogenous chaperones and folding factors. Following incubation, the membranes were washed and the area corresponding to HcpE was visualized by Western blotting so that it could be excised. Bound proteins were removed by tryptic digestion and sent to mass spectrometry for peptide identification. A schematic overview of the method is depicted in Figure 8. Detailed methods can be found in section 2.15 and are reviewed in section 3.2.5.

Figure 8: Schematic overview of the method known as "affinity blotting of the immobilized substrate." Detecting interactions between chaperones and/or folding factors with their cargo proteins requires the cargo to be in a denatured native form. In affinity blotting, the substrate protein is denatured by SDS-PAGE and immobilized by immunoblotting onto a PVDF membrane. Membranes are incubated with cell extracts to allow for local interactions. Chaperones/ folding factors within the extract will bind their unfolded substrates on the membrane. The interactions can be identified by digesting the proteins bound to the membrane and sending to MS for protein identification. The schematic represents the experimental protocol used in this study to identify interactions between HcpE and its endogenous *H. pylori* folding factor. Histidine-tagged TsaA, an *H. pylori* protein not related to Hcps, served as a negative control to eliminate non-specific interactions.

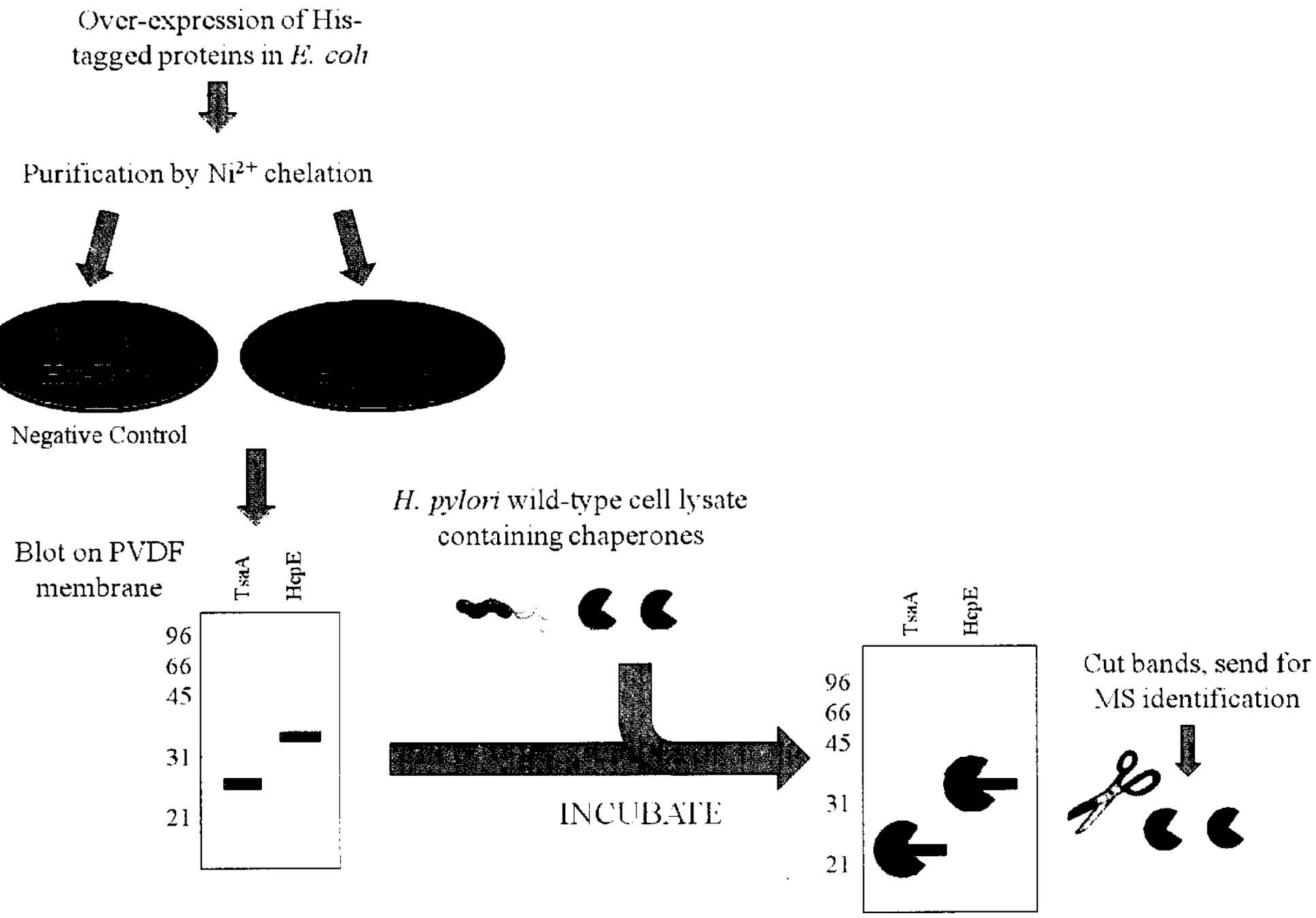
Over-expression of His-tagged proteins in E. coli
Purification by Ni2+ chelation
Negative Control
Blot on PVDF membrane
TsaA
HcpE
96
66
45
31
21
H. pylori wild-type cell lysate containing chaperones
INCUBATE
TsaA
HcpE
96
66
45
31
21
Cut bands, send for MS identification

1.7 Hypotheses and objectives

Based on the presence of high antibody titers to the HcpE protein in *H. pylori* infected individuals and the established role of other Hcp family members in immune modulation, the following hypotheses were proposed:

- **HcpE is secreted by *H. pylori* and contributes to bacterial virulence mediated by its interaction with host cells.**
- **Being a member of the Hcp protein family, HcpE may have β-lactamase activity.**
- **Based on its high cysteine content and the presence of a signal peptide, we propose that HcpE interacts with periplasmic folding factors to acquire its proper structure before secretion.**

To address these hypotheses, the objectives of this thesis were to:

1) **Determine if HcpE is secreted by *H. pylori***
2) **Identify *H. pylori*-specific factors that facilitate and/or assist in HcpE secretion**
3) **Assess the intrinsic activity of HcpE**
4) **Characterize the effect of HcpE on host cells and/ or identify an interaction with host cells**

CHAPTER 2: MATERIALS AND METHODS

2.1 Bacterial strains, growth conditions, and reagents

Bacterial strains and plasmids used in these studies are listed in Table 1. *H. pylori* NCTC 11637 cells were grown under microaerophilic conditions of 5% O_2, 10% CO_2, and 85% N_2 for 48 hours on agar plates containing 37 g/L Brain Heart Infusion (BHI) media (BDH), 2.5 g/L yeast extract (YE; BioShop), 0.05 μg/ml sodium pyruvate (BioShop), 10% Horse serum (HS; Gibco) supplemented with the antibiotics: trimethoprim (5 μg/mL), vancomycin (10 μg/mL), and amphotericin B (5 μg/mL) (Sigma). To grow the *hcpE::kan* knockout mutant the media was supplemented with kanamycin (5 μg/mL; Fisher). Unless stated otherwise, growth of *E. coli* for all over-expression studies was done at 37˚C, in Luria-Bertani (LB; BioShop) media supplemented with chloramphenicol (34 μg/mL), kanamycin (30 μg/mL), or ampicillin (100 μg/mL) as required for selection of expression plasmids.

2.2 SDS-PAGE and Western blot analysis

Bacterial cells or proteins at various stages of purification were denatured in sodium dodecyl sulfate (SDS) sample buffer (0.625M Tris pH 6.8, 2% SDS, 2% 2-β-mercaptoethanol, 10% glycerol, and 0.002% bromophenol blue), boiled for 5 min at 100°C and separated on 12 or 15% SDS polyacrylamide gels. Individual proteins were visualized by Coomassie blue staining (10% acetic acid, 25% ethanol, 0.01% (w/v) Brilliant Blue R-250), Western blotting, or silver nitrate staining. For Western blotting, proteins were transferred to a nitrocellulose membrane (BioRad) using standard procedures. Transfer occurred for 45 min at 180 mAmp. The membrane was washed in distilled water and stained with Ponceau Red stain

Table 1: Bacterial strains and plasmids

Strains and plasmids	Description	Reference
Strains		
H. pylori		
NCTC 11637	Wild-type strain	Lab stock (provided by Dr. D. E. Taylor)
E. coli		
DH5α	*supE Δlac U169 (Φ80lacZΔM15)hsdR recA endA gyrA hri relA*	(52)
BL21(DE3)pLysS	F^- *ompT hsd*S_B(r_B^- m_B^-) *gal dcm Δ(srl recA)* 306::*Tn*10(*DE3*) pLy	Novagen, USA
Plasmids		
pHel3	Shuttle vector containing kanamycin resistance cassette; Kan^R	(57)
pUC18	Cloning vector; Ap^r	(144)
pET-MTF	A pET23 derivative with a N-terminal histidine-tag	(96)
pET-30a	A pET30 derivative with a C-terminal histidine-tag	Novagen, USA
Expression plasmids		
pET30a-*hcpE*	The *hp0235* gene (1085 bp) cloned into pET30a expressing a C-terminal Histidine tagged HcpE protein	This study (made by J. Chahal)
pET30a-*dsbG*	The *hp0231* gene (856 bp) cloned into pET30a expressing a C-terminal Flag tagged DsbG protein	This study (made by L. Meng)
pET23-*tsaA*	The *hp1563* gene (840 bp) cloned into pET-MTF expressing a N-terminal histidine tagged TsaA protein	Merkx-Jacques *et al.*, unpublished
pET23-*cj1427*	The *cj1427* gene (941 bp) cloned into pET-MTF expressing a N-terminal histidine tagged Cj1427 protein	Creuzenet Lab

(0.1% (w/v) Ponceau S in 1% (v/v) acetic acid) for 5 min, shaking, then washed briefly in distilled water and scanned. The membrane was subsequently washed in Tris Buffered Saline (TBS) buffer (50mM Tris-HCl pH 7.5, 150mM NaCl) for 10 min and was then blocked O/N at 4°C in 10% milk, unless indicated otherwise. The membrane was washed twice in TBS-Tween/Triton (0.05% Tween-20, 0.2% Triton-X 100) buffer and once in TBS buffer, for 10 min each. The membrane was incubated in primary antibody for 1 hr at room temperature on the shaker. After incubation, the membrane was washed twice in TBS-Tween/Triton-X 100 and once in TBS at room temperature, as above. All antibodies were centrifuged at 6300 *g* for 10 min prior to use. The membrane was incubated in secondary antibody for 1 hr at room temperature in the dark and then washed three times as above. Proteins were visualized using the Licor Infrared Imaging System with detection at a wavelength of 700 or 800 nm.

2.3 Transformation of *E. coli* competent cells

The following method was used to transform all plasmid DNA into *E. coli* cells. $CaCl_2$-competent cells were thawed on ice, and a 150 µL aliquot was used for each transformation. To the cells, 1 µL DNA or 15 µL of a ligation mixture was added and incubated on ice for 30 minutes. The cells were heat shocked at 42˚C for 90 seconds and then put back on ice for 1 minute. 600 µL of LB was added and the cells were grown at 37˚C while shaking for 1 hr and 30 minutes. 50 µL of each culture were plated on LB plates with the appropriate selection antibiotics using glass beads. For the pET30 constructs kanamycin was used for transformation into DH5α cells and kanamycin + chloramphenicol were used for transformation into BL21(DE3)pLys cells. The remaining culture was centrifuged at 7320 *g* for two minutes. The supernatant was removed, leaving

50-70 μL behind to re-suspend the cells in. 50 μL of the concentrated cell culture was plated on a plate with selection antibiotics. The plates were incubated O/N at 37˚C. To the leftover cells, 600 μL LB was added and grown O/N at 37˚C shaking. If nothing grew on the transformation plates O/N, this culture was re-plated the next day.

2.4 Cloning of *tsaA*, and *hcpE* into the pET system for over-expression

Cloning of the *tsaA* (*hp1563*) gene into the over-expression system to create the N-terminal histidine-tagged pET23-tsaA was carried out by Dr. Alexandra Merkx-Jacques. The *tsaA* gene was PCR amplified using chromosomal DNA from *H. pylori* strain NCTC 11637 with primers HP1563P7 and HP1563P2 (Table 2). The *tsaA* PCR product was digested with *Afl*II and *Bam*HI and cloned into the pET23 derivative with an N-terminal histidine tag yielding pET23-*tsaA*.

Cloning of the *hcpE* gene into the pET expression system was carried out by Jaspreet Chahal and Dr. Carole Creuzenet. First, the pUC18-*hp0235* was generated using primers HP0235P1 and HP0235P2 (Table 2) to amplify *hp0235* from *H. pylori* chromosomal DNA. The PCR product was cloned into the *Bam*HI/*Eco*RI sites of pUC18 using standard procedures. The *hp0235* gene was PCR amplified from pUC18-*hp0235* using the primers HP0235P8 and HP0235P9 (Table 2). The *hp0235* PCR product was digested with *Not*I and *Nde*I and cloned into the pET30a plasmid (Novagen) to create the C-terminal histidine tagged pET30a-*hcpE* construct.

Table 2: List of nucleotide sequences for primers

Primer name	Sequence (5' to 3')
HP0231P1	GGAAGACC**ATAT**GATATTAAGAGCGAGTGTG
HP0231P2	CGG/GATCCTG/CTAGCTCACTTGTCGTCGTCGTCCTTGTA GTC**AGAGCC**TGCCTTATAATGGTATAAGAAAG
HP0235P1	CTC**GAATTT**AGAGCATAAAGAAGAGCGTAAG
HP0235P2	CTC**GAATTC**TCAATACCCCCTAAGTTTAGTG
HP0235P8	GGAAGAC**CATATG**GGTGTCAAATTTTTAAAAATATTAG
HP0235P9	ATAGTTTCGC**GGCCGC**ATACCCCCTAAGTTTAGTGAGGT
HP0235P4	CC**ATCGAT**GAAGATTTTGAAGTGGCG
HP0235P5	GA**AGATCT**ATTCTAGTGCCTTGCCC
HP1563P7	**CCTGT**ACATGTGCATGTTAGTTACAAAACTTGC
HP1563P2	**ACTCT**GGATCCTTAAAGCTTAATGGAATTTTC
Aph3P1	GA**AGATCT**GATAAACCCAGCGAACCA
Aph3P2	CC**ATCGAT**AGACATCTAAATCTAGGTAC
CtermHis	CG**GGATCC**TCAGTGGTGGTGGTGGTGG
T7ProX	TAATACGACTCACTATAGGGG

* Restriction sites are **bolded** and underlined

The over-expression constructs were transformed into *E. coli* DH5α cells and all positive transformants were selected using ampicillin for pET23-*tsaA* and kanamycin for pET30a-*hcpE*. Positive transformants were further verified by restriction enzyme digestion and DNA sequencing. All DNA sequencing was done at the DNA Sequencing Facility at the Robarts Research Institute at the University of Western Ontario.

2.5 Over-expression, and purification of soluble proteins using nickel chelation chromatography

Protein expression was done in *E. coli* BL21(DE3)pLysS (Novagen). The cultures were grown while shaking at 37°C in 1L of LB until they reached an OD_{600nm} of 0.6. For optimal expression of HcpE, cultures were equilibrated to room temperature for 1 hr before induction. TsaA and HcpE were over-expressed from the pET constructs via induction with 0.15 mM Isopropyl β-D-1-thiogalactopyranoside (IPTG, BioShop). The cells were harvested by centrifugation at 2057 *g* for 30 minutes at 4°C and stored at -20°C until needed. For purification of the over-expressed proteins 1L equivalents of culture were re-suspended in 30 mL cold 1X binding buffer (5mM imidazole, 0.1M NaCl, 20mM Tris pH 8.3). Cell pellets representing 3L of the HcpE over-expression culture and 1L of the TsaA over-expression culture were used for purification. Lysozyme was added to the re-suspended cells at a final concentration of 150 μg/mL to promote lysis. To prevent proteolysis 1 mL, for each 1L equivalent, of 1M protease inhibitor cocktail (PIC; Invitrogen) was added to the re-suspended cells. The cells were lysed by mechanical disruption four times using a French press (15,000 psi). Cell debris and insoluble proteins were removed by an initial centrifugation at 12 000 *g* for 30 minutes at 4°C, and membranes were removed by ultracentrifugation (Beckman) at 100 000 *g* for 1 hr. The

supernatant containing the soluble proteins was filtered sequentially through 0.8 μm and 0.45 μm pore size filters (Millipore Millex-HV) and stored on ice until purification. The histidine-tagged proteins were purified by affinity chromatography using Fast Protein Liquid Chromatography (FPLC) system with a POROS 1.6 mL column (Applied Biosciences). The column was washed with 5 column volumes (CV) of water before being charged with 30 CV of 0.1M nickel sulphate. After charging, the column was washed with 7.5 CV 0.1M NaCl and 5 CV of water. The column was equilibrated with 10 CV 1X binding buffer and the soluble fraction was applied at 4 mL/min. A total volume of 230 mL of soluble HcpE and 40 mL of soluble TsaA were loaded onto the column in each of their respective purifications. After loading the sample, the column was washed with 10 CV of 1X binding buffer to remove non-specific proteins. Bound proteins were eluted with an imidazole gradient from 50mM to 1.0M of 1X elution buffer (1M imidazole, 0.1M NaCl, 20mM Tris pH 8.3). Sixty 1 mL elution fractions were collected and analyzed by Coomassie staining and Western blotting. 20 μL of each elution fraction was resolved on a 15% SDS-PAGE gel and detected by Coomassie blue staining. The histidine-tagged HcpE and TsaA were predicted to migrate to 40.2 kDa and 26 kDa, respectively. Fractions containing over-expressed pure proteins were pooled and dialyzed O/N in 50mM ammonium bicarbonate buffer using a molecular weight cutoff of 3.5 kDa to remove all remaining imidazole. Following dialysis the purified HcpE sample was concentrated 3-fold using polyethylene glycol (PEG-8000) such that HcpE could be easily visualized by Coomassie staining. His-TsaA did not need to be concentrated, as it was initially expressed at much higher levels and readily detectable by Coomassie staining.

2.6 Protein quantification using the Bio-Rad Bradford protein assay

For protein quantification, bovine serum albumin (BSA; BioRad) diluted to 1.36 g/l, as recommended by the manufacturer, was used to generate a standard curve. The BSA protein standard was serially diluted (0-0.40 g/L) in 50mM ammonium bicarbonate buffer in a 96-well plate. The protein sample was tested at 3 different concentrations: undiluted, 1:5 dilution and 1:25 dilution, to increase chances of falling within the linear range of the standard curve. 10 µL of protein or standard were added in triplicate to the 96-well plate. The Protein Assay Dye Reagent Concentrate (BioRad) was diluted 1:4 in water, and 200 µL of the reagent was added to each sample. Samples were mixed well, by pitpetting up and down, and the plate was read within 10 min at 595nm on the Microplate reader (BioRad). A plot of the BSA standard was generated and the concentration (g/L) of purified protein was determined using the linear equation $y = mx + b$, where y is the average absorbance of the protein sample as determined by the assay, m is the slope of the line of best fit generated for the standard curve, and b is the y-intercept.

2.7 Solubility assay for over-expression of HcpE

To assess optimal conditions for soluble HcpE expression 1.5 mL of Media II (1% bactotryptone, 0.5% yeast extract, 0.5% NaCl, and 0.2% glucose) or Luria Bertani supplemented with 3 µL of kanamycin and chloramphenicol were inoculated with 30 µL of a 3.0 mL culture of *E. coli* BL21(DE3)pLys containing the IPTG-inducible pET30a-*hcpE* expression plasmid that had been grown overnight at 37˚C in a shaking incubator. The cultures were transferred to 14˚C, 24˚C (room temperature), 30˚C, or 37˚C for 1 hr to equilibrate before being induced with 0.15mM IPTG. All cultures were incubated O/N, after which the cells were pelleted by centrifugation at 14 640 *g* for 5 minutes. The

supernatants were discarded and the cell pellets were re-suspended in ice cold buffer (50mM Tris pH 8, 2mM EDTA) containing 0.1% Triton X-100 and 0.1 g/L lysozyme. The samples were incubated at 30˚C for 30 min to lyse the cells. Once the cell suspension became viscous, 10mM $MgCl_2$ containing 10 mg/mL DNase was added and incubated at 30˚C for 30 min. The resulting lysate consisted of the total proteins; an aliquot was saved for analysis. The cell suspension was centrifuged at 14 640 *g* for 15 minutes to pellet the insoluble proteins. The supernatant containing the soluble proteins was removed and the pellet containing the insoluble protein fraction was re-suspended in buffer (50mM Tris pH 8, 2mM EDTA). HcpE expression levels in the soluble and insoluble protein fractions were analyzed following separation by SDS-PAGE and Western blotting with anti-histidine antibodies.

2.8 Isolation of chromosomal DNA using DNAzol

Bacterial strains were grown on BHI plates under microaerophilic conditions for 48 hrs. Cells from 1-2 plates of confluent growth were re-suspended in 1 mL 0.85% saline. Samples were centrifuged for 20 minutes at 2053 *g* to pellet the cells. The pellet was re-suspended in 1 mL of DNAzol reagent (Invitrogen) and incubated at room temperature for 60 min to allow for lysis of the cells. The lysate was centrifuged at 4880 *g* for 10 minutes, after which the supernatant was removed and transferred to a sterile eppendorf. To this, 500 µL cold 100% ethanol was added and mixed by inverting the tube 5-10 times. The mix was left on ice for 30-45 min to allow the DNA to precipitate. After incubation, the DNA was pelleted via centrifugation at 12 200 *g* for 10 min. The pellet was washed twice in 500 µL 95% ethanol. For this, 500 µL ethanol was added and the sample was spun for 2 min at 15 860 *g*. Following the second wash, the residual alcohol

was removed and the pellets were air dried at room temperature. Once dry, the pellets were re-suspended in 100 µL TE Buffer (10mM Tris-HCl pH 8.0, 1mM EDTA) containing 0.02 µg/µL RNaseA (BioShop). The tubes were left at 4˚C O/N to dissolve the DNA. The next day, the tubes were placed at 37˚C for 30 min to further dissolve the DNA. Chromosomal DNA preparations were stored at 4˚C.

2.9 Construction of the *H. pylori hcpE* mutant

Knockout mutagenesis was performed by Dr. Dinath Ratnayake, a former post-doctorial fellow in the Creuzenet Lab. Inverse PCR amplification of *hcpE* from pUC18-*hp0235* (clone 2D) was performed with the primers HP0235P4 and HP0235P5 (Table 2) using Expand Long-Range template polymerase (Roche) at an annealing temperature of 66°C. The kanamycin cassette was inverse amplified from the pHel3 vector using Aph3P1 and Aph3P2. The *hp0235* PCR product was ligated to the extracted kanamycin cassette from the shuttle vector pHel3 (57), using *Cla*I and *Bgl*II creating the plasmid *phcpE::kan*. The plasmid was transformed into *E. coli* DH5α cells with selection on ampicillin and kanamycin. The knockout *hcpE* mutant was generated by electroporation-mediated allelic exchange into *H. pylori* NCTC 11637 as described by McGee *et al.* (83). Briefly, *H. pylori* cells were re-suspended and washed three times in ice-cold 15% glycerol and 9% sucrose. The cells were re-suspended to a final OD_{600nm} of 2.5. 70 µL of the cells and 10 µL of approximately 1 µg DNA were gently mixed together and transferred to ice-cold 0.2 cm wide electroporation cuvettes (Bio-Rad). The cells were electroporated at 2.5 kV, 800Ω and 25 µF. After electroporation ice-cold BHI containing 5% FCS and 20mM glucose was added to the cells. The transformed bacteria were allowed to recover for two days on BHI plates containing no selection antibiotics and

were then plated onto BHI plates containing 4 μg/mL kanamycin. Transformants were analyzed for proper gene integration by PCR (see below). Clones were stored at -80˚C in 15% glycerol.

2.10 PCR screening of *hcpE::kan* knockout mutagenesis clones

Potential clones were screened using PCR amplification of genomic DNA. Genomic DNA was isolated using the InstaGene Matrix (BioRad) according to the manufacturer's instructions. In short, a small amount of bacteria was re-suspended in 1 mL autoclaved water. The suspension was centrifuged for 1 minute at 12 200 *g* and the supernatant removed. To the pellet, 200 μL of the InstaGene matrix was added and incubated at 56˚C for 30 minutes. Following incubation, the suspension was vortexed at high speed for 10 seconds and then placed in boiling water for 8 minutes. The suspension was vortexed a second time, for 10 seconds, and then centrifuged at 12 200 *g* for 2 minutes. 20 μL of the resulting supernatant was used per 50 μL PCR reaction. The PCR reactions were conducted on genomic DNA prepared from clones 2 and 3, on wild-type chromosomal DNA, prepared as previously described, as a negative control and on the pUC-*hcpE* and pUC-*hcpE::kan* plasmids as positive controls. PCR was done using Expand Long Template polymerase (Roche). The reactions were set-up as follows; 20 μL of InstaGene DNA, or 1 uL plasmid/ chromosomal DNA (1/10 dilution), 1 μL HP0235P1, 1 μL HP0235P2, 5 μL dNTPs (BioRad), 5 μL Buffer 1 (Roche), 0.5 μL Expand enzyme, 36.5 μL autoclaved water. All reactions were prepared using a master mix of the reagents. The PCR program consisted of an initial denaturation step at 93˚C for five minutes, followed by 25 cycles of denaturation at 93˚C for 30 seconds, annealing at 55 ˚C for 30 seconds, and elongation at 68 ˚C for two minutes, followed by a final

elongation at 68 ˚C for seven minutes. The PCR products were visualized following separation using a 0.7% agarose gel and imaging using the GelDoc (BioRad). To determine if the insertion was in the correct orientation, additional PCR reactions were conducted as described above on the positive clones and wild-type chromosomal DNA using the primer sets HP0235 P2/P10 and HP0235 P5/P10 employing the same reaction set-up and PCR conditions.

2.11 Production and screening of anti-HcpE antibody

2.11.1 His-tagged protein purification under denaturing conditions

HcpE was over-expressed from the pET30a construct in BL21(DE3)pLys cells via with induction by 0.15mM IPTG at 37˚C. As HcpE was found to be expressed mainly in an insoluble form, the protein was purified from inclusion bodies by metal chelation in the presence of 6M guanidine-HCl. The cell pellet was re-suspended in binding buffer (20mM Tris pH 8.3, 0.5M NaCl) in the presence of lysozyme and lysed by passage through the French press, as previously described. The insoluble proteins were pelleted by centrifugation at 12 000 *g* for 30 minutes at 4˚C. The pellet was re-suspended in binding buffer containing 6M guanidine-HCl. The solubilized proteins were recovered in the supernatant after centrifugation at 12 000 *g* for 20 minutes. The supernatant was ultra centrifuged at 100 000 *g* for 1 hr. HcpE-His was purified by nickel affinity chromatography as described above except that all buffers contained 6M guanidine-HCl. Eluted fractions were dialyzed O/N in 50mM ammonium bicarbonate before being analyzed by SDS-PAGE (15%). The concentration of purified HcpE was determined using the Bio-Rad protein quantification assay.

2.11.2 Antibody generation

The dialyzed pure HcpE sample purified from inclusion bodies was lyophilized, re-suspended in 1.7% saline and used to immunize rabbits after a 1:1 (vol/vol) dilution with complete or incomplete Freund's adjuvant (Sigma). Briefly, 300 μL purified protein (2 mg/mL) was mixed with 300 μL saline (1.7%), and added to 600 μL complete Freud's adjuvant yielding a total of 1.2 mL mix which was filter sterilized using a 0.2 μm pore filter. Prior to the first injection, pre-immune serum was obtained from each rabbit to test for any cross-reactive antibodies before the immunization process. For the first injection (day 1), New Zealand white rabbits were immunized with 1 mL, containing 500 μg purified-HcpE prepared as described above. For the subsequent injections, the rabbits were boosted with 150 μg of purified-HcpE. The inoculation sample was prepared by mixing 125 μL pure protein (2 mg/mL) with 475 μL saline (1.7%) and 600 μL Incomplete Freud's adjuvant. The mix was filter sterilized, and the rabbits were boosted with a 1 mL injection of the mix on days 14 and 28. Blood was collected prior to each injection. The final bleed and harvesting of the serum was performed on day 36, two weeks after the second boost. Animal care, including inoculations and general caretaking was performed at the Animal Care and Veterinary Services (ACVS) at the University of Western Ontario according to the approved protocol for raising antibodies from Dr. I. Welch (protocol #: 2007-103). Blood received from the rabbits was allowed to coagulate at room temperature for one hour, followed by incubation overnight at 4°C. The serum was separated from the plasma via centrifugation at 12 000 *g* for 10 minutes. All serum was stored at -20°C for testing.

2.11.3 Testing antibody specificity using slot blot

The specificity of the antibody was determined using slot Western blotting on total cell extracts from *E. coli* over-expressing HcpE-His. Briefly, the serum was diluted 1:500, 1:1000, 1:2500, 1:5000 and applied to nitrocellulose membrane. Buffer and pre-immune serum served as negative controls. The membrane was probed according to the standard Western Blotting protocol, and final detection was done with goat anti-rabbit IgG secondary antibody detected at 800 nm.

To further enhance the specificity of the antibody, the serum was absorbed against *E. coli* BL21(DE3)pLysS, for detection of HcpE in our *E. coli* system, and against the *hcp::kan* mutant to enhance detection in *H. pylori*. Cells were lysed by French pressing three times (8000 psi), as previously described, and cellular debris were removed by centrifugation at 12 000 *g*. Four nitrocellulose membranes, 5cm x 3cm were incubated in the cell supernatant for one hour. The membranes were then washed with TBS 3 times, for ten minutes each, blocked in 10% milk for one hour, and then washed in TBS 3 times. The anti-HcpE antibody was applied to each membrane and incubated for one hour while shaking gently. Following the incubation period, the antibody was recovered and applied to the next membrane. The same process was repeated for each membrane. The absorbed antibody was then re-tested for its specificity in each system via Western blotting as previously explained.

2.12 Analyzing the *H. pylori* secretome for detection of HcpE

Wild-type and *hcpE::kan H. pylori* strains were grown on BHI medium with background and selective antibiotics for 48 hrs. After 48 hrs, the cells were harvested in

brucella broth supplemented with 1% β-cyclodextrin (138) and the required antibiotics, and the OD_{600nm} was adjusted to 0.2 in a final volume of 30 mL. The cell suspensions were exposed to gentle agitation in the shaking incubator for 12, 16, or 20 hrs at 37˚C under microaerophilic conditions using sealed anaerobic jars and gas packs (CampyGen; Oxoid). At each time point, the cell suspensions were harvested and pelleted via centrifugation at 2057 *g* for 30 minutes at 4˚C. Aliquots of each culture were set aside for OD_{600nm} readings and quantification of cell lysis. The total cell pellets were re-suspended in 100 µL of 1X SDS-PAGE protein loading buffer. Proteins recovered in the supernatants were concentrated by Trichloroacetic acid (TCA) precipitation. For TCA precipitation, 10% ice-cold TCA was added to the eluate samples in a 1:1 (vol/vol) ratio and incubated on ice for 15 minutes. The samples were centrifuged at 16 000 *g* for 15 minutes at 4˚C, the supernatant was removed, and the precipitated proteins were washed in acetone to remove residual TCA. The samples were re-centrifuged for 5 minutes at 16 000 *g* and pellets were air dried at room temperature. The precipitated proteins were re-suspended in 200 µL 1X SDS-PAGE loading buffer. The secreted proteins were separated by SDS-PAGE (15%) and detected by Western blotting with the anti-HcpE primary antibody and goat anti-rabbit IgG secondary antibody detected at 800nm.

2.13 Phenol red urease activity assay for quantification of cell lysis

To compare the urease activity of the total cells, cell pellets, and cell supernatants, a 2 mL aliquot of both the wild-type and *hcpE::kan* liquid cultures were recovered. For comparison, OD_{600nm} of each culture after growth in liquid was set to be 0.2. The 2 mL aliquot was divided in two; 1 mL was set aside to determine the urease activity of the total cells and the other 1 mL was centrifuged at 2057 *g* for 15 min to pellet the cells. The

supernatant was recovered and the pellet was re-suspended in 1 mL of brucella broth. 30 µL of each sample was added to 200 µL of urease reagent (50mM sodium phosphate pH 7.5, 0.15M NaCl, 1M Urea, 0.001% phenol red). Urease activity was assayed by monitoring OD_{565nm} over time in a 96-well plate using the Microplate Reader (BioRad). The colour change of phenol red reagent from yellow to pink reflects the change of pH occurring upon the conversion of urea to ammonia and carbon dioxide by urease in a slightly buffered solution. All experiments were done in duplicate.

2.14 Affinity chromatography protein-protein interaction assay with soluble *H. pylori* cell extract

H. pylori cell pellets (representing 20 plates of confluent growth) were lysed in 20 mL of 1X binding buffer and French pressed, as previously explained, but in the absence of lysozyme. Cellular debris were removed by centrifugation at 12 000 *g* for 30 min at 4˚C and membranes were removed by ultra centrifugation at 100 000 *g* for 1 hr. The *H. pylori* cell lysate was added to the purified dialyzed protein samples of HcpE and TsaA, and incubated at room temperature for 1 hr on a nutator (Labnet). The purified proteins were added to the soluble *H. pylori* cell extract in a 1:1 volume ratio. After the 1 hr incubation, the cell extracts were purified using a second round of affinity chromatography. The volume of sample loaded onto the column was topped up to 15 mL via the addition of 1X binding buffer. The samples were loaded onto the nickel charged column and purified as previously described. Bound proteins were eluted in sixty 1 mL fractions. Fractions eluting before, or at the same time as the purified over-expressed proteins were thought to contain potential interacting partners. The proteins were separated by SDS-PAGE (15%) gel electrophoresis and detected by Coomassie blue

staining. Bands unique to each individual interaction assay, present in HcpE and not TsaA and vice-versa, were subjected to in-gel trypsinolysis. The peptides were analyzed by liquid chromatography mass spectrometry (MS) (Q-TOF2) at the Protein Identification Facility at the University of Western Ontario.

2.15 Affinity blotting of the immobilized substrate using soluble *H. pylori* cell extracts or enriched DsbG

Purified proteins (HcpE-His and His-TsaA) were separated by SDS-PAGE (15%) and transferred to Polyvinylidene Difluoride (PVDF) membranes (Roche). For confirmation of the identity of the over-expressed proteins their position on the membrane was determined via Western blotting with anti histidine-tag primary antibody (Amersham Biosciences) and the goat anti-mouse IgG secondary antibody (Molecular Probes). Following detection of the histidine tagged protein on the membrane, the membranes were reduced in size and pre-incubated O/N in 10% milk at 4°C. The membranes were washed 3 times in TBS buffer. A soluble cell extract of wild-type *H. pylori*, prepared as explained above, was added directly to the membrane and incubated at room temperature for 1 hr on the nutator. After incubation the membrane was washed 3 times in TBS buffer. Sections of the membrane containing the purified protein bands were isolated and subjected to in-gel trypsinolysis for MS, as described below.

The affinity blotting protocol was modified slightly to facilitate detection using Western blotting as opposed to MS. For this, total cell lysates of the *E. coli* over-expressed HcpE-His, DsbG-Flag, and pET30 vector were separated by SDS-PAGE (15%) and the gels were then transferred to nitrocellulose membrane (BioRad). After transfer was complete, the membranes were stained with Ponceau Red stain to visualize

the protein pattern, scanned and washed 3 times in TBS to remove all residual stain. The membranes were blocked O/N and at room temperature for 1 hr in 10% HS, to prevent non-specific binding, and washed 3 times in TBS. Membranes were spotted directly with either: (a) 1 mL buffer (20mM Tris pH 7.5, 0.5mM NaCl), (b) 1 mL enriched DsbG-Flag, or (c) 500 µL enriched DsbG-Flag containing 500 µL wild-type *H. pylori* cell lysate. Membranes were incubated for 2 hours at room temperature. The *H. pylori* cell lysate was prepared from 2 plates of wild-type *H. pylori* of confluent growth. For this, the bacteria were harvested in 1 mL of 0.85% saline and pelleted by centrifugation at 2057 *g* for 15 minutes. The pellet was re-suspended in 700 µL buffer (20mM Tris pH 7.5, 0.5mM NaCl) and the cells were lysed using glass beads (Sigma). Following the 2 hr incubation period, the membranes were washed 3 times in TBS and then blocked in 10% HS for 1 hr at room temperature and O/N at 4˚C. Western blotting was performed to detect the binding of DsbG-Flag to HcpE-His. Detection was carried out in two successive steps: first with the anti-Flag primary antibody (Sigma) and the goat anti-mouse secondary antibody that fluoresces at 700nm, and then with the anti-HcpE primary antibody and the rabbit anti-mouse secondary antibody that fluoresces at 800nm.

2.16 Protein in-gel trypsin digestion and preparation for mass spectrometry

Samples for protein identification by mass spectrometry were prepared according to the procedures outlined by the Mass Spectrometry Facility at the University of Western Ontario. Following SDS-PAGE, bands were excised from polyacrylamide gels with a clean scalpel, cut into $1mm^3$ cube pieces and stored in a clean silicon-treated eppendorf tubes at -20˚C. The gel pieces were washed in one volume of autoclaved-distilled water for 15 min, followed by one volume water/ acetonitrile (1:1) for 15 min.

All liquid was removed and the gel was incubated completely submerged in acetonitrile. When the gel pieces shrunk, the acetonitrile was removed and the gel was rehydrated in one volume 0.1M ammonium bicarbonate for 5 min. One volume of acetonitrile was added to the ammonium bicarbonate yielding 0.1M ammonium bicarbonate/ acetonitrile and incubated for 15 min. All liquid was removed and the gel was dried in the vacuum centrifuge (Eppendorf) for 30 min under the organic phase setting. The gel pieces were swelled in 0.1M ammonium bicarbonate containing 10mM DTT and incubated for 45 min at 56˚C to reduce the protein. The tubes were cooled to room temperature, excess liquid was removed and freshly prepared 0.1M ammonium bicarbonate containing 55mM iodoacetamide was added and incubated for 30 min at room temperature, in the dark. The iodoacetamide solution was removed and the gel was washed with ammonium bicarbonate and acetonitrile as previously explained. After washing and removal of all residual stain the gel was dried in the vacuum centrifuge. For enzymatic digestion, the gel was rehydrated in 50 µL digestion buffer (50mM ammonium bicarbonate, 5mM $CaCl_2$, 10 ng/µL trypsin) on ice for 45 min. The gel was centrifuged at high speed (12 000 *g*, 2 min) and the supernatant was removed. The gel was incubated in 20 µL buffer (minus trypsin) O/N at 37˚C. To extract the peptides from the gel, the gel pieces were incubated in 25mM ammonium bicarbonate for 15 min. The same volume of acetonitrile was added and incubated for 15 min. The sample was centrifuged at 14 640 *g* for 2 min, the supernatant was recovered and placed in a new tube. The extraction was repeated twice with 5% formic acid and acetonitrile (1:1). The supernatants were pooled, dried in the vacuum centrifuge and stored at -20˚C for submission to MS for LC-MS analysis.

2.17 Assessing beta-lactamase activity of HcpE

2.17.1 Beta-lactamase activity in *H. pylori*

Wild-type and *hcpE::kan* strains were grown for 48 hrs on standard BHI, or BHI with kanamycin selection (30 ug/mL) and transferred to liquid culture in a sterile 24-well plates with 12 wells/strains for 12 hrs, as previously described. The OD_{600nm} was recorded to ensure the bacteria had reached logarithmic phase. All cultures were normalized to an optical density of 0.4. The cultures were exposed to ampicillin (Biobasics) and carbenicillin (Biobasics) concentrations of 0.02, 0.07, 0.22, 0.66, 2 μg/mL, or no antibiotic for 12 or 24 hr, in duplicate. After the 12 or 24 hrs incubation period, bacterial density was determined as a measure of the OD_{600nm} of each well on a plate reader. To determine susceptibility to antibiotic treatment, each culture was serially diluted 5-fold, 6 times in a sterile 96-well plate and 10 μL drops were pipetted directly onto the surface of square BHI plates in duplicate. The drops were allowed to dry and the plates were inverted and incubated under microaerophilic conditions as previously described. Growth was monitored every 24-48 hrs. To check for strain identity, chromosomal DNA was extracted from both the wild-type and *hcpE::kan* strains that grew following antibiotic exposure using DNAzol (Invitrogen), as previously described. PCR amplification of the *hcpE* gene was conducted on both the chromosomal DNA preps using HP0235P1 and HP0235P2 (Table 2) using the reaction conditions that were previously optimized for screening the *hcpE* mutant (refer to section 2.9 for detailed methods). PCR products were visualized following electrophoresis on a 0.7% agarose gel.

2.17.2 Beta-lactamase activity in *E. coli*

To assess the intrinsic activity of HcpE in the *E. coli* over-expression system, three strains were used: (i) pET30a-*hcpE* containing the over-expressed HcpE-His

protein, (ii) pET30a-empty vector as a negative control, and (iii) pET23-*cj1427* as a positive control with constitutive ampicillin expression in the vector backbone. Protein expression was done in *E. coli* BL21(DE3)pLysS (Novagen). 3 mL O/N cultures were grown while shaking at 37˚C in LB media. The cultures were diluted 1/60 the next morning, split in two and allowed to grow for 4 more hours. Over-expression from the pET constructs was induced in half the cultures via addition of 0.1mM Isopropyl β-D-1-thiogalactopyranoside (IPTG). When the cultures reached an OD_{600nm} of 0.4, they were inoculated into a 100-well honeycomb plate (MTX Lab Systems) at two concentrations: OD_{600nm} of 0.4 and 0.2. β-lactam antibiotics, ampicillin (0.1 g/L), carbenicillin (0.1 g/L) or no antibiotic were added to both the induced and un-induced cultures and growth was monitored for 22 hrs at 37˚C using the automated bioscreen. The cultures were recovered and used to assess protein solubility, expression and secretion. A solubility assay was conducted as previously explained to confirm that HcpE was expressed and secreted under the conditions tested. To confirm that HcpE was secreted in the *E. coli* system, proteins recovered from culture supernatants were precipitated via TCA precipitation and the presence of HcpE was determined by Western blotting with anti-HcpE antibodies.

2.18 LPS extraction and analysis

LPS was extracted from the wild-type and *hcpE::kan* strains according to the solubilization protocol by Hitchcock and Brown (58). Cell pellets from each strain were washed in 0.85% saline and re-suspended in 100-200 µL lysis buffer (2% SDS, 4% β-mercaptoethanol, 10% glycerol, 1M Tris pH 6.8, and bromophenol blue). The samples were boiled for 30 minutes at 100°C. Proteinase K (BioShop) was added to a final concentration of 0.5 µg/mL and incubated for 1 hr at 60°C. The LPS was resolved by

18% SDS-PAGE containing 0.88mM NaCl in Tris-glycine buffer (0.025M Tris pH 8.8, 0.192M Glycine, 0.1% SDS). Gels were visualized by silver nitrate staining.

2.19 Silver nitrate staining of LPS preparations

LPS preparations were stained using the modified Ultra-Fast silver staining protocol by Fomsgaard *et al.*, (43) modified from the conventional silver staining method of Tsai and Frasch (134). All glassware used for staining was freshly washed to remove contaminants. Following separation by SDS-PAGE gel electrophoresis, LPS was oxidized in the gel with 0.7% periodic acid, 40% ethanol, 5% acetic acid for 20 minutes, at room temperature on the gel surfer. The oxidizing solution was removed using a vacuum filter and the gel was washed in distilled water 5 times, for 3 minutes. The gel was stained for ten minutes with freshly prepared staining solution (20% (w/v) $AgNO_3$, 0.002% (v/v) NaOH, 0.4% (v/v) NH_4OH). The stain was removed and the gel was washed with distilled water 5 times, for 3 minutes. The color was developed via reduction in water containing 0.00005% (w/v) citric acid and 0.00054% (v/v) formaldehyde. The reaction was stopped via addition of 10% acetic acid for 1 min followed by thorough washing with distilled water.

2.20 Preparation of inner membranes

Samples enriched in inner membrane proteins were prepared by sodium lauroyl-sarcosine treatment. Briefly, *H. pylori* cell pellets (4 plates of confluent growth) were re-suspended in 0.85% saline containing 150 μg/ml lysozyme. After incubation on ice for 10 min and lysis by French pressing three times (8 000 psi), cell debris was removed by centrifugation at 12 000 *g* for 30 minutes. The supernatant was recovered, and the membranes were separated from the soluble proteins in the supernatant by

ultracentrifugation at 100 000 *g* for 1 hr at 4°C. After centrifugation the supernatant was removed and stored at -20 °C. The pellet was re-suspended in 50mM Tris-HCl pH 7.5 containing 1% (w/v) N-lauroyl-sarcosine sodium salt (Sigma) and incubated at room temperature for 1 hr. The inner membranes were recovered following a second ultracentrifugation at 100 000 *g* for 1 hr at 4°C. The supernatant, containing inner membrane proteins was recovered and the pellet, enriched in outer membrane proteins was re-suspended in 50mM Tris-HCl pH 7.5. The soluble, inner membrane and outer membrane fractions were visualized following separation by SDS-PAGE (15%) and staining with Coomassie blue.

2.21 Enrichment of DsbG-Flag using anion exchange chromatography

DsbG was over-expressed from the pET30a construct in BL21(DE3)pLys cells via induction with 0.1mM IPTG at 37°C O/N. For purification 1 L of culture containing the over-expressed protein was used. Cells were harvested via centrifugation at 2057 *g* for 30 minutes and re-suspended in 30 mL of protein loading buffer (20mM Tris pH 7.5, 0.5mM NaCl). Lysozyme was added to the final concentration of 150 μg/mL and incubated on ice for ten minutes. Cells were lysed by passage through the French press four times (15, 000 psi) and the insoluble proteins were pelleted by centrifugation at 12 000 *g* for 30 minutes at 4°C. Membrane proteins were pelleted via ultracentrifugation (Beckman) at 100 000 *g* for 1 hr. The supernatant was filtered through a sterile 0.2 μm filter (PALL Life Sciences) and stored on ice until purification. The soluble protein extract was purified by anion exchange chromatography using the AKTA purification system with the 1.04 mL AcroSep™ Q Ceramic HyperD F column (PALL Life Sciences) according to the manufacturer's instructions. The column was washed with 5 CV of

protein loading buffer, followed by 5 CV of elution buffer (20mM Tris pH7.5, 1M NaCl). After washing, the column was equilibrated with 10 CV of protein loading buffer before the sample was loaded. The protein sample was injected with a 30 mL syringe using the super-loop and applied to the column. After loading the sample, the column was washed with 5 CV of protein loading buffer to wash all unbound proteins. Bound proteins were eluted using a gradient of elution buffer with increasing NaCl concentrations from 50mM to 0.5M. Fractions (1mL) were collected and analyzed via SDS-PAGE (12%) and Western blotting with anti-Flag primary, and goat-anti-mouse secondary antibodies. Fractions containing the pure protein were stored in glycerol (25% final concentration) at -20˚C. Following purification, the column was stripped with the addition of 10 CV of elution buffer and re-equilibrated with 5 CV of protein loading buffer. The column was stored in 20% (v/v) ethanol at 4˚C until further use.

2.22 Refolding assay to assess the enzymatic activity of DsbG in the presence of insoluble HcpE

HcpE-His was over-expressed in a 40 mL culture from the pET30a construct in BL21(DE3)pLys cells via induction with 0.1mM IPTG at 37˚C O/N. The cells were pelleted by centrifugation at 2057 *g* for 30 minutes at 4˚C. The pellet was re-suspended in 4 mL buffer (50mM Tris-HCl pH 7.5) and lysed by passage through the French press as previously described. After lysing the cells, the insoluble proteins were pelleted by centrifugation at 12 000 *g* for 30 minutes at 4˚C. The supernatant containing the soluble proteins was discarded and the pellet, containing insoluble proteins was re-suspended in 2 mL buffer (50mM Tris-HCl pH 7.5). Enriched DsbG-Flag, from above, was dialyzed overnight in 2 L 50mM Tris-HCl pH 7.5 to remove glycerol used for its storage at -20˚C.

The reactions were setup, in duplicate, as follows: each reaction tube received 40 µL of insoluble HcpE cell lysate, 27 µL of DsbG (undiluted, diluted 1:2, or 1:4), 3 µL protease inhibitor cocktail (PIC) and either 10 µL wild-type *H. pylori* cell lysate or 10 µL buffer. Reactions with no DsbG both in the presence and absence of the *H. pylori* cell lysate were set-up as negative controls. Wild-type *H. pylori* cell lysate was prepared as described in section 2.14 for affinity blotting. The reaction tubes were incubated at 37˚C for 1 or 2 hours. At each time point, the tubes were quickly removed and immediately placed on ice to stop the reaction. Once cooled, the tubes were centrifuged at 10 000 *g* for 10 min at 4˚C. 60 µL of the resulting supernatant, containing the solubilized proteins was carefully removed so as not to disturb the pellet. Solubilized HcpE in the supernatants was assessed by Western blotting with anti-HcpE antibodies.

2.23 Interaction assays with gastric adenocarcinoma (AGS) cells

Gastric adenocarcinoma (AGS) cells were cultured in tissue culture flasks containing F12K Medium (F12K; Gibco), supplemented with 10% heat inactivated Fetal bovine serum (FBS; Gibco), 100 µg/ml penicillin; 0.1 µg/ml streptomycin (Gibco), 5% MEM non-essential amino acids (Gibco) and incubated in a 90% humidity, 5% CO_2 incubator at 37˚C. For each experiment, AGS monolayers of 85% confluence were grown in tissue culture flasks until they reached 100% confluence. The concentration of cells per milliliter was calculated by counting the cells with a hemacytometer and 4 x 10^6 cells were plated in each well of a 24-well plate. The cells were incubated overnight to reach 100% confluence before being infected. Wild-type and *hcpE::kan H. pylori* strains were grown for 48 hours on BHI plates with background and selective antibiotics after which an inoculum with an OD_{600nm} of 0.3 was transferred to liquid culture in serum-free

brucella broth, supplemented with β-cyclodextrin for 12 hrs, as previously described. The bacterial cultures were centrifuged at 2057 *g* for 30 minutes at 4˚C to pellet the cells. The cell pellet, representing the total cells, was re-suspended in F12K media such that the AGS monolayers were infected with approximately 5 x 10^8 cfu of *H. pylori* resulting in a multiplicity of infection (MOI) 100 bacteria per AGS cell. The cell supernatants were diluted 1:3 with F12K media and used to infect the AGS monolayers. The AGS cells were infected for 5 or 10 hours. At each time point, the supernatants were recovered and centrifuged at 4880 *g* for 20 min to pellet any unattached bacteria. A portion of the supernatant was kept for cytokine analysis (stored at -20˚C), and the remainder (900 µL) was TCA precipitated, as previously described, for detection of HcpE via Western blotting with anti-HcpE antibodies. The attached cells were washed 3 times with sterile-PBS to remove all unbound bacteria. To recover bacteria that adhered to the AGS cells, monolayers were treated with 200 µL 0.08% saponin (Sigma) for 5 min to lyse the AGS cells thereby releasing bound bacteria into the supernatants. The supernatants were recovered and centrifuged for 20 min at 4880 *g*. Pellets were re-suspended in 100 µL sterile-BHI media, diluted 1:5 and serially diluted 5-fold, 7 times. 10 µL of the last 6 dilutions were dispensed onto antibiotic free plates. Growth was monitored every 24 hrs for 2 weeks and used to determine percent adherence.

To determine if growing in tissue culture media, under non-microaerophilic conditions imparted a growth defect on wild-type and *hcpE::kan* strains, bacterial growth was monitored at 5 and 10 hrs post-inoculation. Both strains were grown in liquid culture as described above. Cell pellets were re-suspended in the appropriate volume of media to achieve the same MOI equivalent as above, but in the absence of AGS cells. 100 µL of

the bacterial suspensions were inoculated into 900 µL of media in a sterile 24-well plate, in triplicate. At each time point, the bacterial cultures were recovered, and centrifuged at 4880 *g* for 20 minutes. The pellets were re-suspended in 100 µL sterile-BHI media, serially diluted and spot plated as explained above. Bacterial growth was monitored every 24-48 hrs, and the viability of each strain was determined.

2.24 Quantification of IL-8 production by ELISA

The IL-8 ELISA was carried out using the READY-SET-GO! Human Interleukin-8 kit (eBioscience) according from the manufacturers' recommendations. A 96-well plate was coated with 100 µL/well of capture antibody (purified anti-human IL-8) in Coating buffer. To prepare the coating buffer, 1 packet of ELISA Coating Buffer Power (provided in kit) was added to one liter of distilled water and mixed until dissolved. Before use, the buffer was filter sterilized using a 0.2 µm pore size filter. For one plate, 48 µL of capture antibody was added to 12 mL coating buffer. The plate was covered and incubated O/N at 4˚C. The next morning, the wells were aspirated and washed 5 times with >250 µL Wash Buffer (1X PBS, 0.05% Tween-20), allowing the buffer to soak for one minute between washes. The plate was blotted dry on absorbent paper after the final wash to remove residual buffer. To block the plate, Assay Diluent (provided in kit) was diluted 1 in 5, to make a 1X solution, and 100 µL were added to each well and incubated for 1 hr at room temperature. After incubation, the plate was aspirated and washed 5 times, as before. To generate a standard curve, the standard recombinant human IL-8 (provided in kit) was diluted 2-fold into 1X assay diluent. The stock solution, 500 pg/mL, was prepared by adding 5 µL of the standard to 10 mL of assay diluent. The stock was then diluted 6 times yielding solutions of 250, 125, 63, 32.5, 15, 7 and 0 pg/mL. The standard and

experimental samples were added to the plate, 100 µL/well in triplicate. The plate was sealed and incubated at room temperature for 2 hr (or O/N at 4˚C). The wells were aspirated and washed 5 times with wash buffer as previously explained. Detection antibody diluted in 1X assay diluent was added, 100 µL/well and incubated at room temperature for 1 hr. The detection antibody (Biotin-conjugated anti-human IL-8, polyclonal) was prepared by adding 48 µL of antibody solution to 12 mL 1X assay diluent. The plate was washed 5 times and Avidin-HRP* diluted in 1X assay diluent was added, 100 µL/well and incubated as room temperature for 30 minutes. The Avidin-HRP enzyme was prepared by adding 48 µL of the enzyme solution to 12 mL assay diluent. The plate was washed as above, allowing the wells to soak in wash buffer for 1 to 2 minutes prior to aspiration. This was repeated for seven washes. After thorough washing and blotting the plate dry, 100 µL Substrate solution (1X tetramethylbenzidine; TMB) was added to each well and incubated at room temperature for 15 minutes. To end the reaction, 50 µL/well Stop solution (1M H_2SO_4) was added. The plate was read within 30 minutes of adding the stop solution using the plate reader (PerkinElmer VICTOR 1420-40 Multilabel Counter) at the Proteomics Facility at the University of Western Ontario at 450 and 570 nm. To analyze the data, the 570 nm readings (background) are subtracted from the 450 nm readings.

CHAPTER 3: RESULTS

3.1 Molecular tools developed to study HcpE

To facilitate the study of HcpE, a number of molecular tools had to be developed. This included generating recombinant proteins for over-expression and purification, developing an *H. pylori hcpE* knockout strain to use as a negative control, producing a polyclonal antibody to detect the HcpE protein and many other tools that will be discussed below.

3.1.1 *hcpE::kan* knockout mutagenesis

To investigate the function of HcpE, the *hcpE* gene was knocked out in our laboratory strain, NCTC 11637. The *hcpE* mutant was constructed by Dr. Dinath Ratnayake by disrupting the chromosomal copy of the *hcpE* gene with a kanamycin resistance cassette. The cassette was placed in the same transcriptional orientation as *hcpE* so as to reduce the risk of polarity effects of knocking out the gene (Figure 9A). Clones were screened for the presence of the *hcpE*/kan construct by PCR amplification with the primers HP0235P1 and HP0235P2 (Table 2) that were used to generate the knockout construct. PCR amplification of a 2186 bp band in the *hcpE* mutant indicated that the kan cassette was integrated in the genome (Figure 9B), and the absence of a band at 1211bp indicated that the wild-type copy of the gene was eliminated. To confirm that the insert was in the proper location and correct orientation, and to ensure that when generating the knockout the neighbouring genes were not affected, PCRs were conducted using the primers P2/P10 and P2/P5. For the PCR with HP0235 P2/P10 the presence of a 2607 bp band in the mutant confirmed that the location and orientation were correct (Figure 9C). Likewise, for the PCR done with HP0235 P5/P10, a band of 797 bp in both

Figure 9: PCR screening of knockout mutagenesis clones. To facilitate the study of HcpE in wild-type *H. pylori*, an *hcpE* knockout mutant was generated using a kanamycin insertion cassette to disrupt the chromosomal copy of the *hcpE* gene. **Panel A:** Graphic representation of the HP0235 coding region in wild-type and mutant *H. pylori* showing all primers used in the PCR screening and the expected PCR fragment sizes. **Panel B:** PCR screening with HP0235 P1/P2 indicate that the *hcpE* gene was effectively knocked out in clone 3. Amplification of *hcpE* from wild-type chromosomal DNA, or the pUC-HP0235 plasmid results in a 1211 bp product; whereas clone 3, with the kanamycin insertion cassette, yields a larger fragment at its predicted size of 2186 bp. The absence of a band at 1211 bp in the mutant indicates that the wild-type copy of the gene was removed. **Panel C:** Primers HP0235 P2/P10 were used to ensure the insertion was integrated in the correct orientation and location. A product of 1632 bp in the wild-type (Lane 2) and 2607 bp in the knockout (Lane 3), established that the kanamycin cassette inserted as desired, in the correct location and orientation. PCR with HP0235 P5/P10, yielded the same size fragment in the wild-type (Lane 4) and knockout (Lane 5), indicating that the upstream neighbouring gene, HP0236, had not been disrupted.

A-

Wild-type

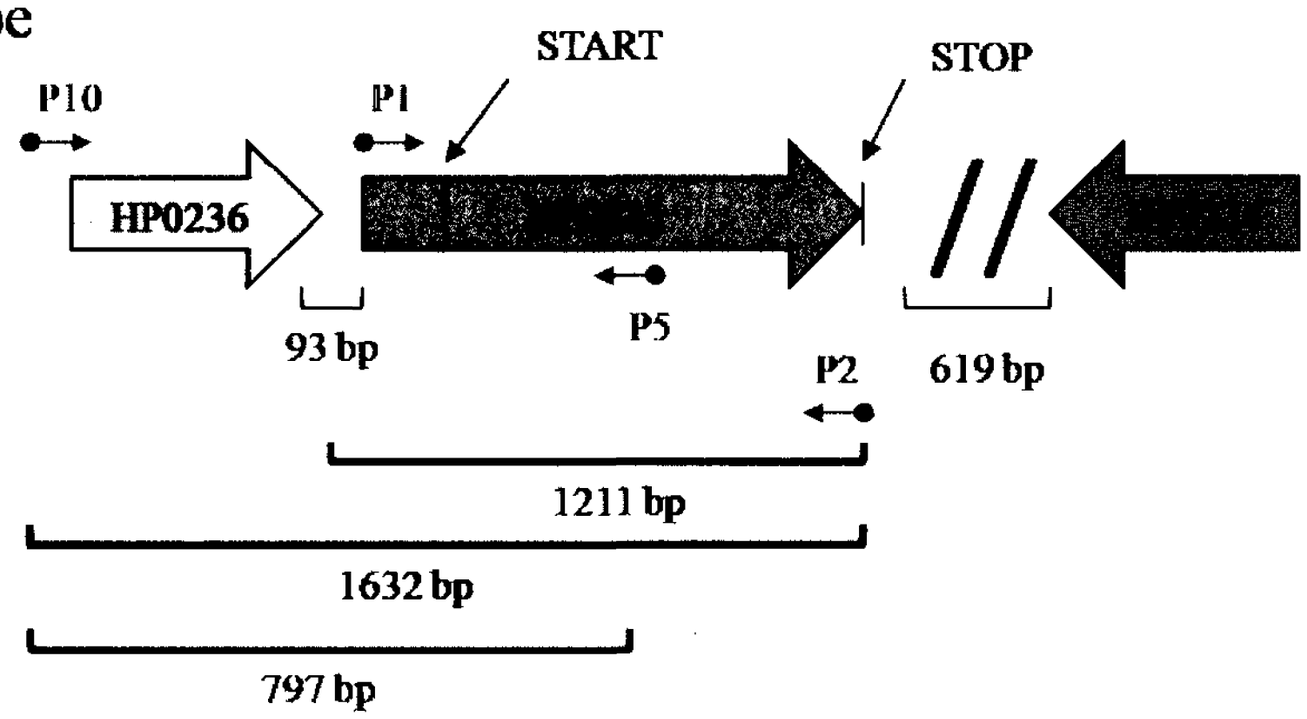

hcpE::kan

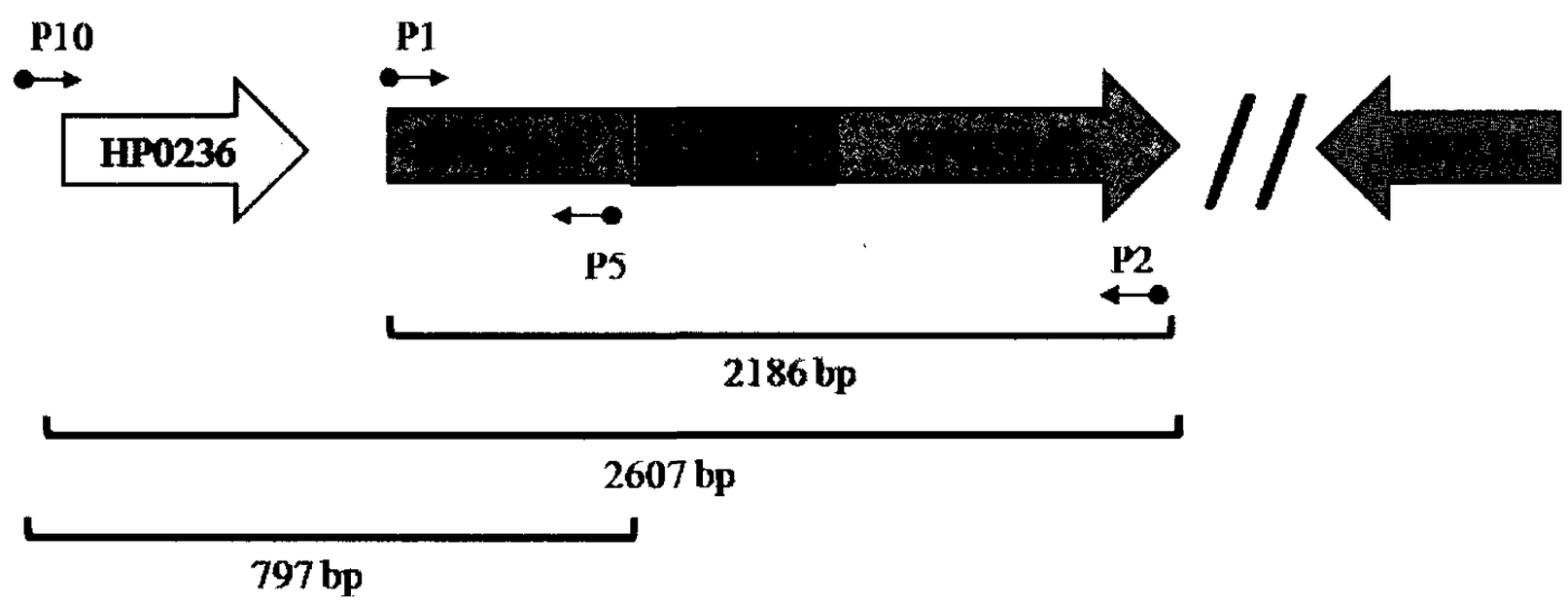

B-

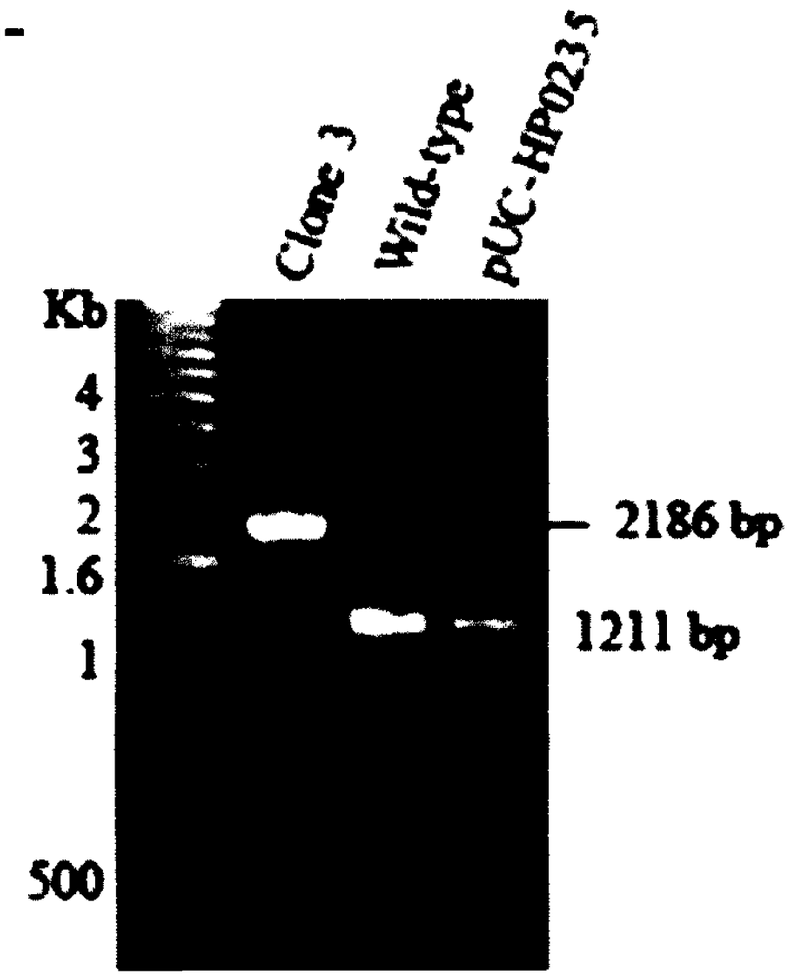

C-

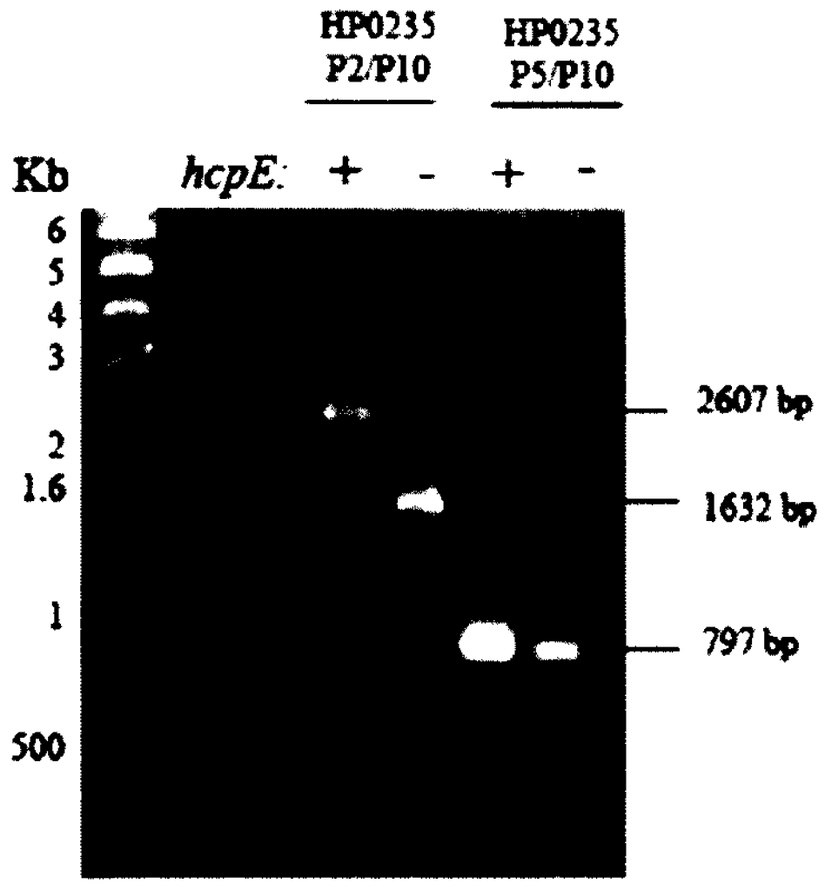

the wild-type and mutant (Figure 9C) established that the mutant had been generated properly, and that its neighbour HP0236 was still intact. No coding region is found in the 619 bp downstream of HcpE and the next gene (HP0234) is found in the reverse direction from HcpE. Therefore, this gene is not anticipated to be affected by the mutagenesis process and no further PCR was performed.

3.1.2 Wild-type and *hcpE::kan* growth is sustained in liquid for up to 20 hrs

H. pylori is a microaerophilic organism that is difficult to grow. Different methods for the isolation and subculture of the bacterium on different solid media have been established, but cultivation of the organism in serum-free broth, which is necessary for secretion experiments, has remained a problem. Growth in liquid culture was previously optimized by the Creuzenet lab for wild-type *H. pylori,* using broth consisting of brucella broth supplemented with 1% β-cyclodextrin. Using this growth media, gentle shaking, and microaerophilic conditions provided by sealed jars and gas packs, the lab strain NCTC 11637 was able to grow in broth.

To determine whether the loss of the *hcpE* gene conferred a growth defect in liquid culture, growth was monitored over a 20 hour time period. For this, wild-type and *hcpE::kan* strains were inoculated at the same starting optical density (OD_{600nm}) and grown for 12, 16, or 20 hrs. At each time point the cultures were harvested and growth was recorded as a function of the OD_{600nm} reading. Comparing the growth rates of the wild-type and mutant strain, it is evident that loss of the *hcpE* gene did not confer a growth defect in liquid media (Figure 10).

Figure 10: Culturing in liquid media does not impose a growth defect on the *hcpE::kan* mutant compared to wild-type. Similar growth is observed for wild-type (blue) and *hcpE::kan* (purple) *H. pylori* grown in liquid media for 12, 16 or 20 hrs. Liquid media consisted of serum-free brucella broth supplemented with 1% β-cyclodextrin. Growth is plotted as function of the normalized OD_{600nm} at each time point. Normalized OD_{600nm} was calculated by subtracting the OD_{600nm} of media alone. All readings were collected in triplicate.

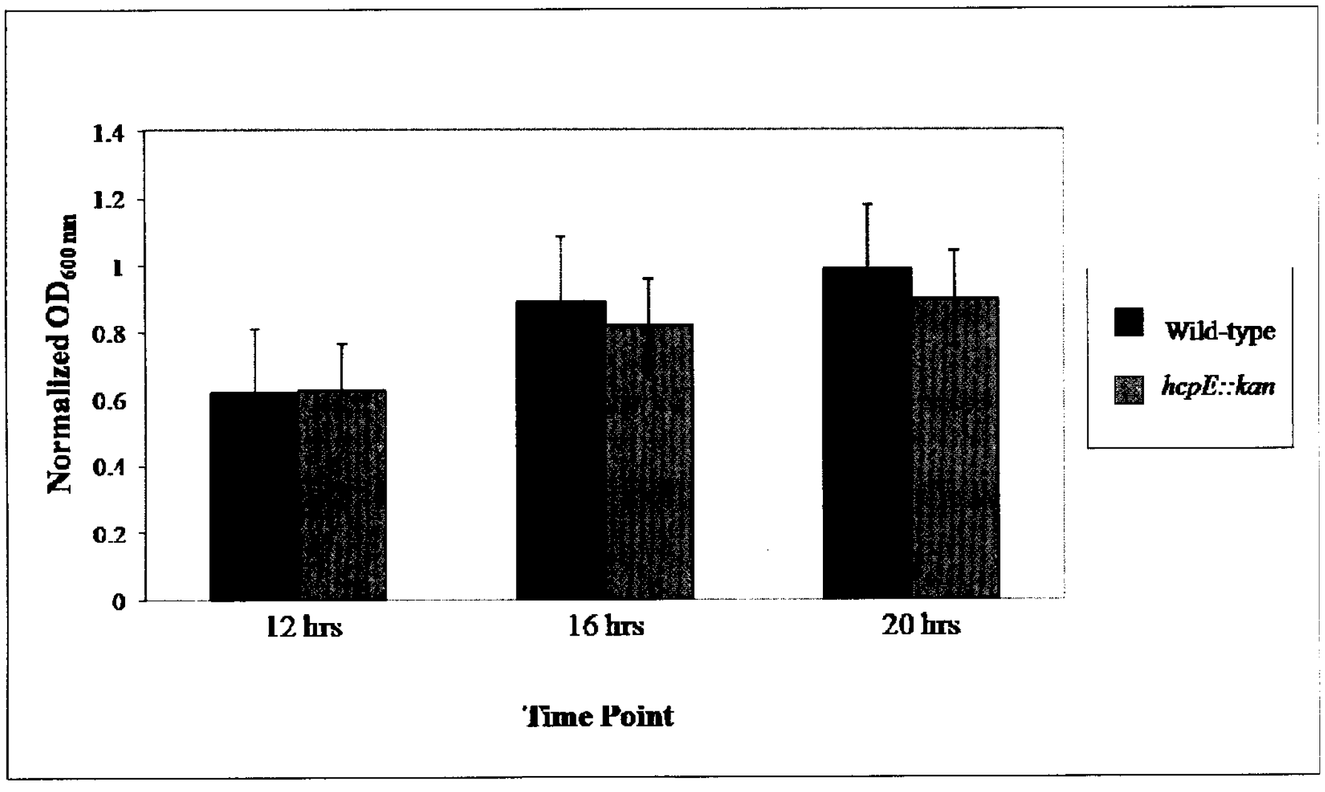
1.4
1.2
1
0.8
0.6
0.4
0.2
0
Normalized OD600 nm
12 hrs
16 hrs
20 hrs
Time Point
Wild-type
hcpE::kan

3.1.3 Comparison of the inner and outer membrane protein profiles of the wild-type and *hcpE* mutant

The protein profile of the inner and outer membranes of our wild-type and mutant strains were compared to determine if the loss of the *hcpE* gene had an impact on the expression of cell surface components. The inner and outer membranes were prepared from wild-type and *hcpE* mutant pellets by lauroyl-sarcosine extraction of total membranes. These fractions, as well as the total cell lysates were analyzed by SDS-PAGE and the proteins were subsequently detected by Coomassie staining. The protein profiles of both strains appeared very similar (Figure 11) indicating that disruption of *hcpE* did not have general pleiotropic effects on the production and localization of other proteins. The only difference noted was one prominent protein migrating to approximately 45 kDa (arrow) present in the outer membrane fraction of the *hcpE* mutant strain that was absent in our wild-type strain. A band corresponding to HcpE was not observed in our wild-type strain by Coomassie staining alone, suggesting that within cells the protein was present at low levels. This is consistent with the fact that HcpE is anticipated to be secreted.

3.1.4 Flagellin production by *hcpE::kan* is comparable to wild-type levels

To complete the characterization of phenotypes directly associated with the loss of the *hcpE* gene, the production and expression of the flagellum was assessed. The flagellum in an essential bacterial virulence factor whose production is often affected by pleiotropic effects that affect membrane stability. To determine whether knocking out *hcpE* had an effect on the bacterial flagella, flagellin production was assessed by Western blotting. Bacterial pellets from wild-type and mutant strains were resolved by

Figure 11: Inner and outer membrane protein profiles of wild-type and *hcpE::kan* extracted using lauroyl-sarcosine. The membrane proteins of wild-type and *hcpE* mutant bacteria were extracted from total cell pellets by ultra centrifugation, and the inner and outer membrane proteins were separated using differential solubilization with lauroyl-sarcosine. The total cell lysates (before ultracentrifugation), inner and outer membrane proteins of each strain were resolved by SDS-PAGE and Coomassie staining. Both strains show a relatively similar protein distribution, with the exception of one prominent protein (arrow) present in the *hcpE::kan* strain that is absent in the wild-type. IM; inner membrane, OM: outer membrane.

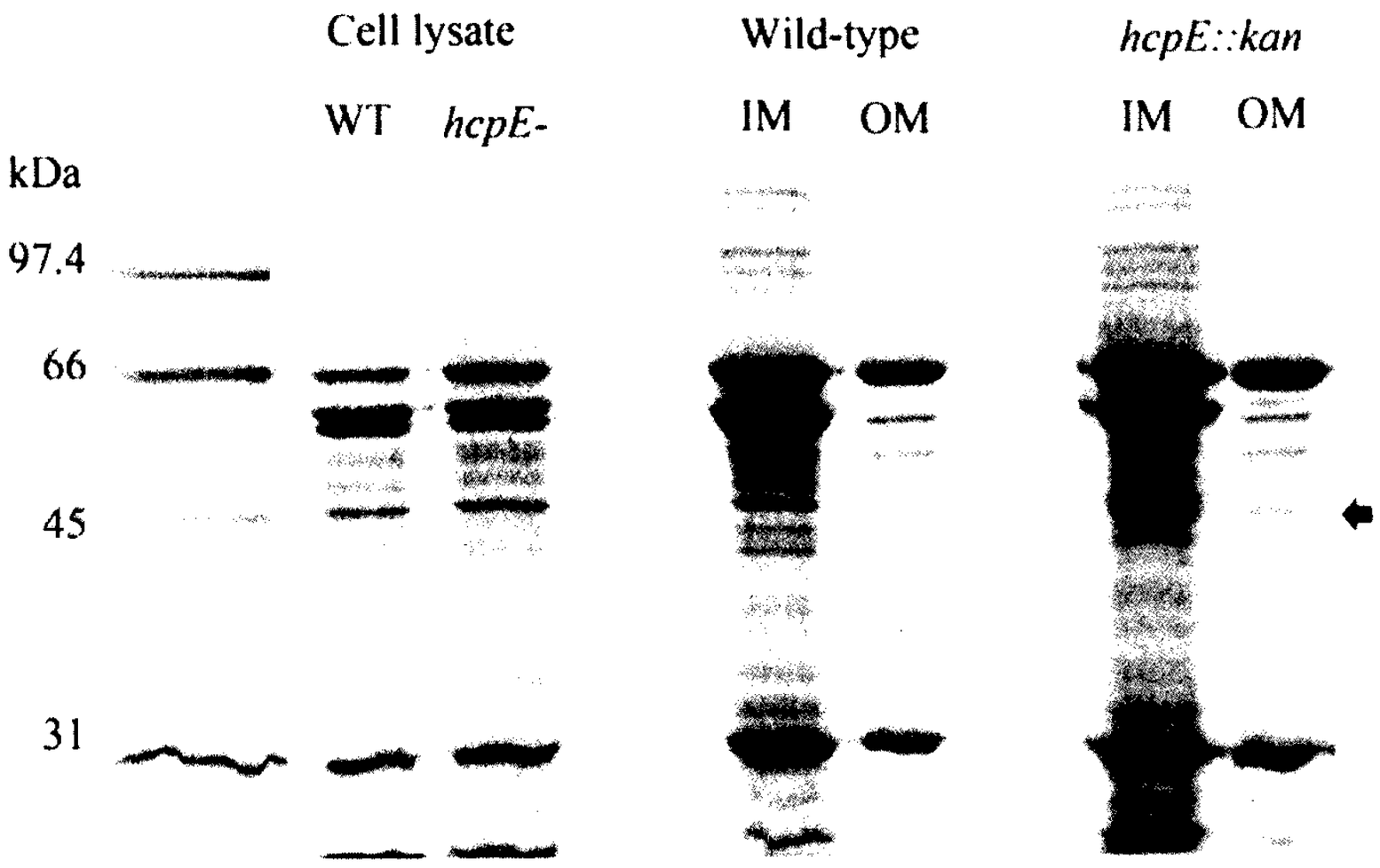
Cell lysate
WT
hcpE-
Wild-type
IM
OM
hcpE::kan
IM
OM
kDa
97.4
66
45
31

SDS-PAGE and immunoblotted. Flagellin production was evaluated using the polyclonal rabbit anti-flagellin-A antibody, which was made and characterized by a previous member of the Creuzenet lab. Similar levels of flagellins were present in the wild-type and *hcpE::kan* samples (Figure 12) indicating that disruption of the *hcpE* gene does not affect the production of mature flagellin subunits by the bacterium.

The analysis of the *hcpE::kan* mutant with regards to growth rate, the production and localization of proteins and production of an essential virulence factor demonstrate that disruption of *hcpE* had no pleiotropic effects.

3.1.5 Histidine-tagged over-expressed TsaA can be purified from *E. coli* by nickel-chromatography

For the purposes of these studies, TsaA will serve as a negative control in all experiments related to the over-expression, purification and interactions with HcpE-His. TsaA (AphC, HP1563) is a cytoplasmic alkyl hydroperoxide reductase that has been shown to confer resistance to oxidative stress (12). TsaA was over-expressed in the *E. coli* pET-23 plasmid with an N-terminal histidine tag by A. Merkx-Jacques. Following induction of protein expression and preparation of the total cell extracts from the *E. coli* over-expression strain, His-tagged TsaA was purified using nickel chelation chromatography. After charging the column with nickel, the total cell extracts of the over-expressed protein were loaded onto the column. Proteins that bound non-specifically were removed through gentle washing. The histidine-tagged protein was eluted off the column by applying a gradient with increasing concentrations of imidazole. A small peak

Figure 12: Flagellin production by wild-type and *hcpE* mutant. Flagellin production was assessed by Western blotting total cell pellets of wild-type and *hcpE::kan H. pylori* with the anti-flagellin-A antibody. Cell pellets were analyzed in their concentrated form, diluted 1:5, and diluted 1:25 (as depicted by the gradient). Wild-type and *hcpE::kan H. pylori* strains show similar levels of flagellin production at all dilutions tested. Semi-pure flagellins were included as a positive control. PR; Ponceau Red (loading control), WB; Western Blot.

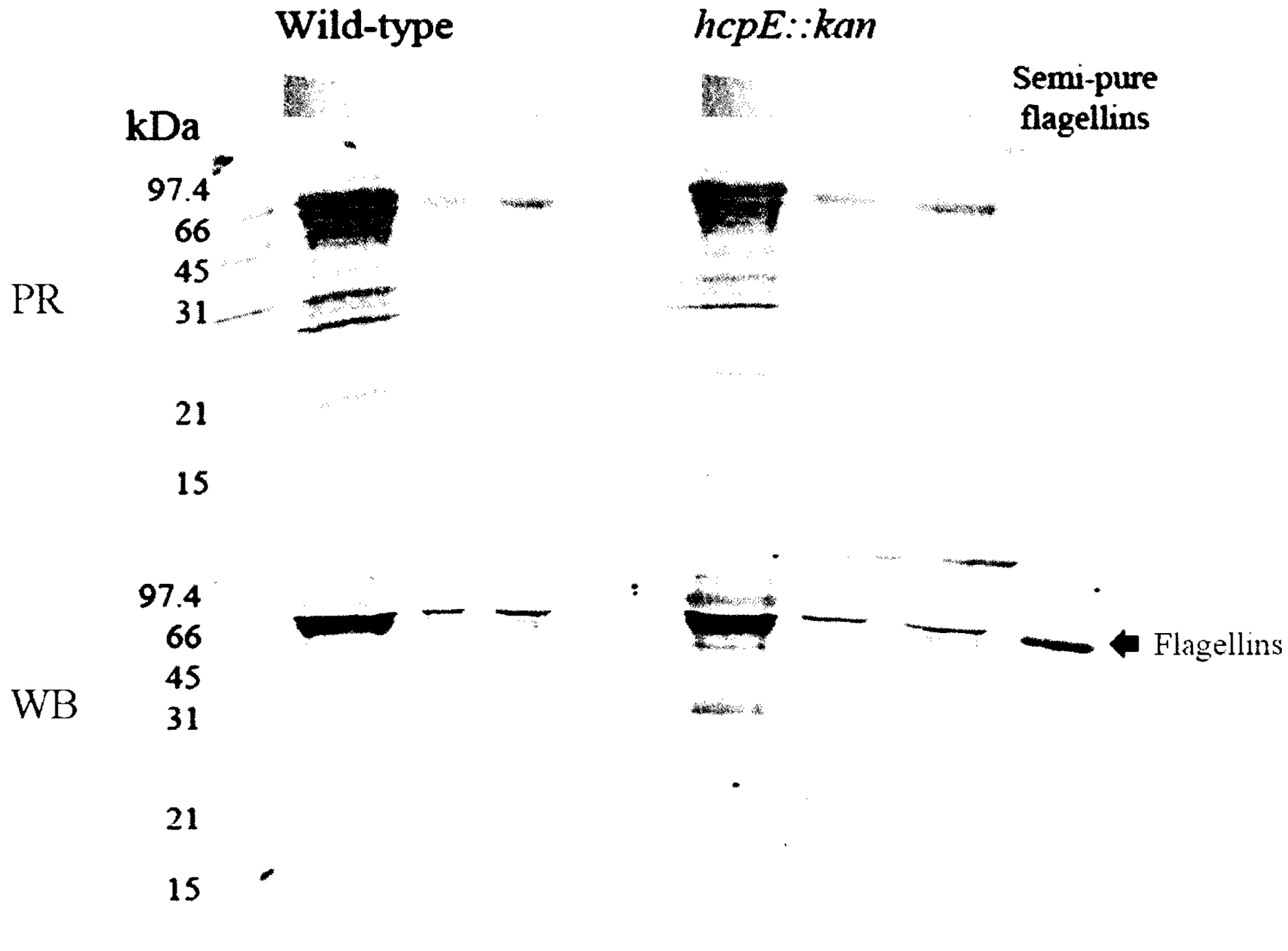
Wild-type
hcpE::kan
Semi-pure flagellins
kDa
97.4
66
45
31
21
15
PR
WB
Flagellins

was visible on the chromatogram (Figure 13A, blue box). Fractions within this peak were analyzed by SDS-PAGE and Coomassie blue staining. Monomeric TsaA was present in fractions A5 through B2, at its migratory size of 26 kDa (Figure 13B). TsaA displays an anomalous migration, as its predicted molecular weight is 22 kDa, and it consistently migrates to ~26 kDa (12). Dimeric TsaA was recovered from fractions B11 to C8. An unidentified *E. coli* protein co-eluted with both monomeric and dimeric TsaA. Given that TsaA served as a negative control in these studies, the contaminating species was not of concern. The identity of the purified TsaA protein was confirmed following Western blotting with anti-histidine antibodies (Figure 13C).

3.1. 6 *E. coli* over-expressed HcpE is insoluble

Pure HcpE was needed to identify its *H. pylori* interacting partner, as well as to generate specific anti-HcpE antibodies to use as a tool to aid in detection of HcpE for future secretion experiments. The C-terminally histidine-tagged HcpE was cloned into the pET30 vector by J. Chahal and was further expressed in *E. coli* BL21(DE3)pLys cells, with induction with IPTG.

To successfully purify HcpE, the conditions favoring its expression in a soluble form had to be determined. Cultures were grown in LB or defined media (Media II, see methods 2.7 for composition) at 14˚C, 24˚C, 30˚C, and 37˚C and induced with IPTG. Cells were lysed with the addition of lysozyme and Triton X-100, and the soluble and insoluble protein fractions were separated by centrifugation. Both the soluble proteins, contained in the supernatant, and the insoluble proteins, present in the pellet, were analyzed by Western blotting with the anti-histidine antibody. HcpE was insoluble under

Figure 13: Purification of TsaA by nickel chelation chromatography. For the purposes of these studies TsaA served as a negative control for all work concerning over-expression of HcpE-His in the *E. coli*-pET system. **Panel A:** TsaA was over-expressed in *E. coli* with an N-terminal histidine tag and purified via nickel chromatography by FPLC. Bound proteins were eluted via application of an imidazole gradient from 50mM to 1M. Protein detection was carried out at 280 nm. **Panel B:** Elution fractions within the protein peak (blue box) were resolved by SDS-PAGE (12%); TsaA was identified in fractions A5 through B2 (marked with asterix) in its monomeric form migrating to 26 kDa. Dimeric TsaA was identified in abundance in fractions B11 through C8 (Lanes 4-10) at its predicted dimeric size, of approximately 44 kDa. An unidentified *E. coli* protein eluted with TsaA both in its monomeric and dimeric forms. **Panel C:** Western blotting with anti-histidine antibodies confirmed the identity of the purified histidine-tagged TsaA. For each panel: PR; Ponceau Red (loading control), WB; Western Blot.

A-

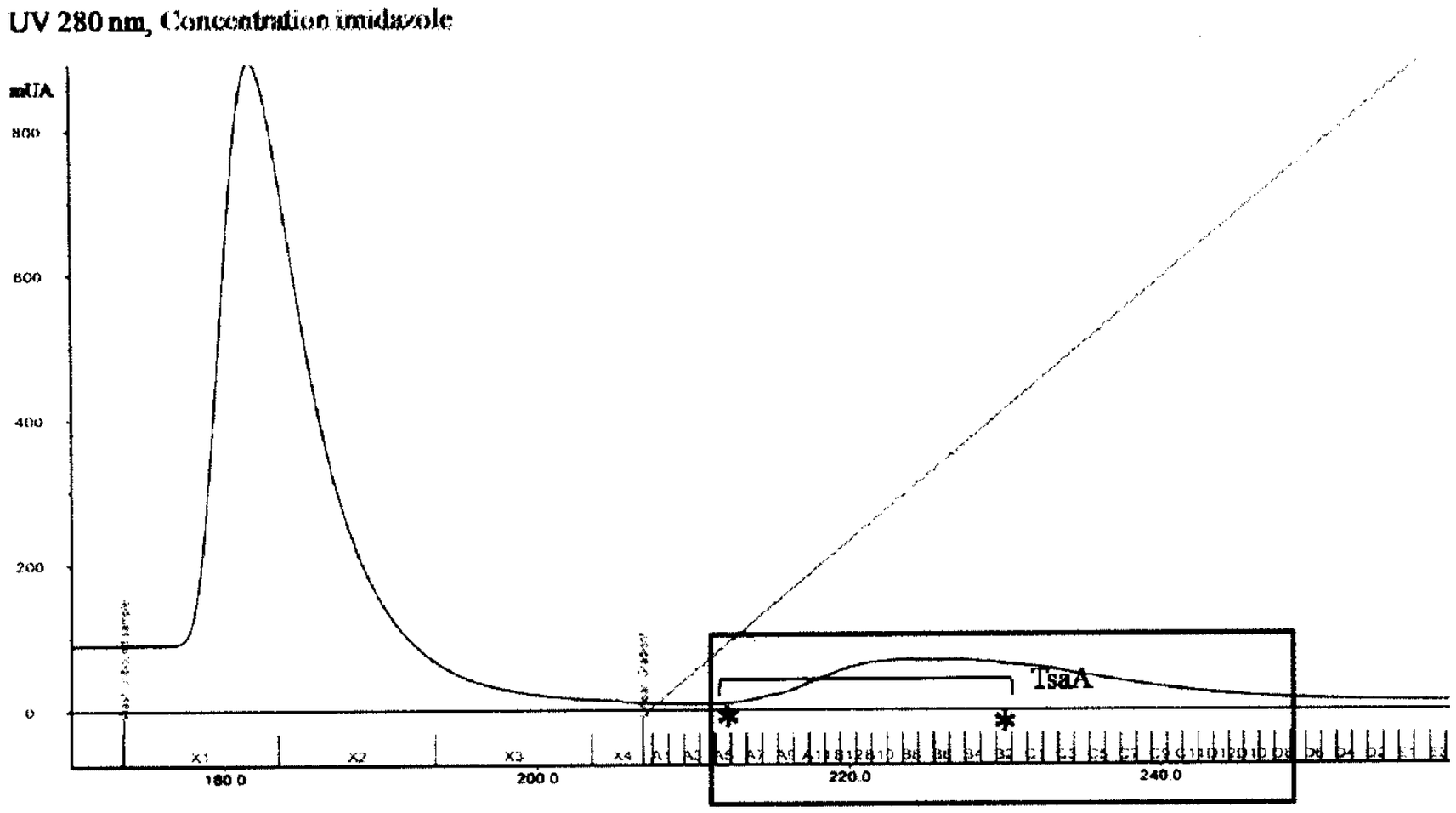
UV 280 nm, Concentration imidazole
mUA
800
600
400
200
0
X1
X2
X3
X4
180.0
200.0
220.0
240.0
TsaA

B-

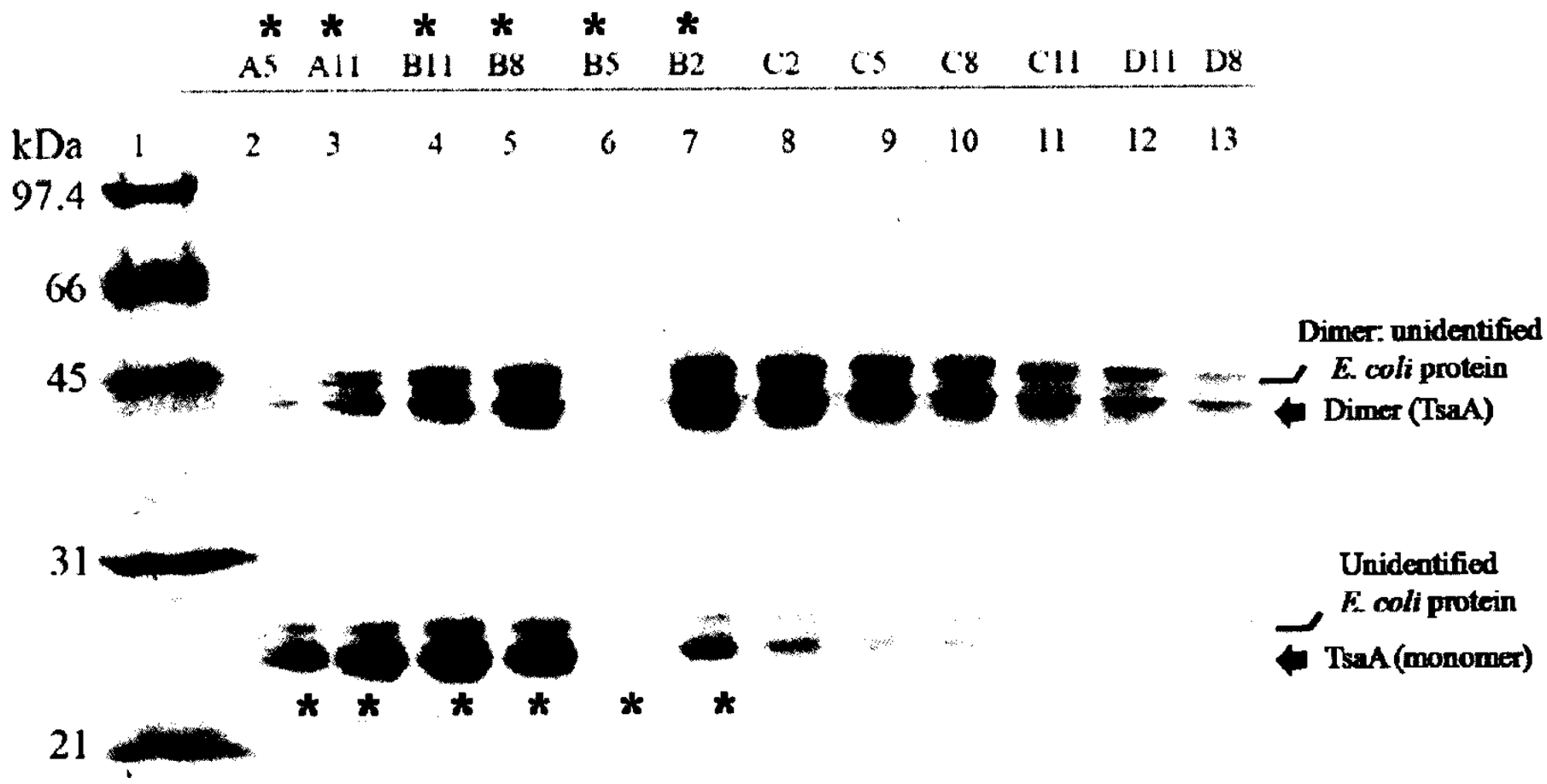
A5 A11 B11 B8 B5 B2 C2 C5 C8 C11 D11 D8
kDa 1 2 3 4 5 6 7 8 9 10 11 12 13
97.4
66
45
31
21
Dimer: unidentified
E. coli protein
Dimer (TsaA)
Unidentified
E. coli protein
TsaA (monomer)

C-

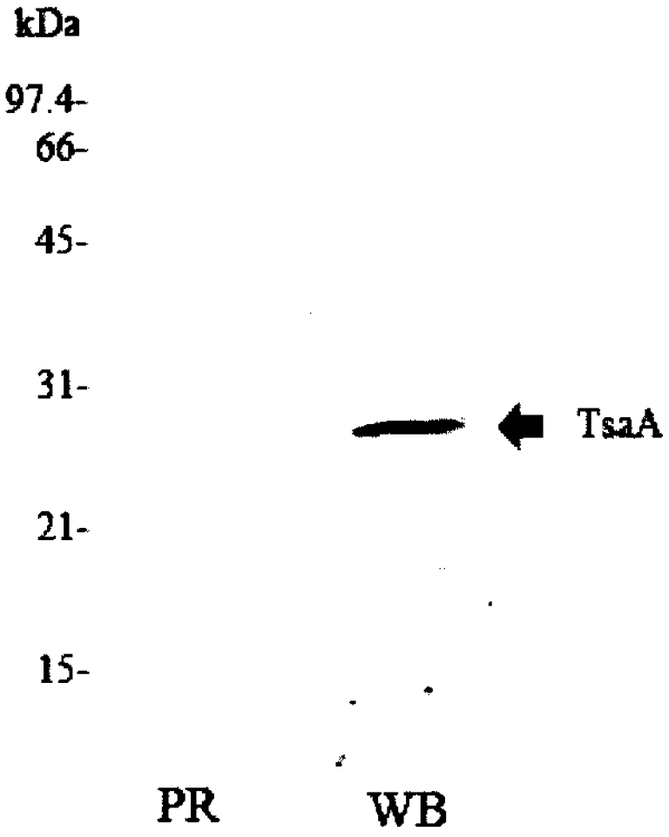
kDa
97.4-
66-
45-
31-
21-
15-
TsaA
PR
WB

Figure 14: Small scale solubility assay to assess solubility of HcpE-His. Solubility of HcpE was assessed under different growth conditions to identify the optimal conditions for over-expression of a soluble protein. Total cells pellets were chemically lysed via incubation in EDTA/Triton X-100 and separated into the soluble and insoluble protein fractions by centrifugation. Soluble and insoluble fractions of the *E. coli* over-expressed, histidine-tagged HcpE were resolved by SDS-PAGE and visualized by Western blotting with anti-histidine antibodies. **Panel A:** Solubility of HcpE-His in Media II and LB at 30˚C, 37˚C and 24˚C (room temperature). **Panel B:** Solubility of HcpE-His at lower temperatures, 14˚C and 24˚C, in Media II and LB. For each panel: PR; Ponceau Red (loading control), WB; Western Blot, S; soluble fraction, P; insoluble fraction. Under all conditions tested HcpE was detected in the insoluble fraction. A 10 kDa C-terminally truncated form of HcpE (arrow) displayed strong reactivity to the anti-histidine antibody, indicating degradation of HcpE. For all future over-expression studies expression was conducted in LB at room temperature (24˚C).

A-

PR

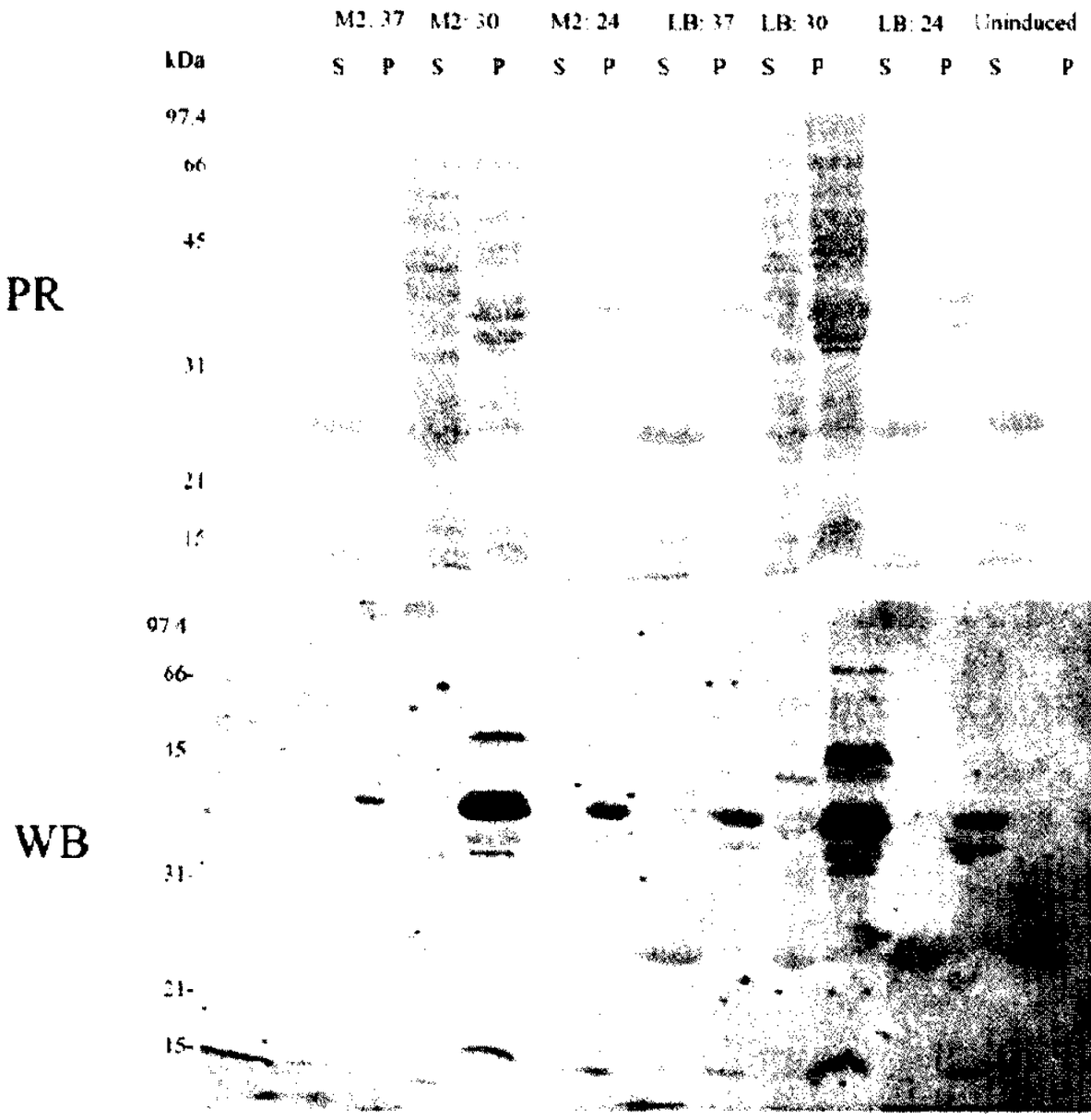

WB

Insoluble HcpE (full length)

Insoluble C-terminal truncated HcpE

B-

PR

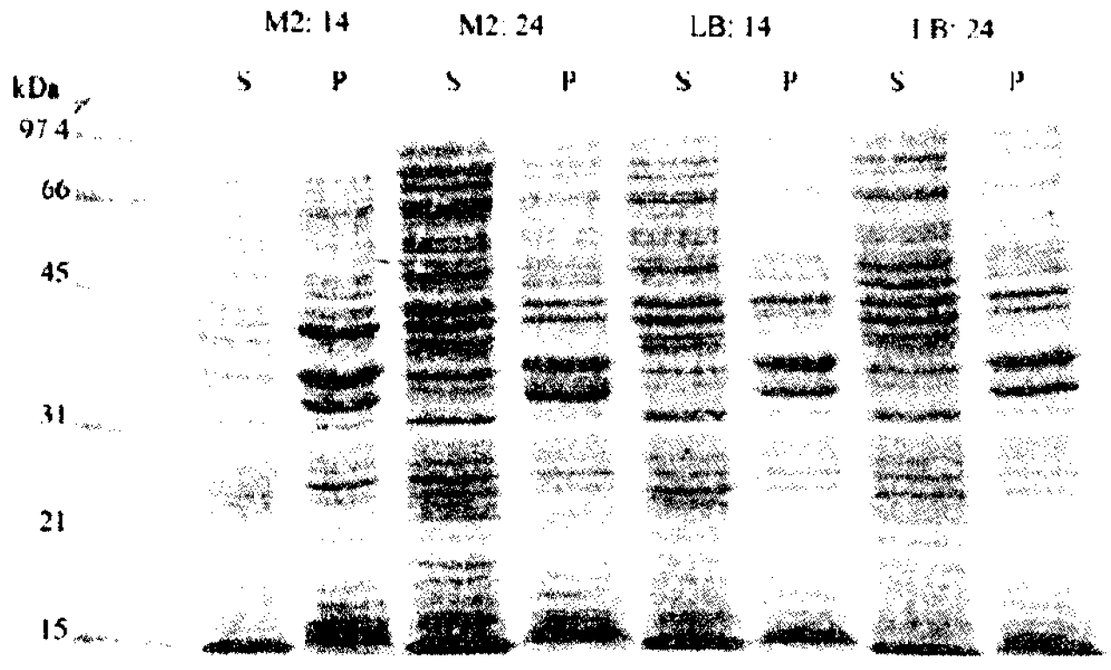

WB

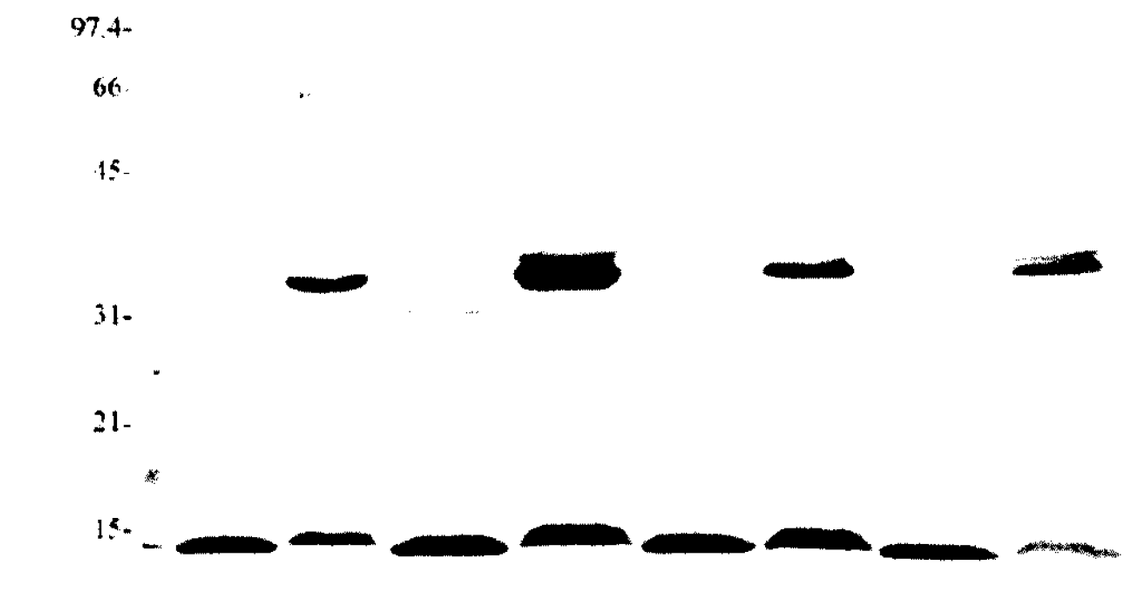

Insoluble HcpE (full length)

Insoluble C-terminal truncated HcpE

all conditions tested (Figure 14A and B). HcpE was targeted for rapid degradation as revealed by the presence of a degraded C-terminal truncated HcpE (Figure 14A and B; arrows). Based on these findings, all subsequent HcpE purifications were performed at 24˚C for convenience and to facilitate large scale expression. In addition, protease inhibitors were added to the cells before lysis to prevent protein degradation.

3.1.7 Purification of histidine-tagged HcpE by nickel chromatography

HcpE was purified from the over-expression system mentioned above. The purification of HcpE was not very efficient, as the protein was still mostly insoluble and prone to degradation. When purified under the same conditions as TsaA, no prominent peak was visible on the chromatogram. Alternating fractions were screened to locate the purified protein (Figure 15A blue box). HcpE was identified in fractions B9 through B1 as a band migrating to its predicted molecular weight of 40.2 kDa. Truncated HcpE eluted along with, and also after the full-length protein (Figure 15B, fractions B1-E4). The identity of the purified HcpE was confirmed by Western blotting with anti-histidine antibodies (Figure 15C). A band reacting with the anti-histidine antibody was identified at 10 kDa. Comparison of the total protein pattern by Ponceau red stain with the Western blot allowed us to infer that HcpE was prone to degradation into a 30 kDa fragment comprising the N-terminus and the majority of the protein and a 10 kDa fragment containing the C-terminal histidine-tag. The same unidentified *E. coli* protein present in the TsaA purification fractions eluted with HcpE just under the 31 kDa marker. The protein appears to bind to the nickel column with equal affinity as the over-expressed proteins, eluting at low imidazole concentrations with our tagged-proteins.

Figure 15: Purification of soluble and insoluble histidine-tagged HcpE by nickel chromatography. Panel A: HcpE was over-expressed in *E. coli* with a C-terminal hexahistidine-tag and purified using nickel chromatography by FPLC. Bound proteins were eluted via application of an imidazole gradient from 50mM to 1M. Protein detection was carried out at 280 nm. Due to the low abundance of over-expressed HcpE, and in the absence of a detectable protein peak, alternating elution fractions (blue box) were screened for the presence of HcpE. **Panel B:** Fractions were resolved by SDS-PAGE (15%) and visualized by Coomassie staining. HcpE was identified in fractions B9 to B1 (marked w/asterix) at its expected size of 40.2 kDa. Truncated HcpE was identified at approximately 30 kDa and 10 kDa eluting after the full length protein. The same *E. coli* protein observed in the TsaA purification was present just below the 31 kDa marker. **Panel C:** The identity of the purified protein was confirmed via Western blotting with anti-histidine antibodies. HcpE-His was degraded into 2 fragments (marked w/x). The 30 kDa fragment was missing the C-terminus based on lack of reactivity with the anti-histidine tag antibody. For each panel: PR; Ponceau Red (loading control), WB; Western Blot. **Panel D:** To enhance the yield of HcpE, purification was performed from the insoluble fraction in the presence of 6M guanidine-hydrochloride. Insoluble protein aggregates obtained after lysis of cells by French press were solubilized via re-suspension in loading buffer containing 6M guanidine-HCl. The solubilized proteins were then purified by nickel chelation chromatography (as above) under denaturing conditions in which all buffers were supplemented with 6M guanidine-HCl. Following elution with an imidazole gradient, full-length HcpE was found to be enriched in seven consecutive fractions (B10 to B4) marked by an asterix.

A- UV 280 nm, Concentration imidazole

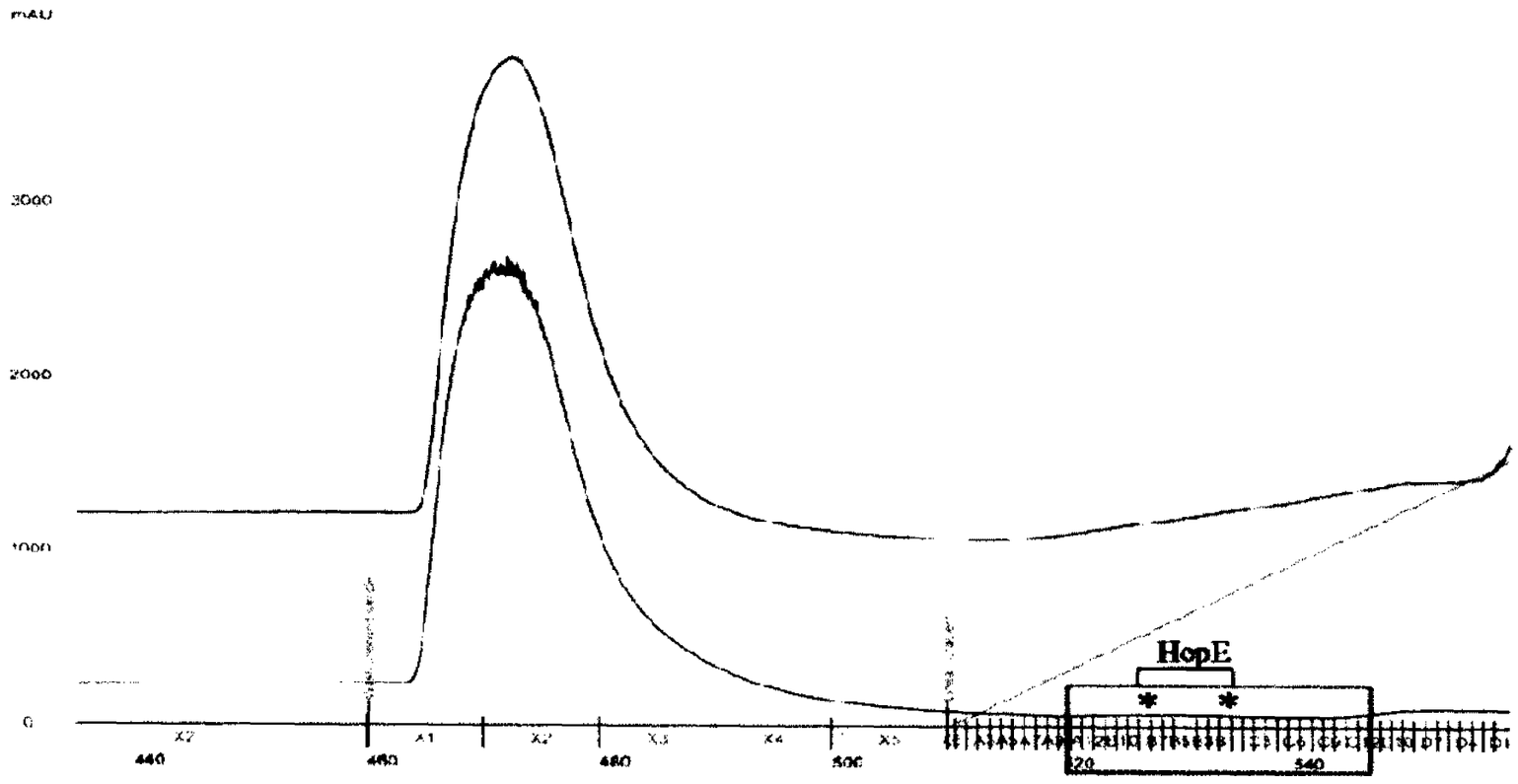

B-

HcpE Fractions:

kDa	1	A11	A8	A12	B9	B5	B1	C4	C8	C12	D9	D5	D1	E4
		2	3	4	5	6	7	8	9	10	11	12	13	14

C-

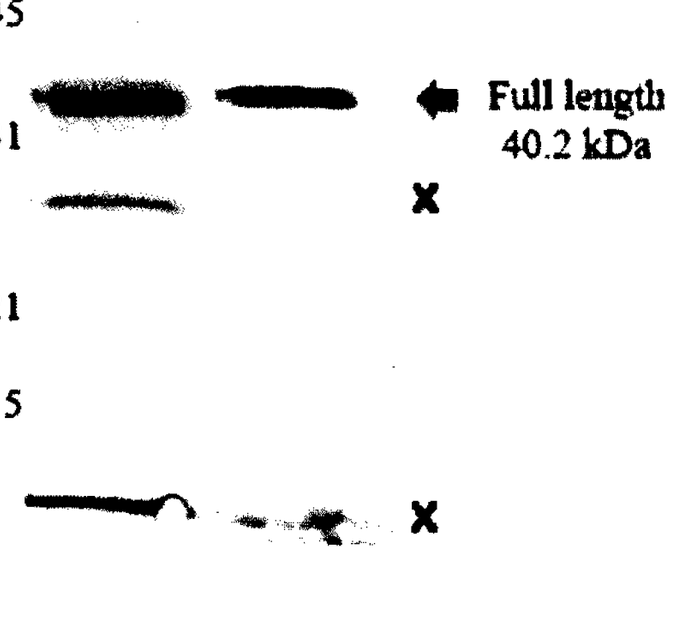

D-

HcpE Fractions:

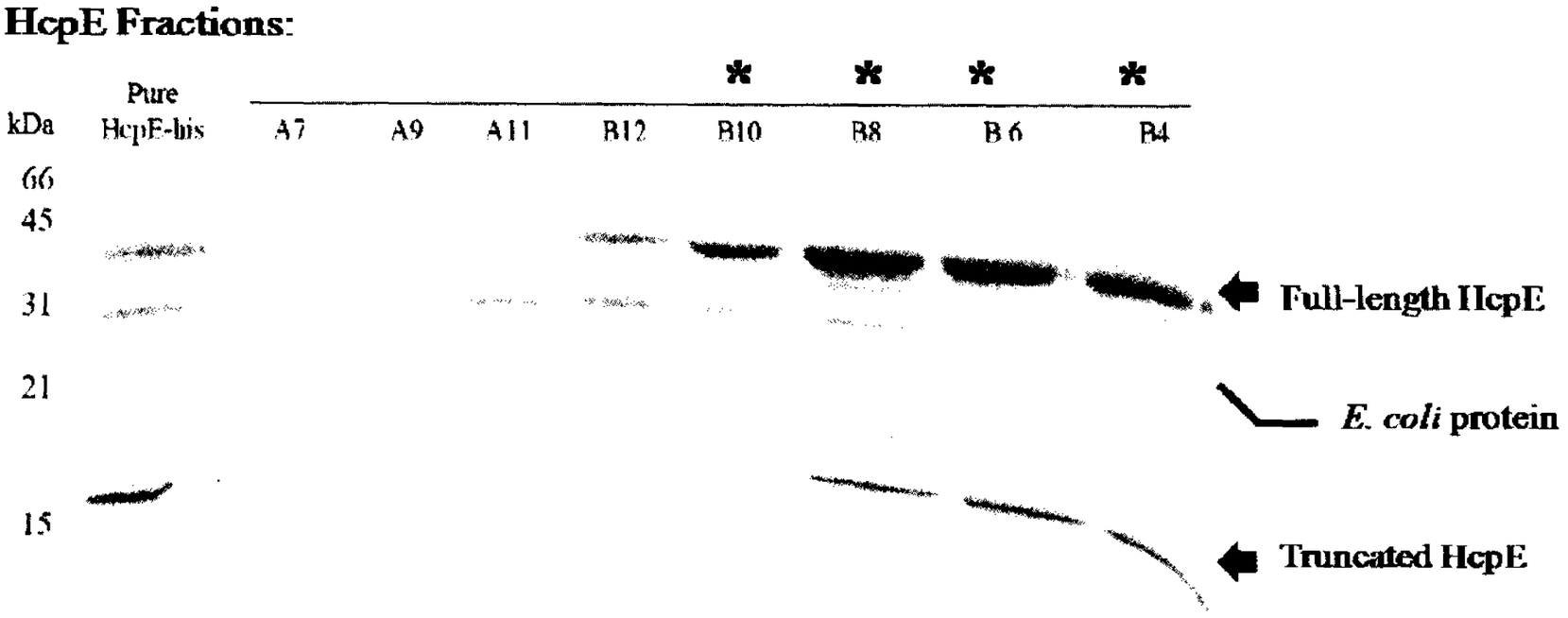

For production of the anti-HcpE antibody in rabbits, a minimum of 800 μg of pure protein was required. Due to the low yields of pure-HcpE obtained from the soluble fraction, our approach was modified to purify the protein from the insoluble fraction in the presence of guanidine-hydrochloride. With this modification, HcpE was purified to near homogeneity, and in large quantities. The protein was identified in its purest form in a total of seven fractions (B10-B4) by SDS-PAGE (Figure 15D). The concentration of purified protein was determined using the Bio-Rad protein quantification assay; 2.45 mg of HcpE was purified using this method. The protein was concentrated by lyophilization, re-suspended in double (1.7%) saline, and this pure, concentrated form was used to inject rabbits at the animal facility to generate the anti-HcpE serum.

3.1.8 Production of the *H. pylori* anti- HcpE antibody

To identify HcpE in the proposed secretion and interaction experiments, an antibody specific to the HcpE protein was needed. Alternatively, a tagged protein could be expressed in the strain of interest to allow detection via an anti-*tag* antibody thereby negating the need for a specific anti-HcpE antibody. However, *H. pylori* is relatively difficult to transform (34). Therefore we opted to purify HcpE to generate a polyclonal antibody. All animal care and handling was performed by technicians at the University of Western Ontario's Animal Care facility. Throughout the duration of the immunization schedule (see methods section 2.11 for details) the evolution of antibody titer and specificity of the anti-HcpE serum was tested by slot blot analysis. Serum dilutions were used to blot membranes containing *E. coli* cell lysates with over-expressed HcpE-His. Following the second injection, a distinct band was identified at approximately 40.2 kDa (Figure 16A) with the newly obtained rabbit serum. Immunoblotting the same membrane

with anti-histidine antibody confirmed that this band corresponded to HcpE-His. The same level of sensitivity was observed with higher dilutions of serum obtained at later time points, indicating that the anti-HcpE antibody titer increased with additional injections. Slight background reactivity was detected to truncated HcpE at 30 kDa (Figure 16A, arrow).

To determine the antibodies ability to detect endogenous HcpE, we tested the reactivity of the serum with total *H. pylori* cell lysates using the *hcpE* mutant as a negative control. Despite cross-reactivity with a number of higher molecular weight *H. pylori* proteins, the anti-HcpE antibody effectively detected HcpE at its predicted size of 39.4 kDa in the wild-type but not mutant strain.

Due to the high sequence homology amongst Hcp family members (31), we predicted that our antibody would potentially cross-react with the other 6 identified *H. pylori* Hcp family members. It was previously documented by Deml *et al.,* that anti-HcpA serum cross-reacted with other Hcp family members, mainly HcpC (31). Thus, it is possible that some of the bands detected by our HcpE anti-serum in *H. pylori* correspond to other Hcp family members.

To reduce non-specific binding and cross-reactivity, the serum obtained following the third injection, day 45 of the injection timeline, was adsorbed against *E. coli* BL21(DE3)pLysS cells to enhance detection of the *E. coli* over-expressed form and against the *hcpE::kan* strain to enhance specificity in detecting the protein endogenously

Figure 16: Production and screening of anti-HcpE polyclonal serum. Panel A: The serum obtained after immunization of New Zealand rabbits with purified HcpE-His was tested for its ability to detect over-expressed HcpE-His in whole cell extracts of *E. coli*. The serum was tested 2 weeks after each injection. Pre-immune serum and buffer served as a negative control. **Panel B:** Serum (from 2nd injection) was used to detect endogenous (untagged) HcpE from wild-type *H. pylori*. The *hcpE* knockout mutant served as a negative control. Although the raw serum cross reacted with other unidentified *H. pylori* proteins, it reacted readily with a band of the expected size for HcpE (39.4 kDa) in the wild-type strain, which was absent in the mutant. The serum was subsequently adsorbed against the *hcpE* knockout mutant to enhance its specificity towards HcpE. The 66 kDa *H. pylori* protein binds readily and non-specifically to the secondary antibody (anti-rabbit antibody) used for the blot. For each panel: PR; Ponceau Red (loading control), WB; Western Blot.

A-

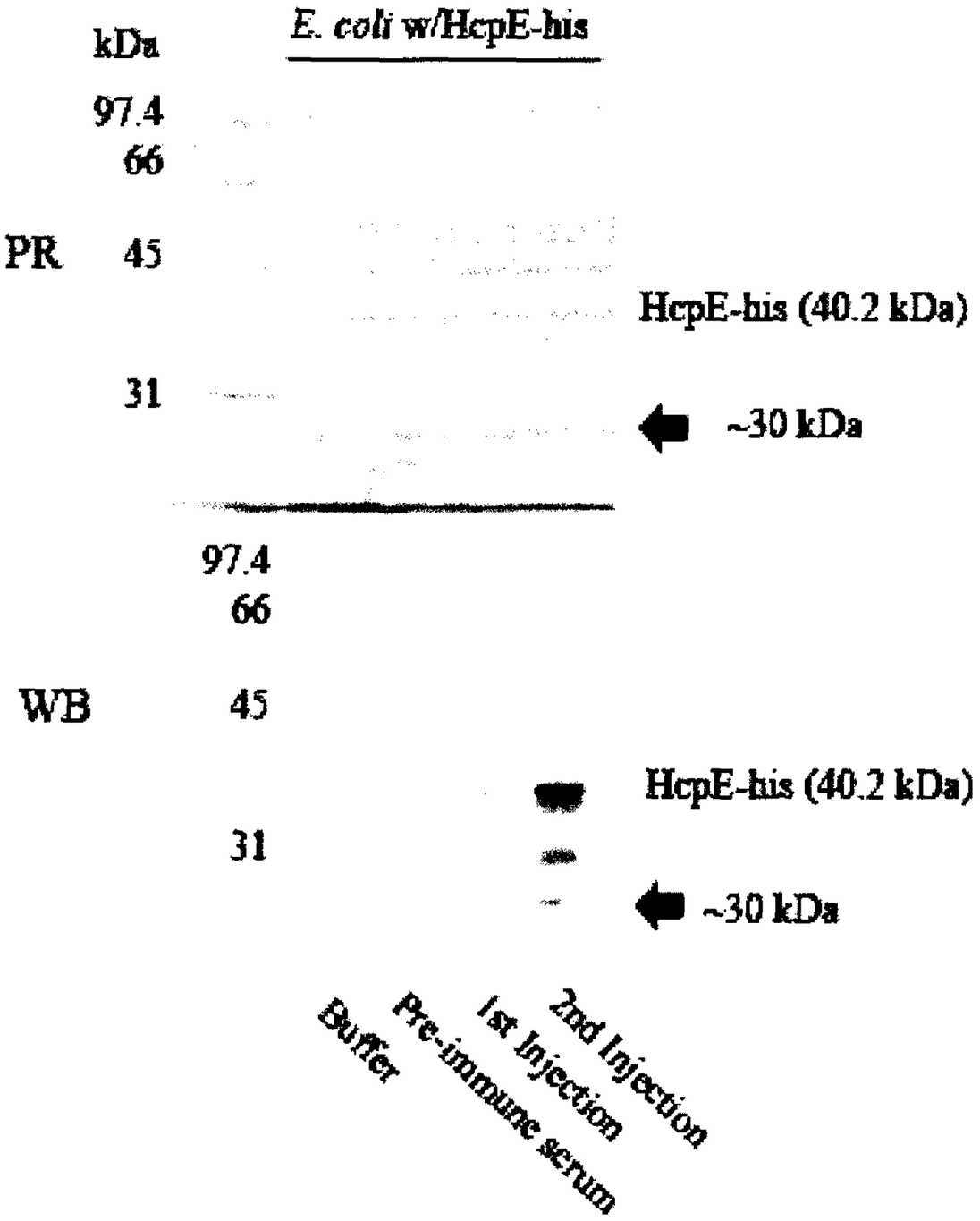
kDa
E. coli w/HcpE-his
97.4
66
PR
45
HcpE-his (40.2 kDa)
31
~30 kDa
97.4
66
WB
45
HcpE-his (40.2 kDa)
31
~30 kDa
Buffer
Pre-immune serum
1st Injection
2nd Injection

B-

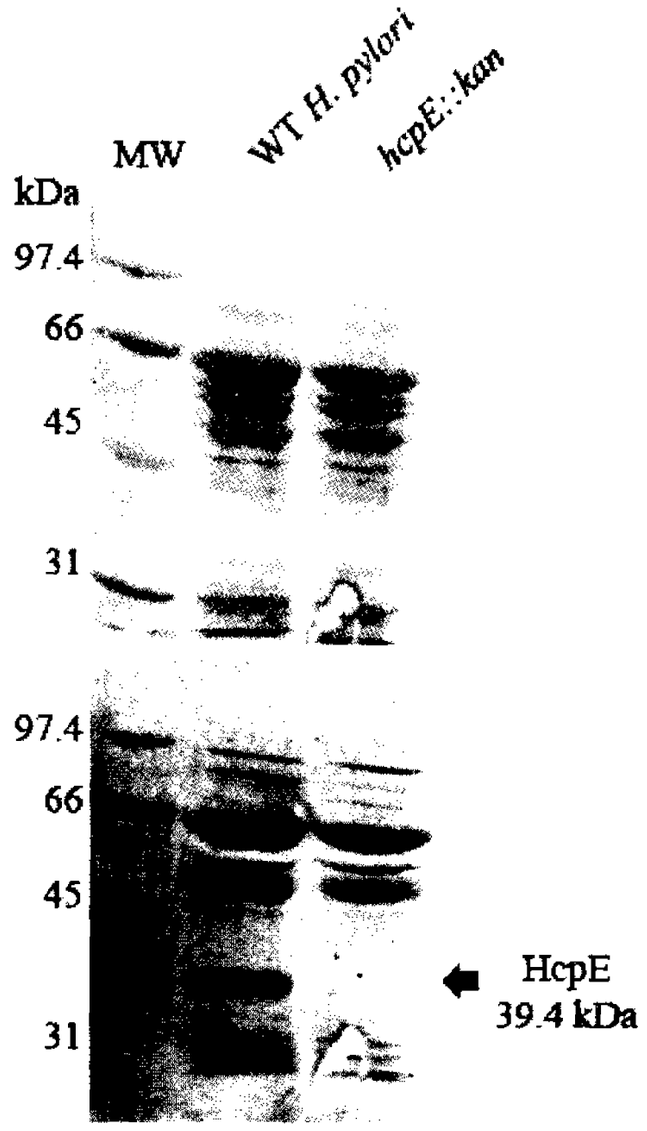
MW
WT H. pylori
hcpE::kan
kDa
97.4
66
PR
45
31
97.4
66
WB
45
31
HcpE
39.4 kDa

in *H. pylori*. The specificity of the adsorbed serum to HcpE-His and *H. pylori* HcpE was increased after absorption.

3.1.9 DsbG is soluble but not over-expressed

As described in section 3.2.5, DsbG was identified by mass spectrometry to interact with HcpE by affinity blotting of the immobilized substrate. To verify the interaction between DsbG and HcpE, purified DsbG was required. For this, a recombinant DsbG protein was generated with a Flag-tag by L. Meng. DsbG-Flag was over-expressed in *E. coli* BL21(DE3)pLys cells carrying the pET30a-DsbG-Flag plasmid via induction with IPTG. A small scale solubility assay was carried out on the induced cultures, as previously described, to assess the protein's yield and solubility. Over-expressed protein was not evident by Coomassie staining alone. Western blotting with an anti-Flag antibody revealed that DsbG-Flag was soluble, but not over-expressing effectively (Figure 17 top panel; PR stain). Moreover, a number of *E. coli* proteins reacted non-specifically with the antibody making it difficult to identify DsbG. A cluster of bands migrating to approximately 30 kDa, the predicted molecular weight of Flag-tagged DsbG showed strong reactivity, obscuring the anticipated DsbG signal. To delineate which of the bands corresponded to DsbG-Flag an *E. coli* cell lysate carrying the empty pET30a vector that had undergone the same preparation was used as a negative control. A prominent band that reacted at 30 kDa in the DsbG-Flag samples was absent in the negative controls and corresponded to DsbG-Flag (Figure 17 bottom panel; WB). Due to the high levels of background of reactivity of other *E. coli* proteins with the anti-Flag antibody, in all future purifications the empty pET30a vector control was run alongside DsbG-Flag to eliminate doubt regarding location of the protein.

Figure 17: Solubility and expression of DsbG-Flag in pET30 expression system. DsbG was expressed with a C-terminal Flag-tag in *E. coli* in the pET expression system. Protein expression and solubility was assessed by small scale solubility assay. Induction with IPTG resulted in production, but not over-expression of DsbG. Detection with the anti-Flag antibody was complicated by its non-specific reactivity with other *E. coli* proteins in the size range expected for Flag-tagged DsbG. The use of the empty pET30 vector as a negative control allowed us to identify DsbG-Flag in the soluble and insoluble fractions at its expected size of 30.6 kDa.

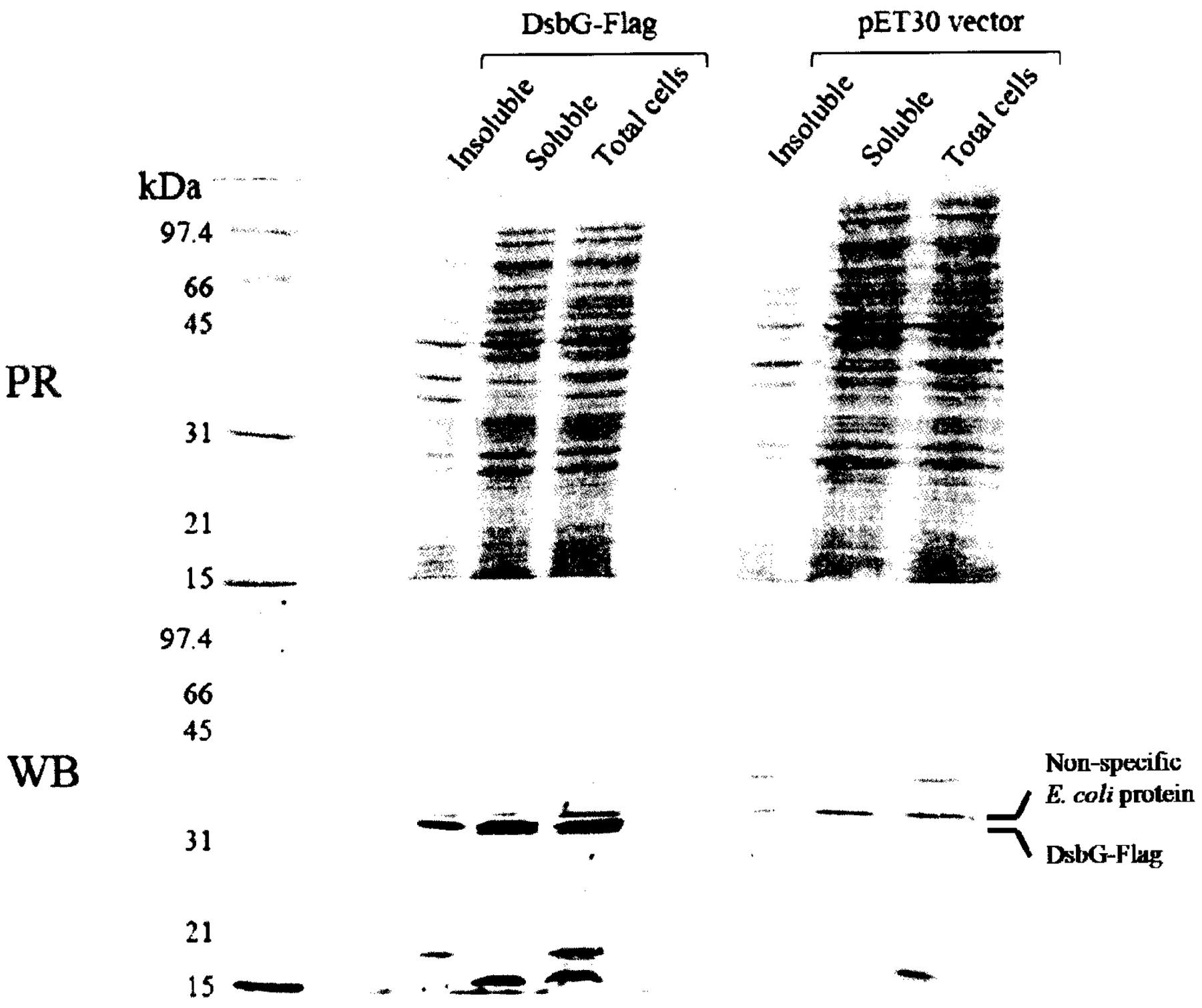
DsbG-Flag
pET30 vector
Insoluble
Soluble
Total cells
Insoluble
Soluble
Total cells
kDa
97.4
66
45
31
21
15
PR
97.4
66
45
31
21
15
WB
Non-specific
E. coli protein
DsbG-Flag

3.1.10 DsbG is enriched by anion exchange chromatography

The soluble DsbG-Flag produced in *E. coli* (see above) was subjected to anion exchange chromatography to obtain enriched samples suitable for interaction assays. Anion exchange chromatography was performed using an S-Hyper-D column at pH 7.5 with a NaCl gradient from 50mM to 0.5M. The chromatogram revealed large quantities of protein were being retained by the column (not shown). Fractions from each independent peak, thought to represent at least one unique protein were screened via SDS-PAGE followed by Western blotting with anti-Flag antibodies (Figure 18). DsbG was identified at its predicted molecular weight of 30.6 kDa in 10 fractions (B8-C1, not shown). An initial screen revealed that the fractions were too dilute to be visualized by Ponceau Red staining. As a result, fractions containing DsbG-Flag were pooled, and concentrated by PEG for visualization by Western blotting with anti-Flag antibodies. DsbG-Flag was present as a doublet (red asterix), which could represent its cytoplasmic and periplasmic forms with and without its signal peptide. Although this step of anion exchange chromatography does not result in full purification of DsbG (refer to Ponceau stain, top pannel), it resulted in a considerable enrichment of the protein which should be sufficient to carry out the interaction assays.

Figure 18: Enrichment of DsbG-Flag by anion exchange chromatography. DsbG was over-expressed in *E. coli* with a C-terminal Flag-tag and enriched using anion exchange chromatography at pH 7.5. Bound proteins were eluted with a gradient from 50mM to 0.5M NaCl. DsbG was identified at its expected size of 30.6 kDa in a very dilute form in ten fractions (data not shown) that were subsequently pooled and concentrated by PEG (arrow). DsbG-Flag was detected as a doublet (red asterix, lane 5) by Western blotting with anti-Flag antibodies, which represent its cytoplasmic and periplasmic forms, with and without its signal peptide. Total cell lysates of the over-expressed DsbG-Flag (lane 2) and of cells harboring the empty pET-30 vector (lane 4, labeled Vector) served as positive and negative controls, respectively.

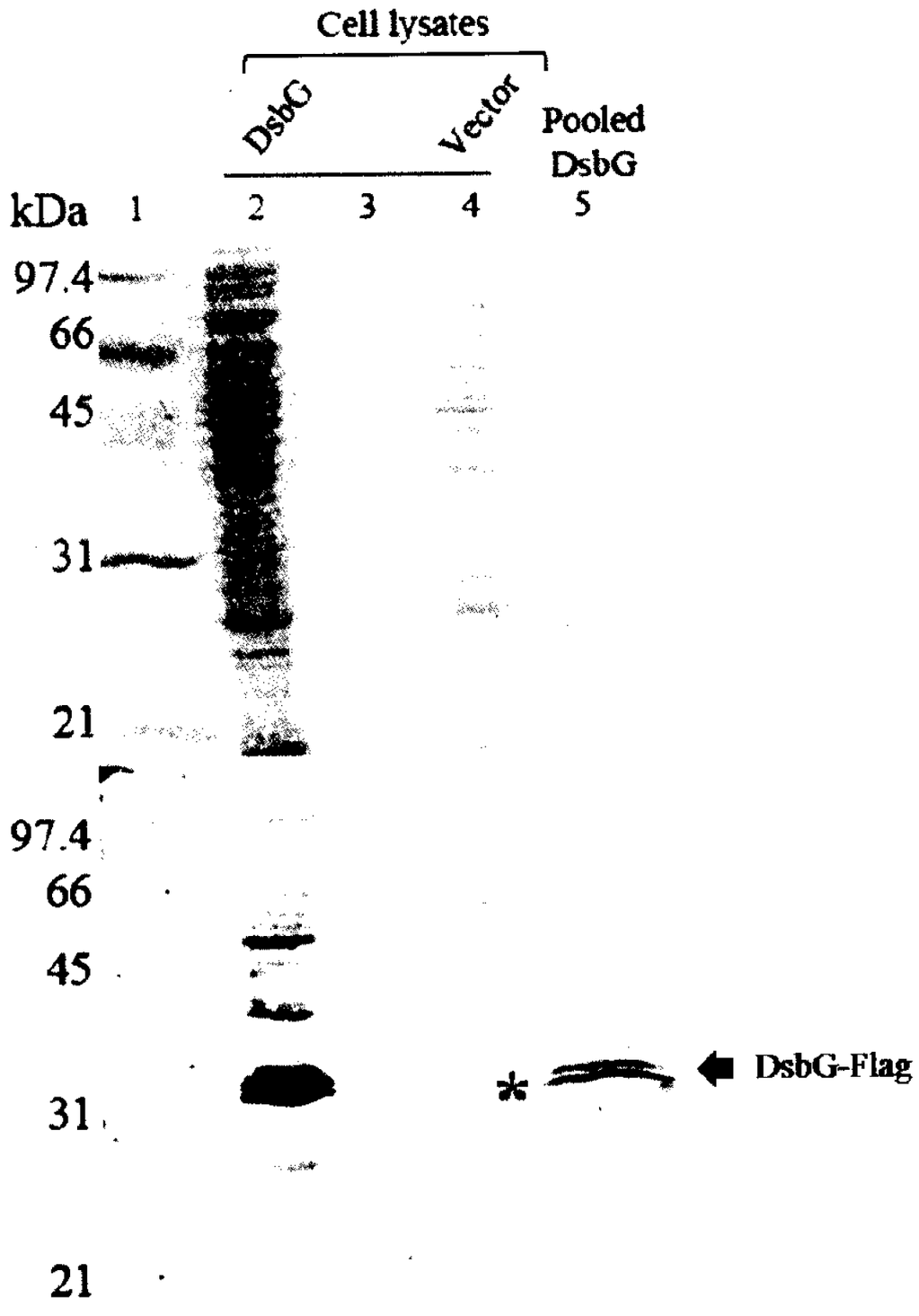
Cell lysates
DsbG
Vector
Pooled DsbG
kDa
1
2
3
4
5
97.4
66
45
31
21
97.4
66
45
31
*
DsbG-Flag

3.2 Secretion and folding of HcpE

3.2.1 HcpE is secreted by *H. pylori* when grown in liquid culture

Previous work by Mittl and colleagues (87) established that patients infected with *H. pylori* have high antibody titers to Hcp proteins, including HcpE. This finding implies that HcpE is secreted, or released by cell lysis during natural infections, thereby eliciting antibody production by the host. The hypothesis that HcpE contributes to bacterial virulence through its interaction with host cells is dependent on HcpE being secreted by the bacterium. Thus, to establish a role for HcpE during infection, its secretion status had to be assessed. To determine if HcpE is secreted by *H. pylori*, the presence of HcpE in culture supernatants after 12, 16 and 20 hours of growth in broth medium was examined by Western blotting with the anti-HcpE antibody. For this, the *hcpE::kan* strain served as a negative control. HcpE was detected at its predicted molecular weight of 39.4 kDa in both the pellets and supernatants of the wild-type but not the knockout strain (Figure 19, red asterix). Similar results were obtained for all three time points tested (data not shown). Despite the non-specific reactivity of the antibody with a number of other *H. pylori* proteins, a distinct band is present in the wild-type strain that is not detectable in the *hcpE::kan* strain.

3.2.2 HcpE secretion is not a result of cell lysis

H. pylori is a fastidious organism, that is not easily culturable (34). When growth conditions are not optimal, the bacteria are known to: (i) transform to a coccoid form, which is thought to be non-culturable, but viable (35, 100) , or (ii) lyse, resulting in the release of all intracellular contents. Growth in liquid media has been optimized by the Creuzenet lab; however, despite finding conditions that encourage growth in liquid,

Figure 19: Secretion of HcpE from wild-type *H. pylori* NCTC 11637 as detected by anti-HcpE Western blot. Proteins recovered in the cell pellets and culture supernatants of wild-type or *hcpE::kan H. pylori* strains grown in brucella broth supplemented with β-cyclodextrin for 12 hrs were analyzed by SDS-PAGE and Western blotting for the presence of HcpE. Detection was performed with Ponceau red staining (PR) of total proteins and anti-HcpE Western blotting (WB). HcpE was detected in the cell pellets and culture supernatants of wild-type, but not *hcpE::kan* at its expected size of 39.4 kDa. Similar results were obtained after 16 and 20 hrs of growth in broth culture (not shown).

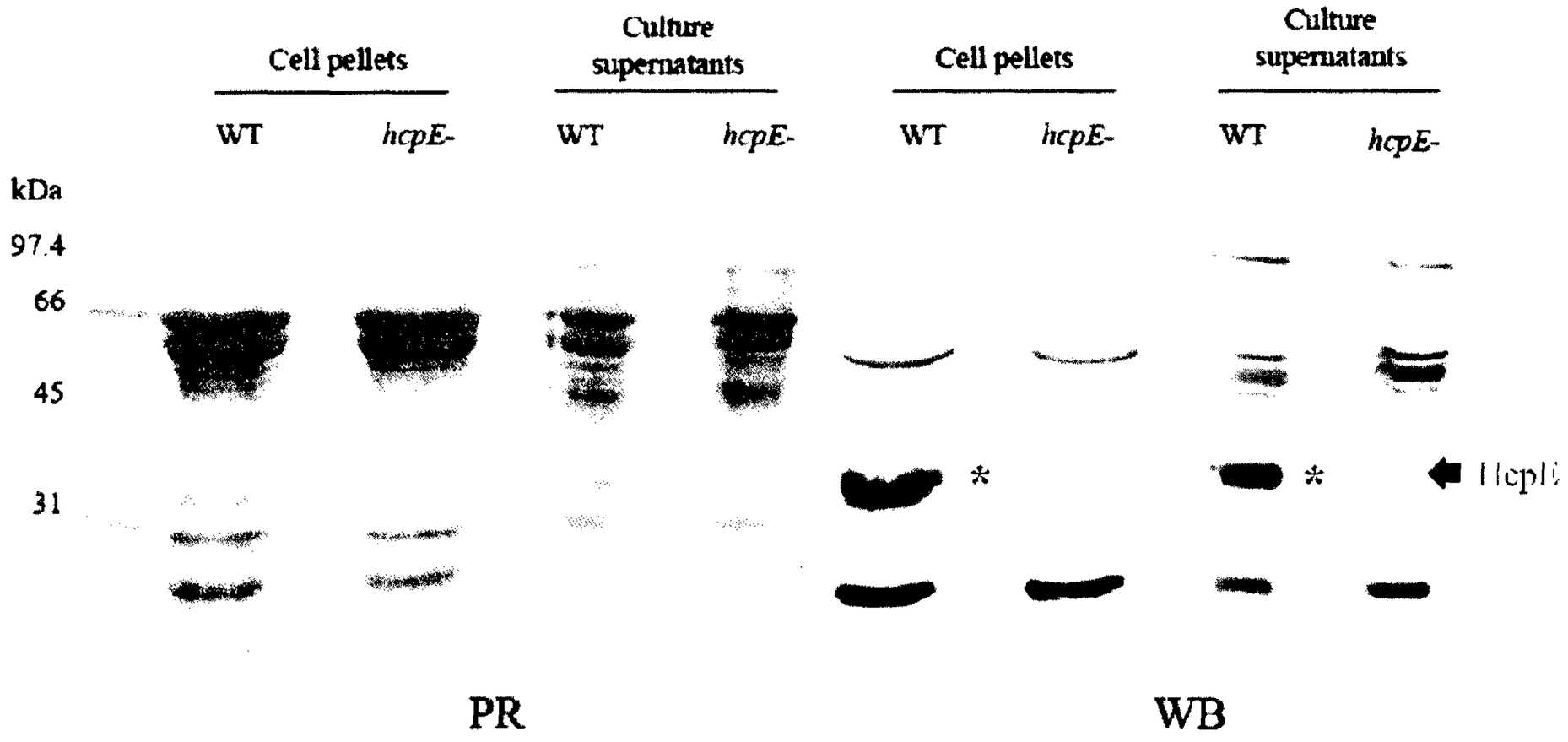
Cell pellets
Culture supernatants
Cell pellets
Culture supernatants
WT
hcpE-
WT
hcpE-
WT
hcpE-
WT
hcpE-
kDa
97.4
66
45
31
*
*
Hcp1
PR
WB

growth is not optimal and lysis does occur. Thus, the presence of HcpE in the culture supernatants could simply be a result of the cells lysing on account of the undesirable growth conditions. To investigate this, the urease activity of the total cells, cell pellets and culture supernatants was compared in the wild-type and *hcpE* mutant strains. Urease is an intracellular enzyme, so its relative abundance outside cells can be used to quantify the amount of cell lysis that took place. The urease activity detected in the supernatants was negligible compared to that detected in the cell pellets. Of the total urease activity detected in the total cell lysate, the majority was contributed by the cell pellets and only a small amount was contributed by the supernatants (Figure 20, bottom series). This indicates relatively low levels of cell lysis occurred and that HcpE was secreted by the bacteria and not present in the supernatants purely as a result of cell lysis.

3.2.3 Structural model for HcpE

Sell-like repeats (SLRs) motifs are 36-44 amino acids in length, are found in tandem, and have been shown to mediate protein-protein interactions (88). They are present in a wide range of proteins with unrelated roles and are encountered in bacteria and mammals. As previously explained, the sequence of HcpE contains nine SLRs, more than any other Hcp family member. The large number and complex structure of these motifs suggests that they are important features of the mature functional protein.

In general, SLRs consist of repeats of 5-40 amino acids that fold into secondary structural elements, such as alpha or beta helices, stabilized by the formation of ionic, aromatic, covalent, or cysteine bonds between residues of each helix. The crystal

Figure 20: Urease activity of wild-type and *hcpE::kan H. pylori* strains grown in liquid media. Cell lysis was controlled for by monitoring the activity of urease in cell supernatants. Urease is a cytoplasmic protein; its presence in limited amounts in the supernatants indicates low levels of cell lysis occurred during growth in broth. The OD_{565nm} which measures urease activity in the phenol red assay was normalized to the cell density (recorded as OD_{600nm}) of the culture before its separation into the cell pellets and the supernatants. Urease activity was recorded for the total cell cultures, the cell pellets and culture supernatants. The negligible amount of urease activity detected in the supernatants indicates that HcpE detected in the supernatants was secreted by the bacteria.

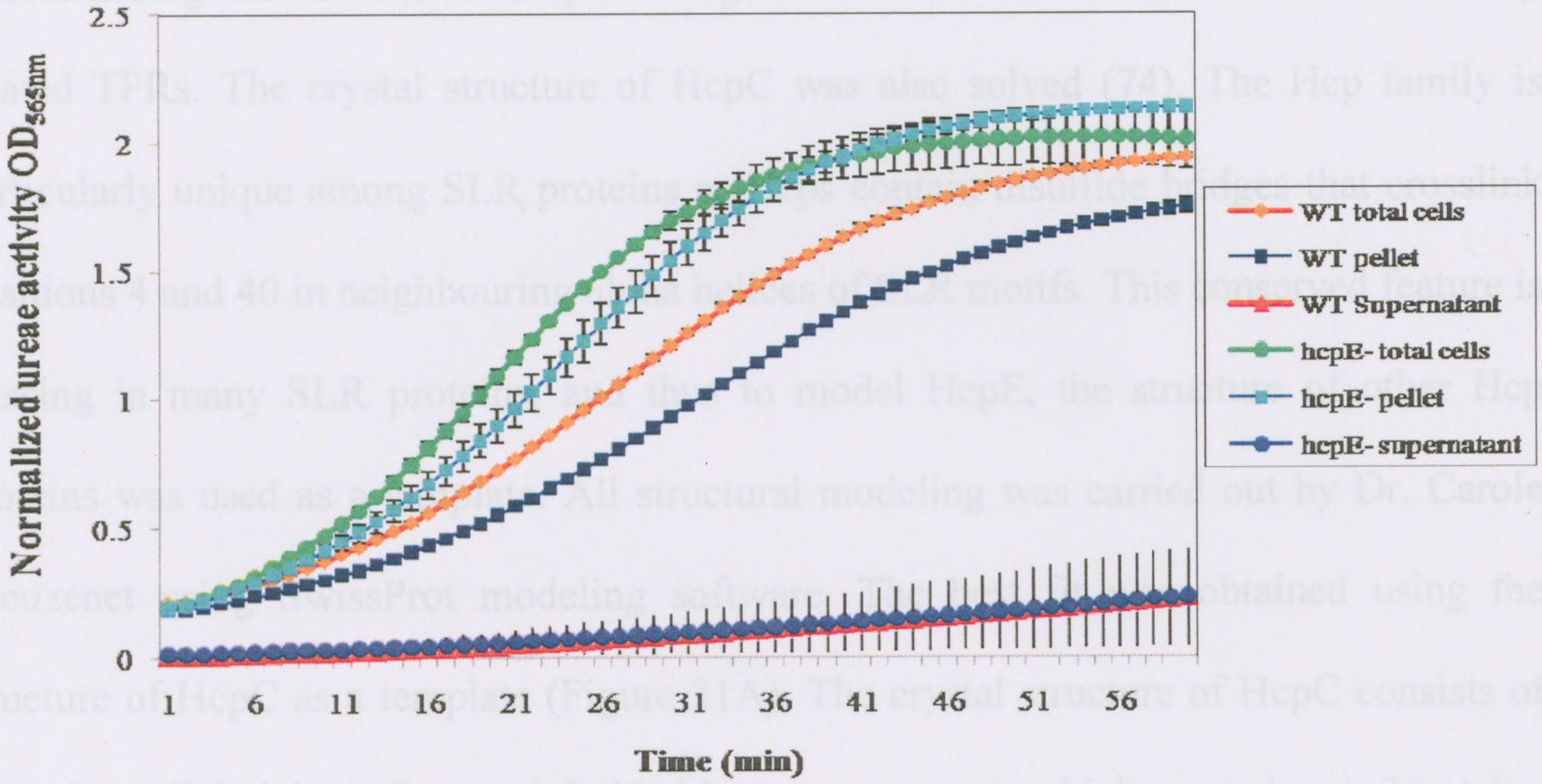
Normalized ureae activity OD565nm
2.5
2
1.5
1
0.5
0
1
6
11
16
21
26
31
36
41
46
51
56
Time (min)
WT total cells
WT pellet
WT Supernatant
hcpE- total cells
hcpE- pellet
hcpE- supernatant

structure of HcpB was previously solved (75) and served as the prototype structure for understanding the difference in spatial organization of different SLRs and the closely related TPRs. The crystal structure of HcpC was also solved (74). The Hcp family is particularly unique among SLR proteins as Hcps contain disulfide bridges that crosslink positions 4 and 40 in neighbouring alpha helices of SLR motifs. This conserved feature is missing in many SLR proteins, and thus to model HcpE, the structure of other Hcp proteins was used as a template. All structural modeling was carried out by Dr. Carole Creuzenet using SwissProt modeling software. The best fit was obtained using the structure of HcpC as a template (Figure 21A). The crystal structure of HcpC consists of 15 anti-parallel alpha helices, subdivided into seven repeats which were always 36 amino acid residues long. The protein contains 14 cysteine residues, all of which form disulfide bridges, with a consistent spacing of seven amino acid residues between each pair of cysteine residues. In the predicted model of HcpE SLRs 1-3 and 6-9 were superimposed directly onto the 7 SLRs of HcpC, leaving a stretch of 62 amino acids (AA152 to 213) comprising the two central SLR repeats of HcpE (SLRs 4 and 5) misaligned (Figure 21B). The predicted secondary structure elements of this misaligned stretch of AA were identified as alpha-helices, suggesting that the structure of this portion of the protein might not be properly modeled using HcpC. As well, the model showed disulfide bonds between cysteine residues of SLR 1-3 and 6-9, as expected; however, it left the 4 cysteine residues in SLR 4 and 5 in their reduced form, which is unexpected for these types of proteins. HcpE with 19 cysteine residues and a total cysteine content of 5.4% has the greatest proportion of cysteine residues of all Hcp family members. HcpC, the template protein, contains fewer cysteine residues arranged in seven predicted SLRs,

Figure 21: Modeling of the 3D structure of HcpE onto the known structure of HcpC. **Panel A:** Structure of HcpC, available in Protein Data Bank as 1ouv. **Panel B:** Direct modeling of the structure of HcpE onto HcpC. Four segments anticipated to form two extra SLR repeats were not properly modeled (highlighted in red, blue, green and orange). The problem was attributed to the extra SLRs in HcpE (9 in HcpE, versus 7 in HcpC). **Panel C:** Modeling of the two overlapping segments of HcpE (AA 1-230, and 143-355) onto HcpC. Each segment contained the mis-folded areas highlighted in panel B and only contained a total of 6 SLRs, which was less than in HcpC. The lower number of SLRs allowed the segments to model properly onto the structure of HcpC and form the expected SLRs. **Panel D:** Model of the reconstituted full-length HcpE. The modeled segments shown in panel C were superimposed using PyMol to provide a model for the full-length HcpE protein. In this final model, the two cysteines of each SLR form a disulfide bridge that covalently links the 2 helices of each SLR together. All proteins shown here are monomers. *Figure courtesy of Dr. Carole Creuzenet.*

A- HcpC

Known structure

Top view

Side view

B- HcpE

Direct modeling

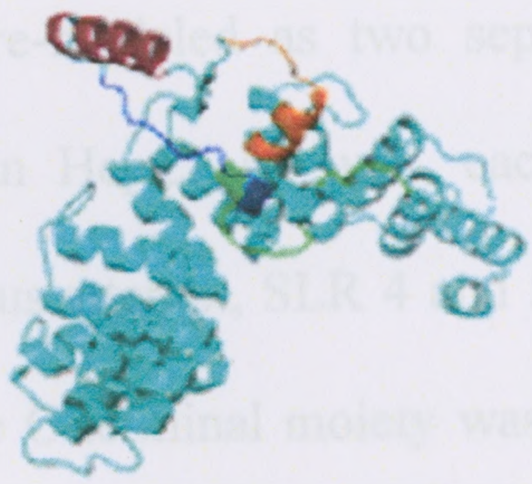

C- HcpE

Modeling of fragments

AA 1-230

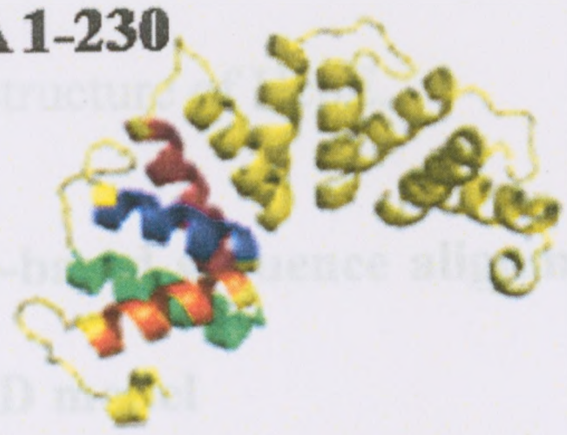

AA 143-355

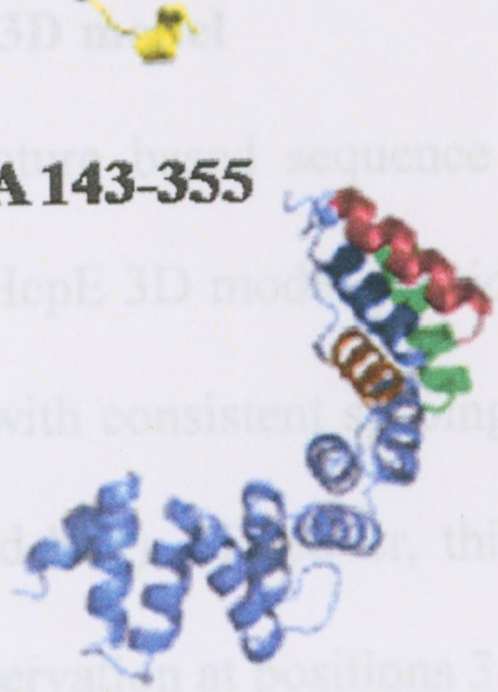

D- HcpE

Reconstituted

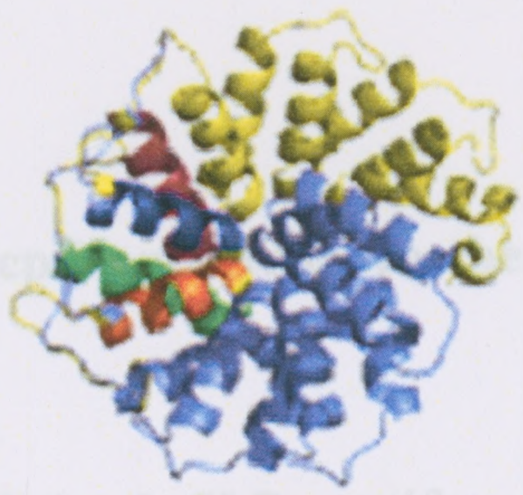

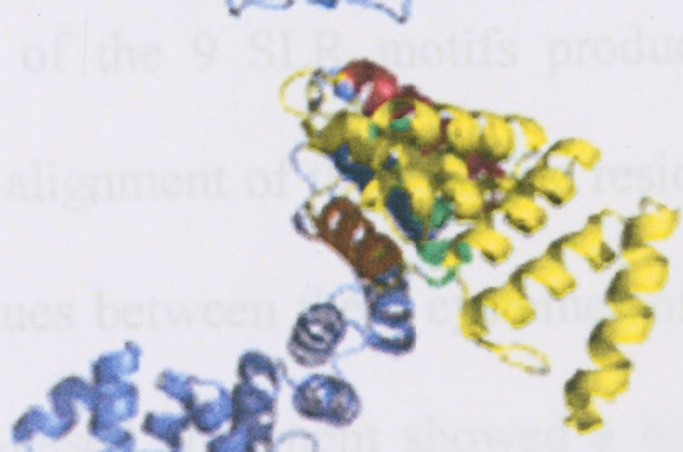

and thus it is possible that the inconsistent model reflects the fact that HcpE simply has more SLRs than HcpC, which prevented proper structural modeling.

To resolve this modeling issue, HcpE was re-modeled as two separate but overlapping moieties each containing less SLRs than HcpC. As well, each moiety contained the mis-folded SLRs identified in the previous attempt, SLR 4 and 5. The N-terminal moiety was modeled using AA 1-230 and the C-terminal moiety was modeled with AA 143-355 (Figure 21C). By modeling the protein in two independent segments, the structure of SLR 4 and 5 was properly modeled onto that of HcpC, in which all cysteine residues were oxidized, forming disulfide bridges which maintain the two helices of each SLR. The predicted structure of the remainder of the protein remained identical to that predicted by modeling the full length sequence; all SLRs were modeled as two helix elements interconnected via a disulfide bridge. Alignment of both the N and C-terminal segments of the newly modeled moieties via their overlapping SLRs (SLR 4 and 5) using PyMol software allowed for the generation of a reconstituted model of HcpE (Figure 21D). In this model, the regular two-helix motif of the SLRs is maintained throughout the structure of HcpE.

3.2.4 Structure-based sequence alignment of HcpE and HcpC further validates the reconstituted 3D model

A structure based sequence alignment of the 9 SLR motifs produced by the reconstituted HcpE 3D model provided perfect alignment of the cysteine residues within these motifs, with consistent spacing of 7 residues between the 2 cysteines of each SLR (Figure 22, red box). Moreover, this structure-based alignment showed a high level of sequence conservation at positions 3 (K), 4 (A), 7 (Y), 8 (F/Y), 10 (K), 11 (A/G), 12 (C),

Figure 22: Structure-based sequence alignment of the SLR motifs of HcpE and comparison with the organization of HcpC. The amino acids present in the helices of the SLR motifs were identified in the modeled structure of HcpE and the known structure of HcpC and are aligned for each motif. The cysteine residues present in each helix are perfectly aligned (red box) and separated by 7 amino acids in each SLR, in both proteins. Conserved amino acids can be identified for each protein but are not necessarily conserved in both proteins. **!**; amino acids conserved in all SLRs for each protein. **+**; amino acids/consensus conserved in 90-99% of SLRs. *; conservation of type of amino acid in 70-89% of SLRs. *Figure courtesy of Dr. Carole Creuzenet.*

```
Prot    # AA      -----Helix A---          ---Helix B---  -linker--
HcpE 1  44        YSKATSYFKKACN-D  GV      SEGCTQLGIIY-E  NGQ-GTRID
HcpE 2  80        YKKALEYYKTACQA-  DD      REGCFGLGGLYDE  -GL-GTTQN
HcpE 3  117       YQEAIDAYAKACVL-  KH      PESCYNLGIIYDR  KIK-GNA--
HcpE 4  152       DQ-AVTYYQKSCNFD  MA      K-GCYVLGVAY-E  KGFLEVKQS
HcpE 5  188       NHKAVIYYLKACRLD  DG      Q-ACRALGSLF-E  NGDAGLDED
HcpE 6  214       FEVAFDYLQKACGL-  NN      SGGCASLGSMYML  -GRY-VKKD
HcpE 7  261       PQKAFNFFKQACDM-  GS      AVSCSRMGFMYSQ  -GDA-VPKD
[HcpE 8  297      LRKALDNYERGCDM-  GD      EVGCFALAGMYY-  N-M-KDKEN
[HcpE 9  332      AIM--I-YDKGCKL-  GM      KQACENLTK
                  *+   *+****!             !   +*   +      *

HcpC  1  47       -TQAKKYFEKACDL   KE      NSGCFNLGVLYYQ  GQGVEKN
HcpC  2  82        LKKAASFYAKACDL   NY      SNGCHLLGNLYYS  GQGVSQN
HcpC  3  117       TNKALQYYSKACDL   KY      AEGCASLGGIYHD  GKVVTRD
HcpC  4  153       FKKAVEYFTKACDL   ND      GDGCTILGSLYDA  GRGTPKD
HcpC  5  190       LKKALASYDKACDL   KD      SPGCFNAGNMYHH  GEGATKN
HcpC  6  225       FKEALARYSKACEL   EN      GGGCFNLGAMQYN  GEGVTRN
HcpC  7  261       EKQAIENFKKGCKL   GA      KGACDILKQ
                  **!    +  !+!*!            +!   ++   +     !  +*   *

                                  7AA
```

21 (C), 24 (L), 25 (G), 28 (Y/F) in HcpE. Some of these features, including the conservation of aligned cysteine residues interspersed by 7 AA (red box) coincided with the sequence alignment generated from HcpC's structure, although the boundaries of helix A differed slightly between HcpE and HcpC. The sequence alignment strongly supports the modifications made in the reconstituted structural model.

3.2.5 Identification of the folding factor DsbG by affinity blotting of the immobilized substrate

For HcpE to be folded properly, it is believed that it may interact with a protein of the Dsb (DiSulfide Bond) family. This presumption is validated by the structural modeling done on HcpE (refer to section 3.2.3). According to this model, HcpE contains numerous disulfide bonds, arranged in a very precise pattern. Furthermore, due to its predicted signal sequence, HcpE is thought to transit through the periplasm during secretion. For this to occur, HcpE may interact with folding factors, such as Dsb proteins, in the periplasm allowing it to acquire its proper structure prior to secretion.

Interactions between folding factors and their target proteins require the target to be reduced and unfolded, thus the method of affinity blotting of the immobilized substrate was employed. This technique has been used extensively to identify interactions between unknown cargo proteins and their type III chaperones (44, 139, 143). We adapted this method to identify unknown folding factors for our known substrate HcpE. Since the interaction between a folding factor and its substrate involves the unfolded substrate, purified HcpE was denatured under reducing conditions and resolved by SDS-PAGE and immunoblotted onto a PVDF membrane. The membrane was incubated with wild-type *H. pylori* cell extracts. A section of the membrane was used for Western

blotting with anti-histidine antibodies to identify the exact location of HcpE such that the band corresponding to HcpE and its interacting partner could be excised. A brief outline of the technique employed is outlined in Figure 23, for a more detailed schematic refer to Figure 8. Proteins were subsequently digested off the membrane by trypsinolysis and analyzed by MS for protein identification. For these experiments, the same affinity blotting protocol was performed with purified histidine-tagged TsaA to eliminate non-specific interactions, as well as in the absence of over-expressed protein. In two independent determinations, MS identified DsbG (HP0231) to interact with both full-length and truncated HcpE, but not with the control protein TsaA. Because truncated HcpE was not reactive with anti-histidine antibodies, its location was determined by lining up the membrane containing full length HcpE with a Coomassie stained gel (Figure 23).

3.2.6 Structural modeling of the *H. pylori* DsbG homologue

The paradigm established in *E. coli* for disulfide bond formation via the oxidative pathway requires DsbA and DsbB, whereas the isomerization pathway to correct mis-folded bonds involves DsbC/G and DsbD. However, there is growing evidence that the components of the oxidative folding machinery in bacteria are highly variable, suggesting that this paradigm is not conserved (56). Moreover, a number of bacterial species have been shown to have only one Dsb protein as opposed to a functional pair as in *E. coli* (37, 122).

Structural modeling of DsbG was done by Dr. Creuzenet using SwissProt modeling software with visualization using PyMol. The best 3D model for *H. pylori*

Figure 23: Identification of a folding factor for HcpE by the method of "affinity blotting of the immobilized substrate." Representative gel of membranes used for the affinity blotting experiment. Purified HcpE (red box) and TsaA (black box) were denatured by SDS-PAGE and immunoblotted on PVDF membranes that were subsequently incubated with wild-type *H. pylori* cell lysates to allow for interactions. To confirm the location of the purified proteins on the membrane, a section was used for Western blotting with the anti-histidine antibody. Membranes were cut (dashed boxes, arrows), and bound proteins (interacting partners) were digested from the membrane by trypsinolysis and sent to MS for protein identification. For HcpE both the full-length (red box) and truncated (green box) proteins were used in the assay. To identify the location of the C-terminally truncated HcpE, which does not react with the anti-histidine antibody, the membrane was lined up with the Coomassie stained gel and then cut. MS identified DsbG (HP0231) to interact with both forms of HcpE, but not TsaA.

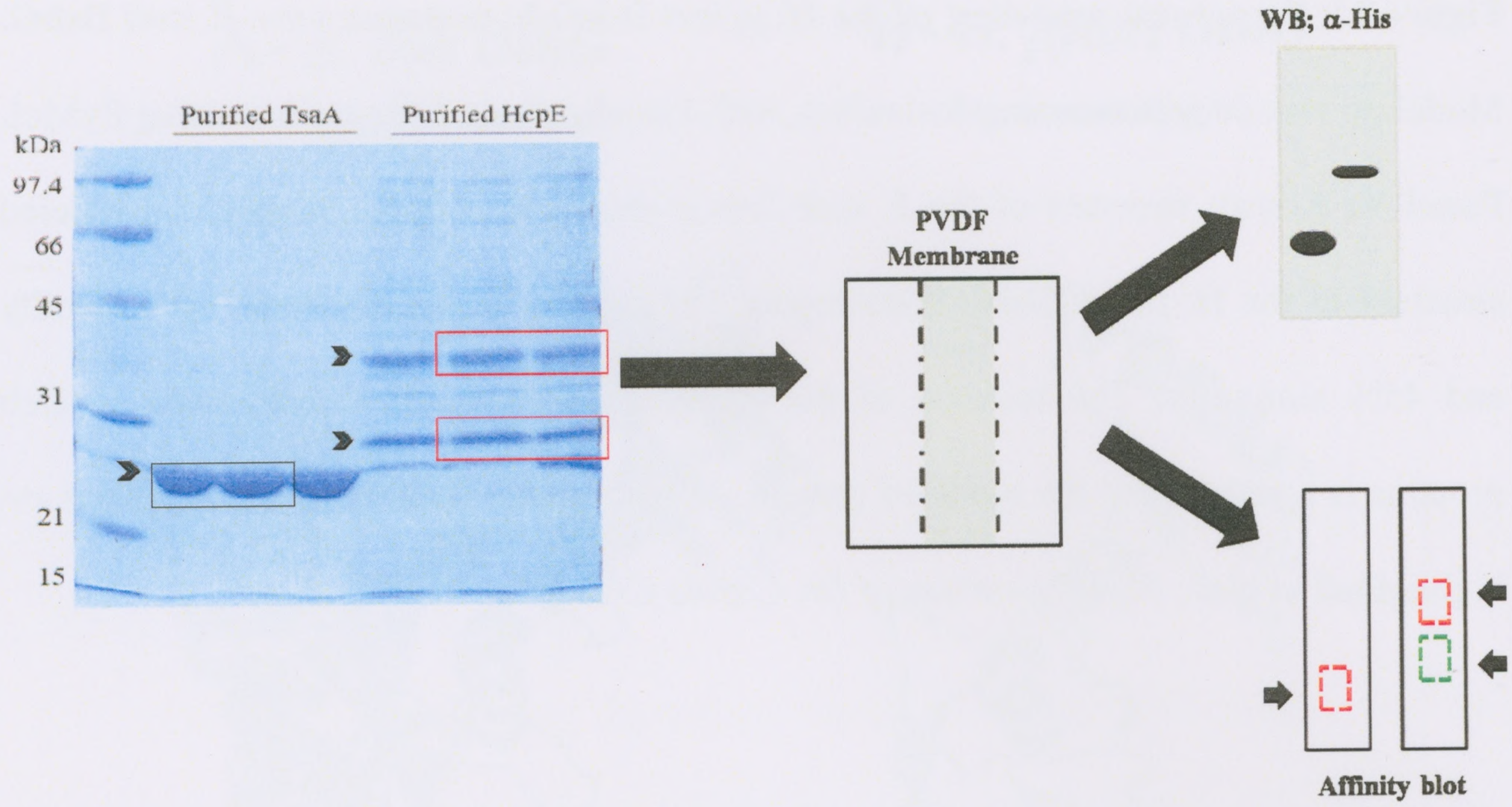
Purified TsaA
Purified HcpE
kDa
97.4
66
45
31
21
15
PVDF
Membrane
WB; α-His
Affinity blot

Figure 24: Structural modeling of the *H. pylori* DsbG homologue onto *E. coli* DsbG. Modeling was performed using SwissProt, with visualization of the models using PyMol. **Panel A:** Known structure of the *E. coli* DsbG, shown as a dimer. **Panel B:** Modeled structure of the *H. pylori* DsbG homologue. The protein sequences share 16% identity and 45% similarity. The location of the catalytic CxxC motif characteristic of Dsb proteins is conserved in the modeled protein. In both panels the conserved cysteines are highlighted in pink. *Figure courtesy of Dr. Carole Creuzenet.*

A- *E. coli* DsbG

Known structure

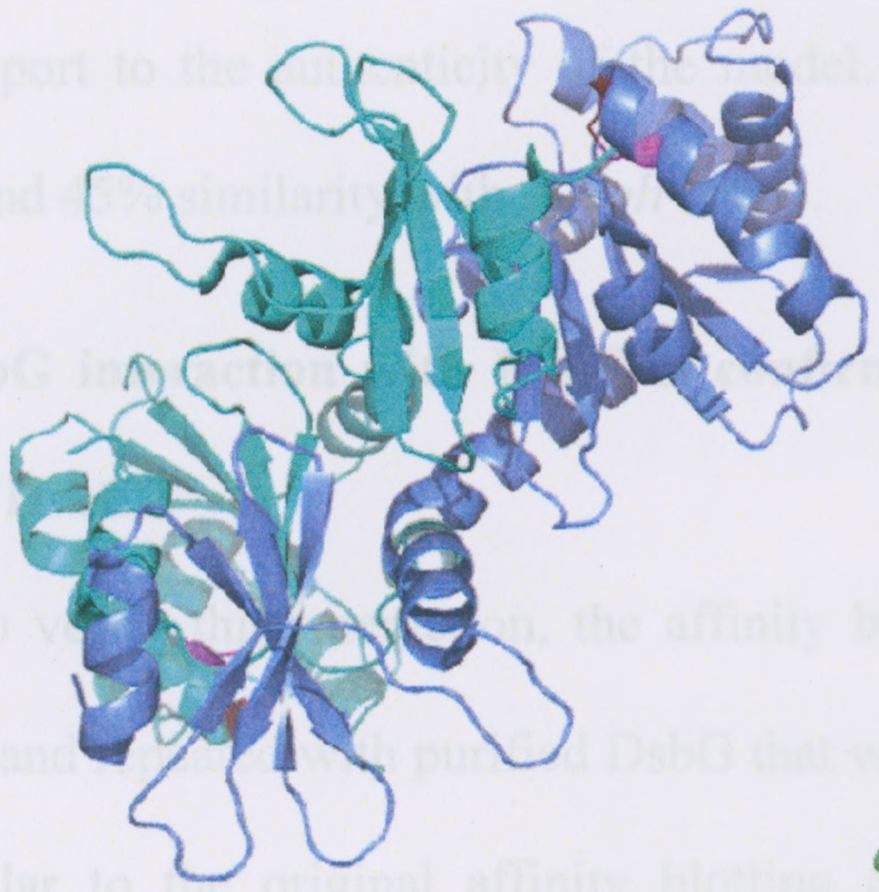

B- *H. pylori* DsbG

Direct modeling

DsbG (HP0231) was obtained using the *E. coli* DsbG as a template (Figure 24). For this, *H. pylori* DsbG was modeled onto a monomer of the *E. coli* DsbG homodimer. With this model, the active site CxxC motif characteristic of Dsb proteins was conserved, which lends support to the authenticity of the model. *H. pylori* DsbG (HP0231) shares 16% identity and 45% similarity with *E. coli* DsbG.

3.2.7 DsbG interaction with HcpE is confirmed by a modified affinity blot using enriched DsbG

To verify this interaction, the affinity blotting protocol (see section 3.1.6) was modified and repeated with purified DsbG that was over-expressed in *E. coli* with a Flag-tag. Similar to the original affinity blotting protocol, HcpE-His was denatured and resolved by SDS-PAGE and immobilized on a membrane. In this experiment, nitrocellulose membrane was used as opposed to PVDF, used previously. Cell extracts of *E. coli* over-expressing HcpE were used instead of pure HcpE, and cell lysates of *E. coli* harboring an empty pET30 vector served as a negative control. The membrane was subsequently incubated with either DsbG-Flag, DsbG-Flag supplemented by wild-type *H. pylori* cell lysate, or buffer only. The addition of *H. pylori* lysate was to test whether the DsbG/ HcpE interaction involved additional *H. pylori* proteins. After the incubation period the membrane was washed and probed with anti-Flag antibodies to probe for binding of DsbG-Flag onto the denatured HcpE. The location of HcpE was determined by probing the same membrane with anti-HcpE antibodies.

Western blotting with the anti-Flag antibody revealed a band reacting at the location of full-length HcpE (as probed by anti-HcpE antibody) which was more reactive

Figure 25: Demonstration of an interaction between DsbG and HcpE using the method of "affinity blotting of the immobilized substrate" with enriched DsbG-Flag. To verify the interaction between HcpE and DsbG, cell extracts of *E. coli* over-expressing HcpE-His were denatured by SDS-PAGE and immunoblotted on nitrocellulose membrane. HcpE-His was used at two different loadings: concentrated and diluted 1:4, to assess whether the amount of HcpE present on the membrane would limit the interaction with DsbG. Cell extracts of the same *E. coli* strain as HcpE harboring the empty vector served as a negative control for non-specific interactions with other *E. coli* proteins. The *E. coli* over-expressed DsbG-Flag cell lysate served as a positive control for reactivity of the anti-Flag antibody. Membranes were incubated with enriched DsbG-Flag (Panel A), buffer only (Panel B), or enriched DsbG-Flag supplemented with wild-type *H. pylori* cell extract (Panel C). The membranes were probed with anti-Flag antibodies to detect DsbG binding to the immobilized HcpE, followed by anti-HcpE antibodies to identify the location of HcpE, and visualized at 700 and 800 nm, respectively. Full length and truncated HcpE are marked by a black arrow; DsbG-Flag (positive control) is marked by a red asterix; non-specific *E. coli* protein reacting with the anti-HcpE antibody is marked by a grey arrow. Figure is representative of three independent experiments. DsbG binds full length HcpE in Panel A and C and the signal detected is stronger than that detected in Panel B, treated with buffer only.

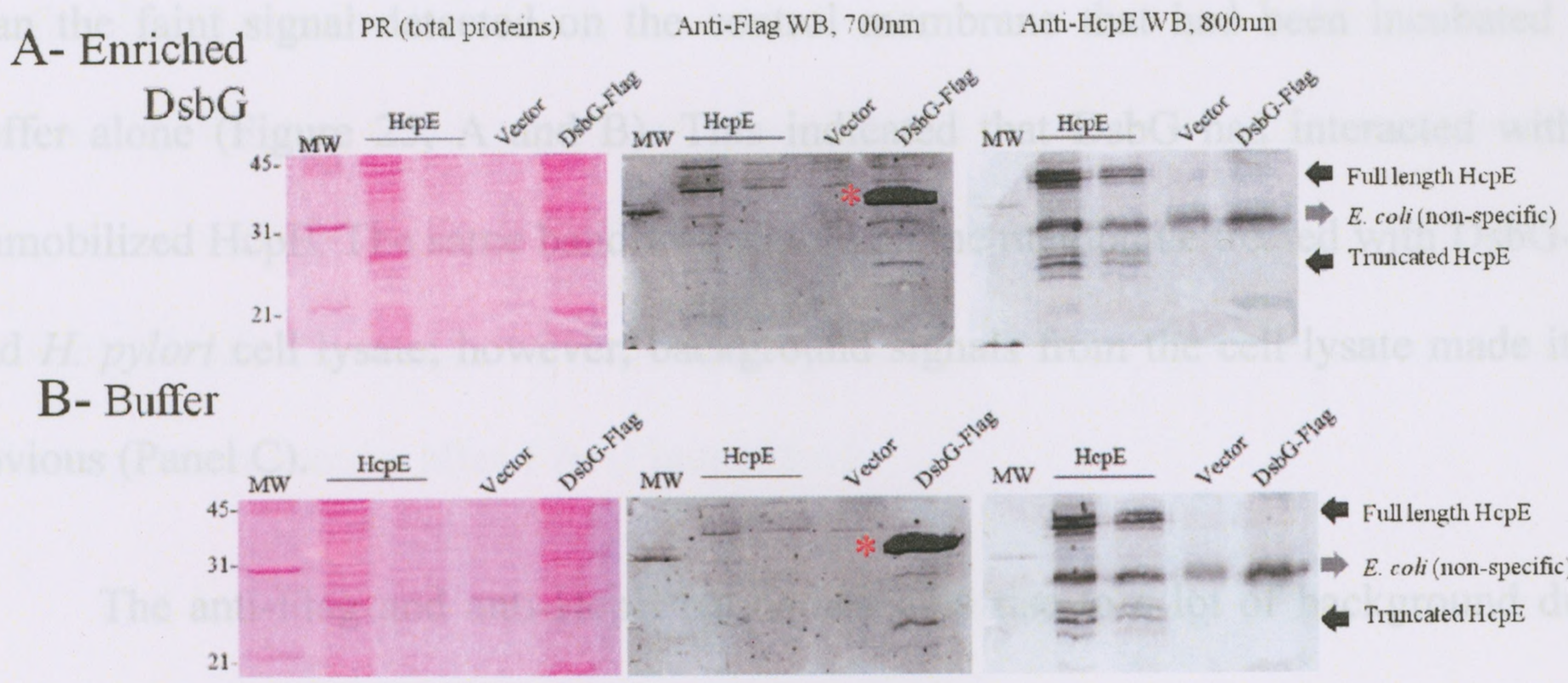
A- Enriched DsbG
PR (total proteins)
Anti-Flag WB, 700nm
Anti-HcpE WB, 800nm
MW
HcpE
Vector
DsbG-Flag
45-
31-
21-
Full length HcpE
E. coli (non-specific)
Truncated HcpE
B- Buffer
C- Enriched DsbG, wild-type H. pylori

than the faint signal detected on the control membrane that had been incubated with buffer alone (Figure 25, A and B). This indicated that DsbG had interacted with the immobilized HcpE. The same band was visible on the membrane treated with DsbG-Flag and *H. pylori* cell lysate; however, background signals from the cell lysate made it less obvious (Panel C).

The anti-Flag and anti-HcpE antibodies give rise to a lot of background due to non-specific binding. To better assess the specificity of the signals obtained, a control lane was included (empty vector). Unfortunately, at the low level of loading used, no difference was observed in the presence of DsbG between the HcpE positive lane, and only non-specific signals were observed. This lack of specificity is inconsistent with the cross blot comparison (Panels A and B, high HcpE loading). It is likely that the low amount of HcpE on the membrane was the limiting factor that prevented DsbG from binding at significant levels. Using larger amounts of purified HcpE-His, similar to what was used in the original affinity blot that allowed us to identify DsbG by MS, should eliminate this discrepancy.

3.2.8 DsbG solubilizes insoluble HcpE

In the proposed model for the interaction of DsbG with HcpE, DsbG acts as an enzymatic catalyst, catalyzing the formation of disulfide bonds between the cysteine residues of HcpE. If this hypothesis is correct and DsbG is responsible for oxidizing HcpE so that it can acquire its mature form necessary for secretion from the cell, and if improper folding and/or the absence of these disulfide bonds prevented HcpE secretion into the soluble fraction, the presence of DsbG alone should be enough to solubilize insoluble HcpE. To test this hypothesis, a re-folding assay was designed in which

purified DsbG was incubated with insoluble HcpE, and its ability to solubilize HcpE was detected by Western blotting proteins present in the supernatant of the reaction mixture using the anti-HcpE antibody. When increasing concentrations of DsbG were added to insoluble HcpE, the amount of HcpE detected in the reaction supernatants increased in a dose-dependent manner after 1 hr (Figure 26A).

Full length HcpE was present as a doublet in this assay. These two bands are thought to reflect the cytoplasmic and periplasmic forms of the protein, with and without its signal peptide, respectively. In the cytoplasm HcpE is unfolded and contains its signal peptide which allows it to be recognized by the Sec machinery for transit into the periplasm. Once in the periplasm, its signal peptide is cleaved and proper folding ensues with the formation of disulfide bonds. The size difference for these two forms of the protein is about 2.7 kDa. Based on the resolution of the gel, it seems plausible that the doublet would reflect these forms of the protein.

The effect of DsbG on solubilization of HcpE is most striking for cytoplasmic HcpE (HcpE +SP). Cytoplasmic HcpE was always in the reducing environment of the cytoplasm, so it has no preformed disulfide bonds, which result in its insolubility. Incubation without DsbG is not enough to render it soluble, but DsbG can clearly solubilize it in a dose-dependent manner. This indicates that DsbG is involved in bond formation and not isomerization. Note that when the highest dose of DsbG was used, the proportion of solubilized cytoplasmic and periplasmic HcpE is the same as in the input samples, indicating that all insoluble cytoplasmic HcpE was solubilized. Full solubilization could also be obtained with the lowest amount of DsbG tested, provided that a longer incubation was performed (Figure 26A). In summary, the data show dose-

Figure 26: DsbG catalyzes the solubilization of insoluble HcpE *in vitro*. Enriched DsbG was incubated with insoluble HcpE that had been over-expressed from the pET30 construct under conditions favoring its insoluble form. Reactions were incubated in the presence or absence of increasing concentrations of enriched DsbG-Flag at 37˚C for 1 or 2 hrs to allow for catalysis to occur. The reactions were spun down and the solubilized HcpE recovered in the supernatant was resolved by SDS-PAGE. Solubilized HcpE was detected by Western blotting with anti-HcpE antibodies. Gradient (+DsbG) refers to the concentration of enriched DsbG-Flag added to each reaction: diluted 1:4, diluted 1:2 and undiluted (from anion exchange enrichment). HcpE was present as a doublet which is thought to reflect its cytoplasmic form with its signal peptide (HcpE +SP) and its periplasmic form without its signal peptide (HcpE -SP). The size difference between these two forms is 2.7 kDa. **Panel A:** Anti-HcpE Western blot and Ponceau red stain of reactions in the absence of wild-type *H. pylori* cell extracts. A dose-dependent response to DsbG is observed, resulting in increased soluble full-length HcpE +SP with increasing amounts of DsbG at 1 hr. A time-dependent response to DsbG is observed at 2 hrs, in which the lowest concentration of DsbG is able to solubilize HcpE +SP to the same level as the highest concentration of DsbG at 1 hr. Solubilization of periplasmic HcpE (HcpE -SP) occurs under the reaction conditions independent of DsbG (compare -DsbG with + DsbG; no difference in signal intensity). DsbG has no effect on the solubilization of truncated HcpE. **Panel B:** Anti-HcpE Western blot and Ponceau red stain of reactions done in the presence of wild-type *H. pylori* cell lysate. In the presence of *H. pylori* extract, which also contains endogenous DsbG, addition of extra DsbG has no effect on the solubilization of HcpE (compare –DsbG with + DsbG lanes). The cell extract was able to facilitate solubilization of HcpE on its own. The same unidentified *E. coli* protein, as seen in previous gels, was detected in this assay. Samples were analyzed twice, the same trend was observed.

A-

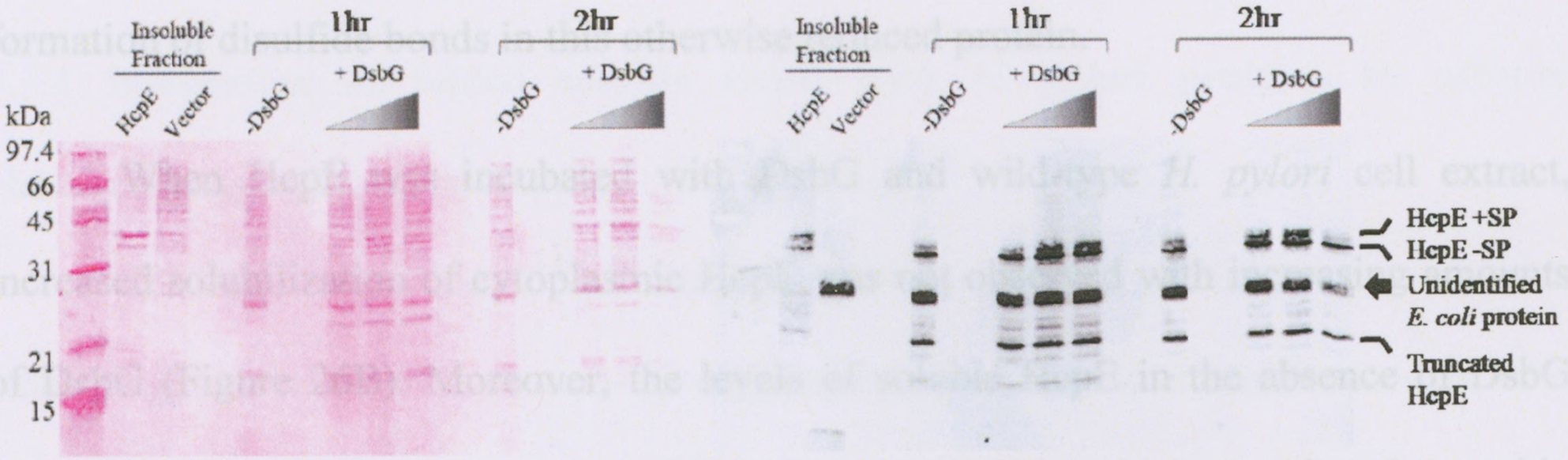
Insoluble Fraction
1hr
2hr
HcpE
Vector
-DsbG
+ DsbG
kDa
97.4
66
45
31
21
15
HcpE +SP
HcpE -SP
Unidentified
E. coli protein
Truncated
HcpE

B-

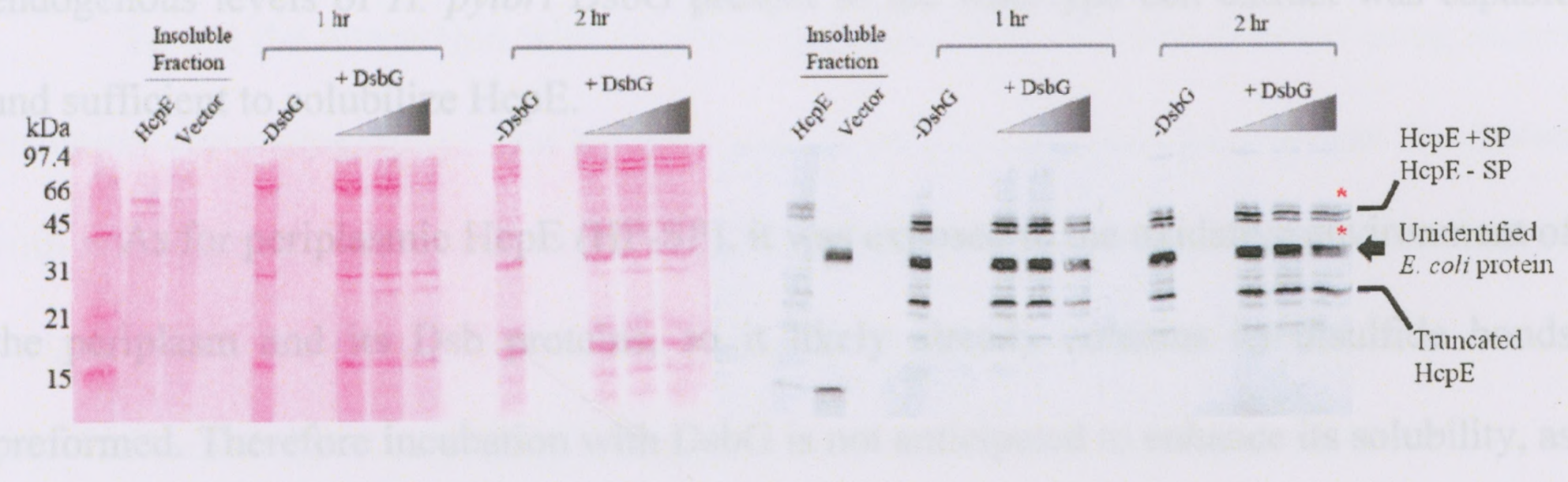
Insoluble Fraction
1 hr
2 hr
HcpE
Vector
-DsbG
+ DsbG
kDa
97.4
66
45
31
21
15
HcpE +SP
HcpE - SP
Unidentified
E. coli protein
Truncated
HcpE

and time-dependent solubilization of cytoplasmic HcpE by DsbG, presumably via formation of disulfide bonds in this otherwise reduced protein.

When HcpE was incubated with DsbG and wild-type *H. pylori* cell extract, increased solubilization of cytoplasmic HcpE was not observed with increasing amounts of DsbG (Figure 26B). Moreover, the levels of soluble HcpE in the absence of DsbG (marked -DsbG) but in the presence of *H. pylori* proteins is equivalent to that observed in the presence of increasing concentrations of DsbG. This observation indicates that endogenous levels of *H. pylori* DsbG present in the wild-type cell extract was capable and sufficient to solubilize HcpE.

As for periplasmic HcpE (HP-SP), it was exposed to the oxidative environment of the periplasm and its Dsb proteins, so it likely already contains its disulfide bonds preformed. Therefore incubation with DsbG is not anticipated to enhance its solubility, as observed. Since it was recovered in the insoluble fraction, it is likely that the final tertiary folding of this HcpE fraction had not occurred in this periplasmic environment but it was able to occur in the absence of specific folding factors under our reaction conditions at 37˚C (see mock samples –DsbG).

3.3 Intrinsic activity of HcpE

3.3.1 Interaction of folded soluble HcpE with *H. pylori* proteins by affinity chromatography interaction assay

The large proportion of SLR motifs in the sequence of HcpE suggests that native HcpE might be involved in protein-protein interactions. These interactions could be with host-cell proteins, which will be tested in a tissue culture system with human gastric cells, or with *H. pylori* proteins.

To test the interaction with *H. pylori* proteins, HcpE-His was purified using nickel chelation chromatography. The soluble, mature and folded pure protein was incubated with wild-type *H. pylori* cell extract in a 1:1 ratio for one hour to allow HcpE to find its partner within the extract and form a complex. The mixture was subjected to a second round of nickel chromatography followed by elution with an imidazole gradient.

In this method, interacting partners for the His-tagged proteins are anticipated to be found in fractions that elute before or with the His-tagged protein along the imidazole gradient. HcpE eluted early on in the imidazole gradient (5% imidazole), so the fractions where potential HcpE interacting partners may be found also contained numerous proteins that were loosely associated with the column matrix and are not interacting partners for HcpE. These non-specific proteins could be eliminated from further analysis by comparison of the protein profiles of equivalent fractions (same % imidazole) obtained with the TsaA control protein. In comparing these fractions (Figure 27A), a band of ~ 24 kDa that was present exclusively in fractions obtained with HcpE, which was not present in fractions obtained with TsaA, could clearly be visualized by

Figure 27: Protein-protein interaction assay based on affinity chromatography. A prospective interaction was identified for HcpE following the protein-protein interaction assay using affinity chromatography with histidine-tagged HcpE. *E. coli* over-expressed HcpE was purified by nickel chromatography and incubated with wild-type *H. pylori* cell lysate before being subjected to a second round of nickel chromatography to purify histidine tagged-HcpE and its associating interacting partner. **Panel A:** A distinct protein was identified in the HcpE fraction eluting at 5% imidazole (circled, red asterix), that was not present in the corresponding TsaA fraction at the same % imidazole. Full-length and truncated HcpE are marked by black asterix, TsaA is marked by yellow asterix, non-specific *E. coli* protein marked by pink arrow heads. **Panel B:** A distinct interacting partner was identified in fractions eluting at the same % imidazole as TsaA, 15 % (circle, red asterix), that was not present in HcpE fractions eluting at the same % imidazole (data not shown, no proteins eluted at 15% imidazole). Both interacting proteins (circled in panel A and B) were cut from the gels and sent to MS for protein identification following in gel-trypsinolysis. For the HcpE interaction, the protein recovered was HP0184 and for the TsaA interaction, the protein recovered was HP0129. To date, there is no known function for either protein.

A-

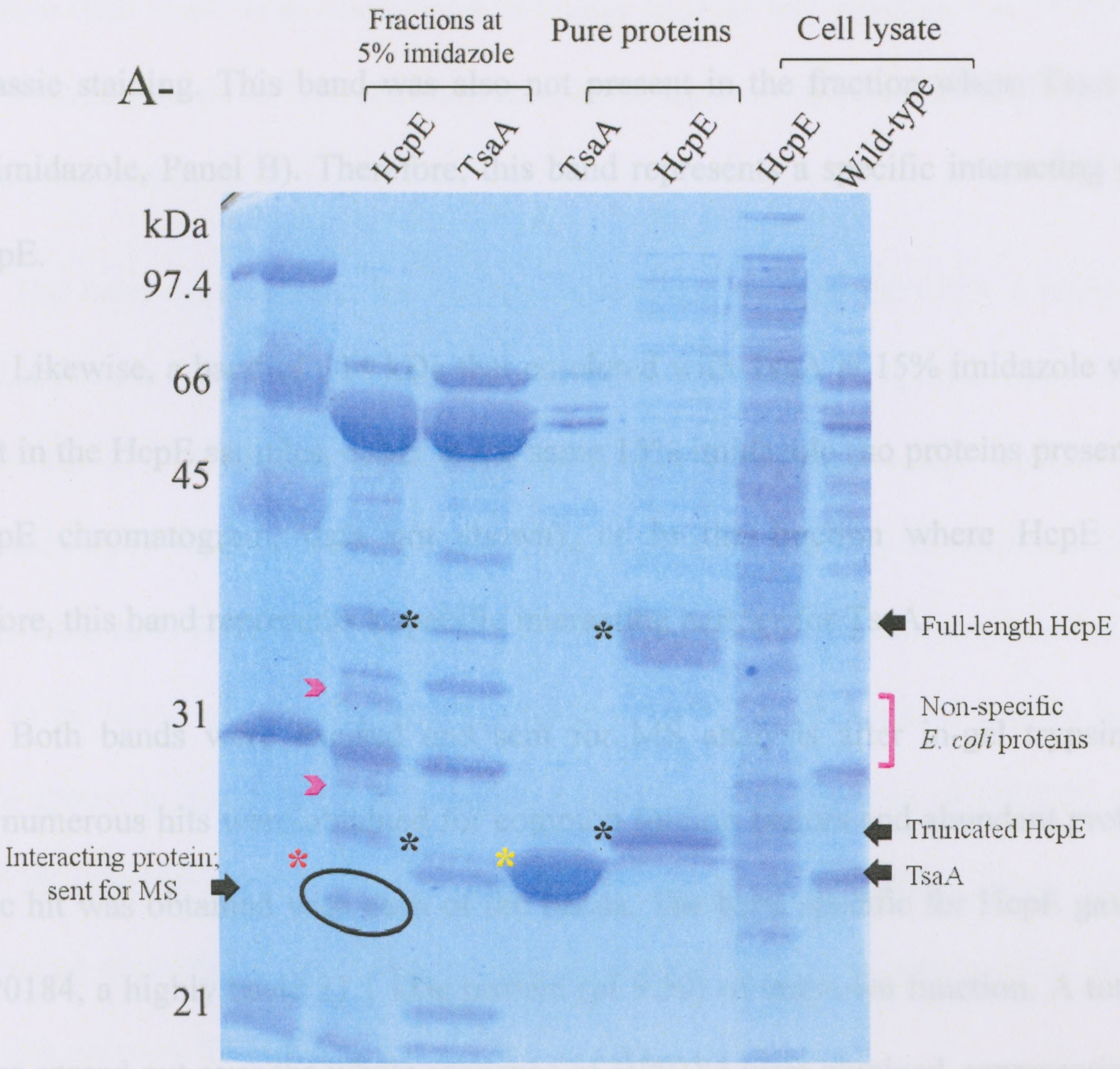
Fractions at 5% imidazole
Pure proteins
Cell lysate
HcpE
TsaA
TsaA
HcpE
HcpE
Wild-type
kDa
97.4
66
45
31
21
Full-length HcpE
Non-specific E. coli proteins
Truncated HcpE
TsaA
Interacting protein; sent for MS

B-

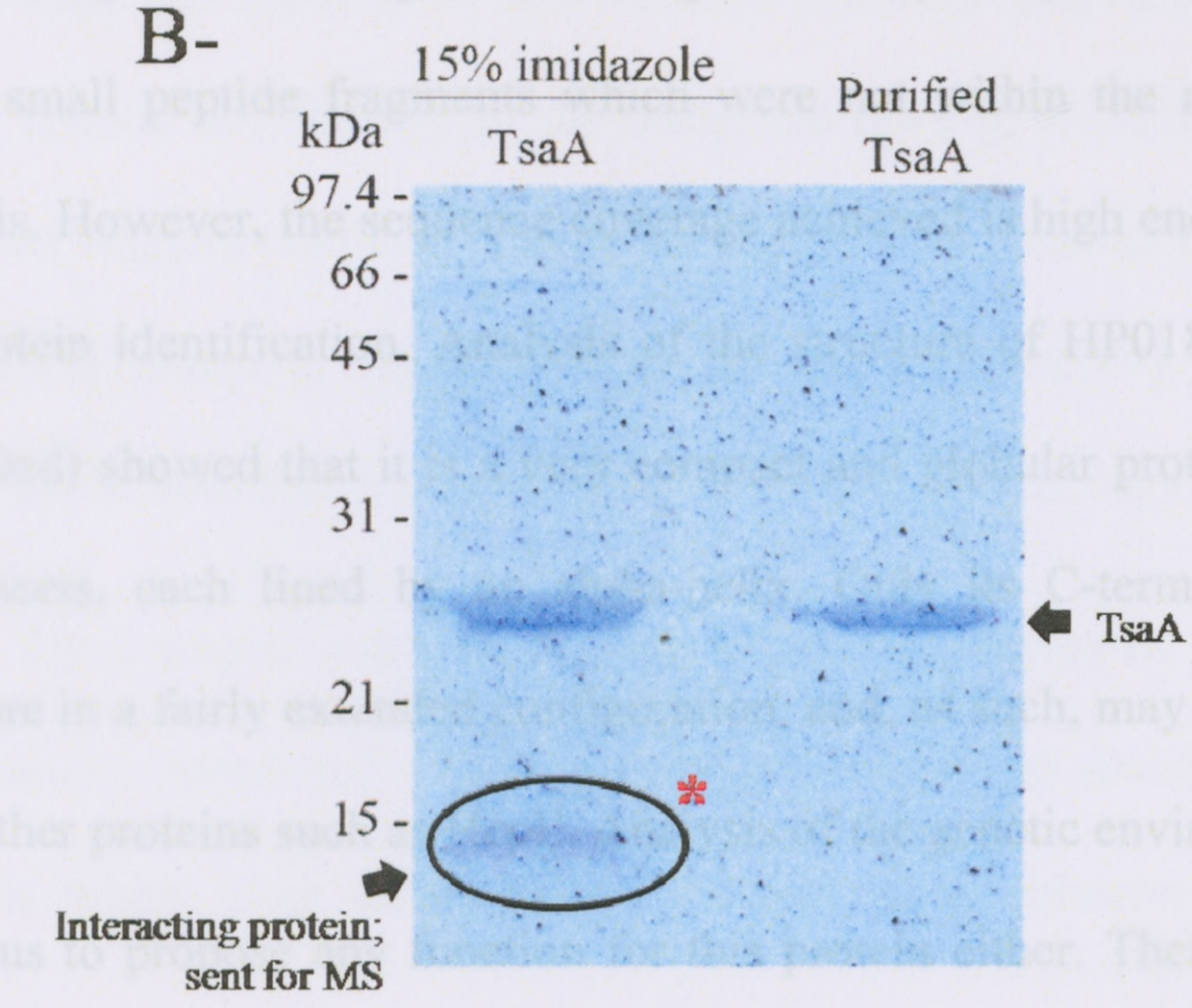
15% imidazole
Purified TsaA
TsaA
kDa
97.4
66
45
31
21
15
TsaA
Interacting protein; sent for MS

Coomassie staining. This band was also not present in the fraction where TsaA eluted (15% imidazole, Panel B). Therefore, this band represents a specific interacting partner for HcpE.

Likewise, a band of ~14 kDa that co-eluted with TsaA at 15% imidazole was not present in the HcpE samples, either at the same 15% imidazole (no proteins present at all in HcpE chromatogram, data not shown), or in the fraction where HcpE eluted. Therefore, this band represents a specific interacting partner for TsaA.

Both bands were excised and sent for MS analysis after in-gel trypsinolysis. While numerous hits were obtained for common folding factors and abundant proteins, a specific hit was obtained with each of the bands. The band specific for HcpE gave a hit for HP0184, a highly basic 21.1 kDa protein (pI 9.30) of unknown function. A total of 4 peptides spread out over the whole sequence of HP0184 were obtained, representing 22% of sequence coverage. The high content in Lys (10%) and Arg (5.6%) residues explains why the sequence coverage was not higher, as trypsinolysis of this protein would result in rather small peptide fragments which were not within the m/z range selected for the analysis. However, the sequence coverage achieved is high enough to have confidence in the protein identification. Analysis of the structure of HP0184 (PDB 2ATZ, no article published) showed that it is a very compact and globular protein comprised mostly of 3 beta-sheets, each lined by an alpha-helix. Only its C-terminus protrudes out of the structure in a fairly extended configuration, and, as such, may be involved in interactions with other proteins such as HcpE. Analysis of the genetic environment of HP0184 did not allow us to propose any function for this protein either. Therefore, the discovery of its

interaction with HcpE is not helpful at this stage to infer any function for HcpE. Future knockout mutagenesis of HP0184 may shed some light on its potential impact on HcpE secretion and function.

The band excised from the TsaA samples gave a hit for HP0129, a highly basic 16.4 kDa protein (pI 9.34) of unknown function. A total of 3 peptides were obtained, representing 22% of sequence coverage. Similar to HP0184, the high content of Lys (17%) and Arg (5 %) residues in HP0129 likely prevented recovery of additional peptides of significant size. HP0129 belongs to a family of proteins of unknown function which appear to be found exclusively in helicobacters. HP0129 has a signal peptide and was recently shown to be secreted (65). While determining the function of HP0129 and the role of its interaction with TsaA is beyond the scope of this study, these data were presented as controls to demonstrate that the method employed was suitable to detect interaction partners for HcpE in a specific manner.

3.3.2 HcpE does not confer resistance to β-lactam antibiotics in *H. pylori*

Hcps are specific to helicobacters and may play a role in maintenance of the typical cellular morphology of the bacterium (18). In *H. pylori*, the helical morphology facilitates flagella-mediated movement through the viscous epithelial mucosa allowing the bacteria to take up residence within the deeper layers (89). Thus, HcpE may indirectly play a role in virulence by contributing to cellular morphology.

The bacterial cell wall consists of multiple layers of peptidoglycan (PG) that is continuously remodeled allowing for cell growth and division. PG is a carbohydrate polymer whose long chains are maintained as a cohesive network by cross-linked

peptides. Penicillin Binding Proteins (PBPs) are bi-functional enzymes that have transpeptidase and transglycosylase activities that result in the local hydrolysis of PG. This activity is important as it allows for cell remodeling that supports cell growth and division (114). PBPs are inhibited by β-lactam antibiotics. β-lactamases are enzymes that hydrolyze the β-lactam ring of these antibiotics, thereby preventing their inhibitory action against PBPs. β-lactamases work in concert with PBPs and support cell survival, growth and division. A number of Hcps (A, B and D) have penicillin binding activity that is thought to be involved in PG biosynthesis, affecting cellular morphology and/ or division as well as enzymatic β-lactamase activity that may prevent inhibition of PBPs and may also support antibiotic resistance (36, 66); however, the biological signficance of such activity remains unknown.

Due to physiological relevance, we first sought to explore the β-lactamase activity of HcpE in *H. pylori*. For this, the differential susceptibility of the wild-type and *hcpE::kan* strains to various concentrations of ampicillin and carbenicillin was tested. Currently there is no literature outlining the minimum inhibitory concentration (MIC) for these antibiotics in *H. pylori*. To determine the appropriate antibiotic concentration to observe bacterial killing, a range of concentrations was tested beginning with 3-fold serial dilutions from 6 μg/mL to 0.02 μg/mL. At concentrations exceeding 2 μg/mL, bacterial killing was observed, so all future experiments were done with concentrations between 2 and 0.02 μg/mL. To assess the activity of HcpE in the presence of β-lactam antibiotics, bacterial strains grown in broth for 12 hrs were exposed to increasing concentrations of antibiotic for another 12 or 24 hrs to allow for 1 to 2 rounds of replication, in which the antibiotics could exert their activity. The cultures were then

serial diluted and spot plated on antibiotic free plates. Growth was monitored every 24-48 hrs.

It was predicted that if HcpE had β-lactamase activity, the mutant would be more sensitive to antibiotic exposure evidenced by reduced growth at higher antibiotic concentrations. However, observation of bacterial growth revealed the opposite. The mutant displayed enhanced growth at increasing antibiotic concentrations compared to wild-type *H. pylori* (Figure 28A and B). This contradictory finding suggested that the mutant was producing some extra surface component that provided resistance to antibiotic challenge. Moreover, thorough examination of the colonies on the *hcpE::kan* plates revealed that they were more mucoid in appearance compared to wild-type *H. pylori*. This mucoid appearance prompted comparison of the LPS produced by the wild-type and mutant strains. The findings of this comparison are discussed in section 3.4.1.

3.3.3 HcpE does not confer resistance to β-lactam antibiotics in *E. coli*

Due to the unexpected resistance of the *hcpE* mutant to antibiotic challenge, the intrinsic activity of HcpE as a β-lactamase could not be assessed in *H. pylori*. As a result, we tested the ability of over-expressed HcpE-His to confer resistance to β-lactam antibiotics in *E. coli* using the pET30-based protein expression system. The pET30 vector backbone does not encode for any β-lactamase activity that could interfere with the experiment. With this experimental system, HcpE-His could function in its natural environment and a steady supply of fresh HcpE-His could be ensured by continuous induction of protein expression with IPTG. *E. coli* strains carrying the pET30 vector with or without HcpE-His were inoculated, and after reaching log-phase growth cultures were

Figure 28: Assessing β-lactamase activity of HcpE in *H. pylori*. The proposed enzymatic activity of HcpE as a β-lactamase was assessed by testing wild-type and *hcpE::kan H. pylori* strains' susceptibility to β-lactam antibiotic exposure. If HcpE has β-lactamase activity, the mutant should be more sensitive to antibiotic exposure. Cultures were grown in the presence or absence of increasing concentrations of β-lactam antibiotics (ampicillin and carbenicillin) for 12 or 24 hrs. **Panel A:** Cultures grown in the presence of ampicillin. **Panel B:** cultures grown in the presence of carbenicillin for 12 hrs. To assess the differential susceptibility to antibiotic exposure, at each time point cultures were serially diluted (5-fold) and spot plated. Under all conditions tested, the mutant showed enhanced growth at higher antibiotic concentrations compared to the wild-type. Similar results were obtained for the 24 hr (not shown) antibiotic exposure. Figure is representative of three independent experiments.

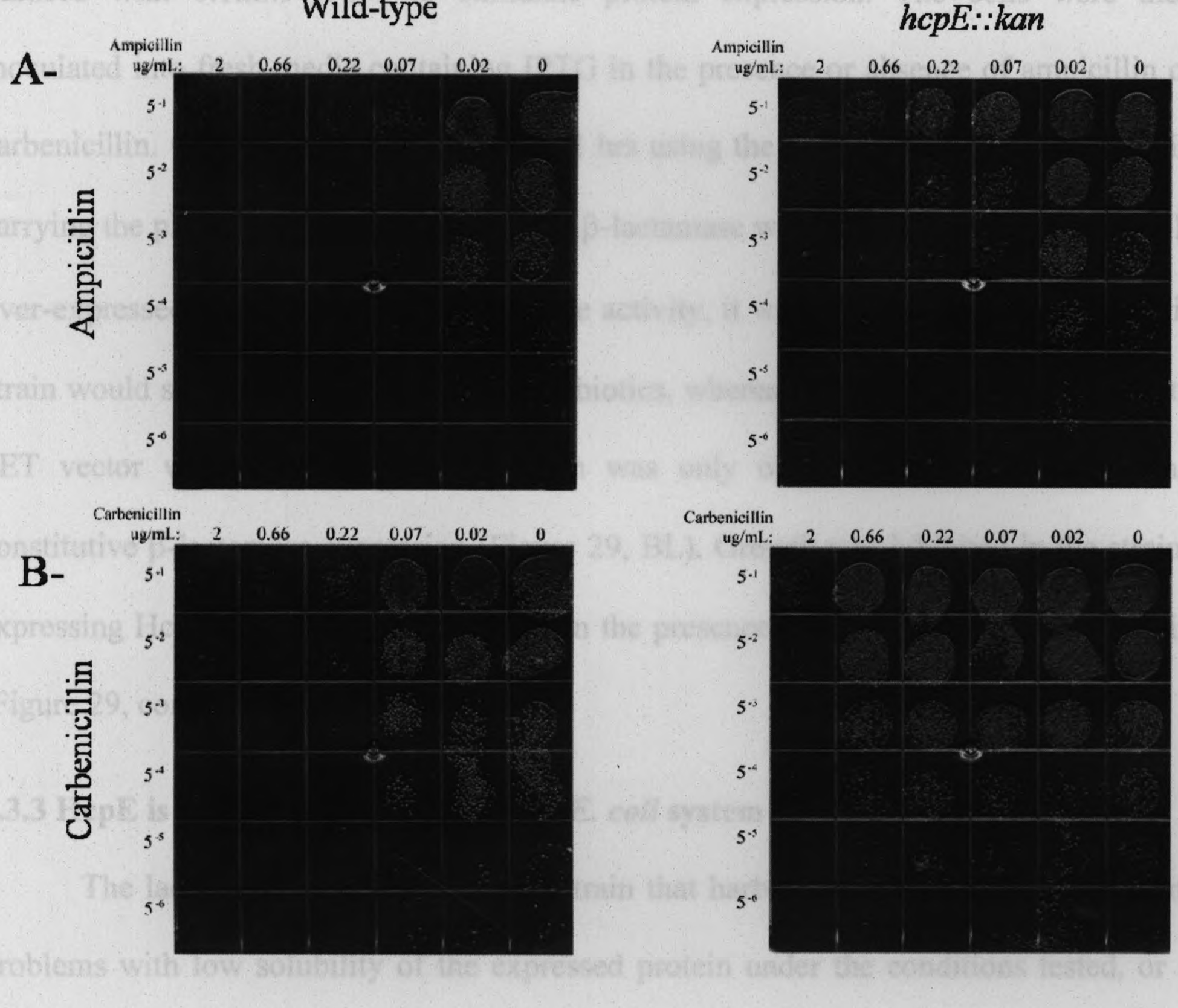
Wild-type
hcpE::kan
A-
Ampicillin
ug/mL: 2 0.66 0.22 0.07 0.02 0
5-1
5-2
5-3
5-4
5-5
5-6
Ampicillin
B-
Carbenicillin
ug/mL: 2 0.66 0.22 0.07 0.02 0
Carbenicillin

induced with 0.1mM IPTG to stimulate protein expression. The cells were then inoculated into fresh media containing IPTG in the presence or absence of ampicillin or carbenicillin. Growth was monitored for 22 hrs using the automated bioscreen. A strain carrying the pET23 vector which encodes a β-lactamase was used as a positive control. If over-expressed HcpE possessed β-lactamase activity, it was predicted that the HcpE-His strain would survive in the presence of antibiotics, whereas the strain carrying the empty pET vector would not. Sustained growth was only observed in strains possessing constitutive β-lactamase expression (Figure 29, BL). Growth was inhibited in the strains expressing HcpE-His or the empty vector in the presence of ampicillin and carbenicillin (Figure 29, compare HcpE+ with HcpE).

3.3.3 HcpE is soluble and secreted in the *E. coli* system

The lack of growth of the *E. coli* strain that harbors HcpE-His could arise from problems with low solubility of the expressed protein under the conditions tested, or a lack of protein secretion by the *E. coli* machinery, as opposed to a genuine lack of β-lactamase activity. Solubility, expression and secretion of HcpE in the *E. coli* induced cultures were monitored via Western blotting with anti-HcpE antibodies. Cell pellets and culture supernatants were immunoblotted for the presence of HcpE. When induced, HcpE was detected in large quantities in the cell pellets (Figure 30, red asterix), as expected for the insoluble protein. Low levels of HcpE were detected in the culture supernatants (blue asterix) indicating that a small portion of the HcpE produced in the *E. coli* system could be secreted by the native *E. coli* machinery. The low levels of secreted HcpE imply that in the absence of its specific folding factor, the process of secretion is rather inefficient. Secretion was possible in the *E. coli* system, as *E. coli*, as mentioned previously, contains

Figure 29: β-lactamase activity of HcpE-His in *E. coli* pET-expression system. The intrinsic enzymatic activity of HcpE-His was assessed in the *E. coli* over-expression system in the presence or absence of ampicillin or carbenicillin (not shown). In both cases, bacterial growth was inhibited in the presence of the β-lactam antibiotics, indicating an absence of enzymatic activity. Growth was monitored as a function of the OD_{600nm} of each strain using the automated bioscreen. A steady supply of HcpE-His was ensured by continuous induction of protein expression with IPTG. Vector refers to a strain carrying the empty pET30 vector used as a negative control; BL refers to a strain with constitutive β-lactamase expression in the vector backbone used as a positive control; + indicates the presence of antibiotic (ampicillin). Similar results were obtained in the presence of carbenicillin. Representative figure of two independent experiments.

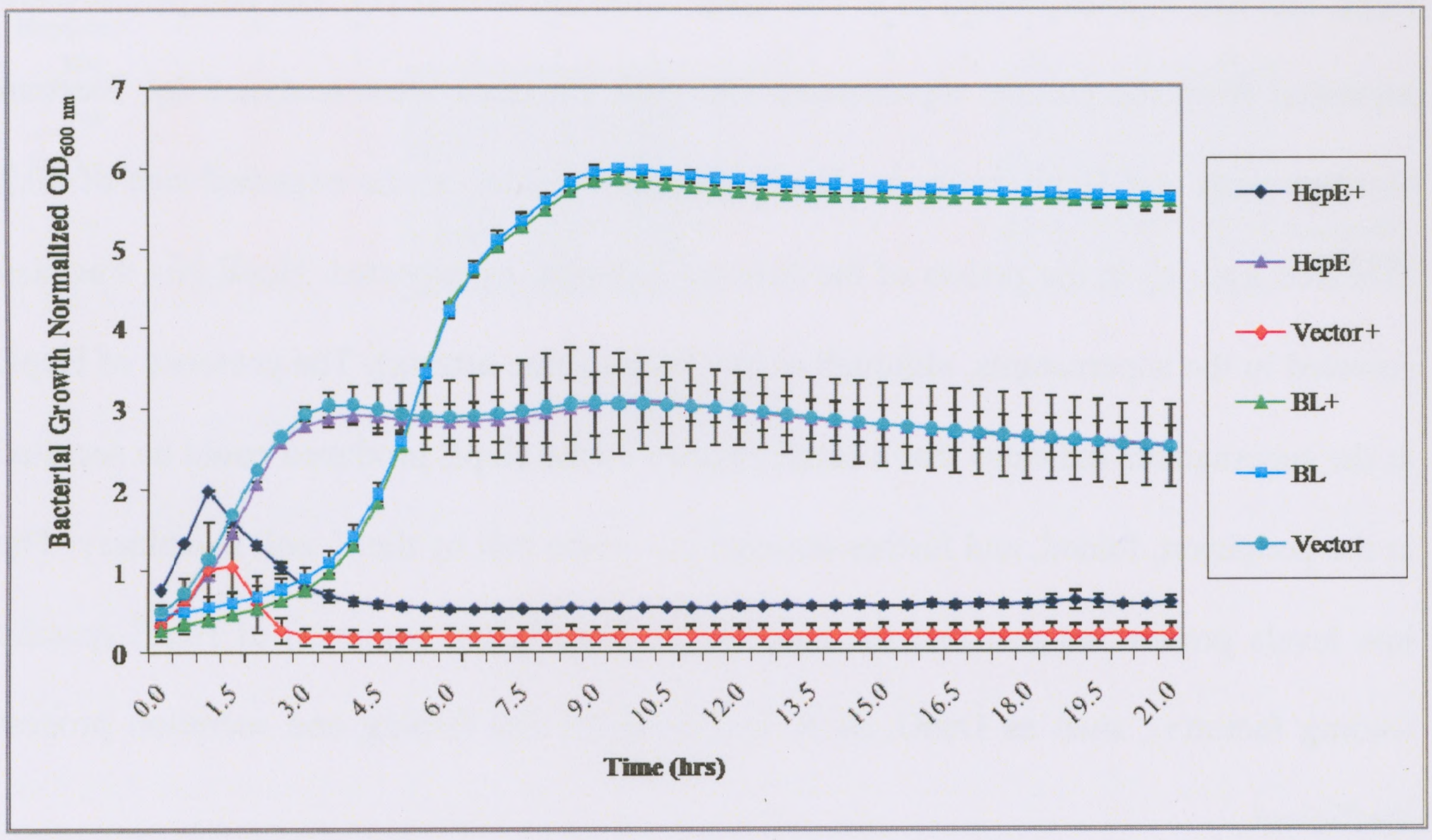
Bacterial Growth Normalized $OD_{600\ nm}$
7
6
5
4
3
2
1
0
0.0
1.5
3.0
4.5
6.0
7.5
9.0
10.5
12.0
13.5
15.0
16.5
18.0
19.5
21.0
Time (hrs)
HcpE+
HcpE
Vector+
BL+
BL
Vector

Figure 30: Demonstration that over-expressed HcpE-His is also secreted by *E. coli*. HcpE-His was over-expressed in *E. coli* upon induction with IPTG. The cell pellets were separated from the culture supernatants and both fractions were analyzed by Western blotting using anti-HcpE antibody. HcpE-His was detected at the expected size of 40.2 kDa (red asterix) in the pellets of the induced cultures, as expected. HcpE-His was also detected in the supernatants, although at low levels (blue asterix). The presence of HcpE in the supernatants indicates that a small fraction of the HcpE produced could be secreted to the periplasm, folded, and further secreted out of the cell by the *E. coli* machinery. The low levels present suggest that the absence (or insufficient amounts) of HcpE-specific folding factor(s), such as DsbG, in *E. coli* rendered the folding and secretion process inefficient.

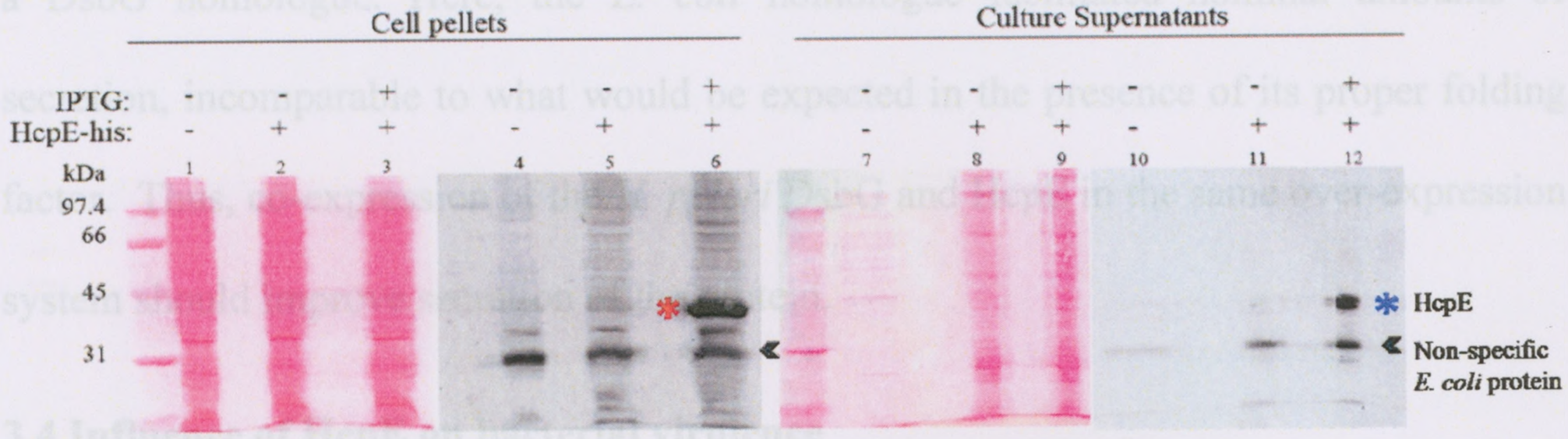
Cell pellets
Culture Supernatants
IPTG:
HcpE-his:
kDa
97.4
66
45
31
1
2
3
4
5
6
7
8
9
10
11
12
HcpE
Non-specific
E. coli protein

a DsbG homologue. Here, the *E. coli* homologue facilitated nominal amounts of secretion, incomparable to what would be expected in the presence of its proper folding factor. Thus, co-expression of the *H. pylori* DsbG and HcpE in the same over-expression system should improve secretion of the protein.

3.4 Influence of HcpE on bacterial virulence

3.4.1 HcpE mutant produces more LPS

Gram-negative bacteria are known to alter the expression of their cell surface components in the face of stress. These changes encompass the bacterial LPS, as it the outermost barrier to the cell (127). It has been shown that when grown in broth, bacteria lengthen their O-antigen chain changing from rough to smooth form (26), and when these bacteria are returned to growth on plates, they will revert to their original rough form.

The enhanced resistance to antibiotic exposure and mucoid colonies generated by the *hcpE::kan* strain prompted investigation into its LPS profile. LPS was isolated from wild-type *H. pylori* and the mutant strain using the classic Hitchcock & Brown method of preparation (58). Extracted LPS was analyzed following separation by SDS-PAGE gel electrophoresis and visualization by silver staining. Our wild-type *H. pylori* exhibited normal LPS distribution (Figure 31A, lane 1) characterized by a prominent lipid-A plus core region at the bottom of the gel and a less prominent lipid-A-core plus O-antigen region in the upper region of the gel, with the distinct banding pattern characteristic of *H. pylori* LPS. Compared to wild-type LPS, *hcpE::kan* appeared to be producing more LPS, evidenced by a more intense band in the O-antigen region (arrow) and less intense expression of its lipid-A plus core region. From this alone, it is not clear whether this

Figure 31: Analysis of wild-type and *hcpE::kan* LPS profiles. Comparison of the LPS profiles of wild-type (Lanes 1, 3) and *hcpE* mutant (Lanes 2, 4) *H. pylori* by silver staining. The mutant shows increased O-antigen production (arrow) compared to wild-type levels. **Panel A:** LPS extracted from bacteria grown on plates, **Panel B:** LPS extracted from bacteria grown in liquid media for 12 hrs. In both cases, LPS was extracted using standard Hitchcock & Brown protocol and was resolved by SDS-PAGE (18%).

A- Growth on Plates

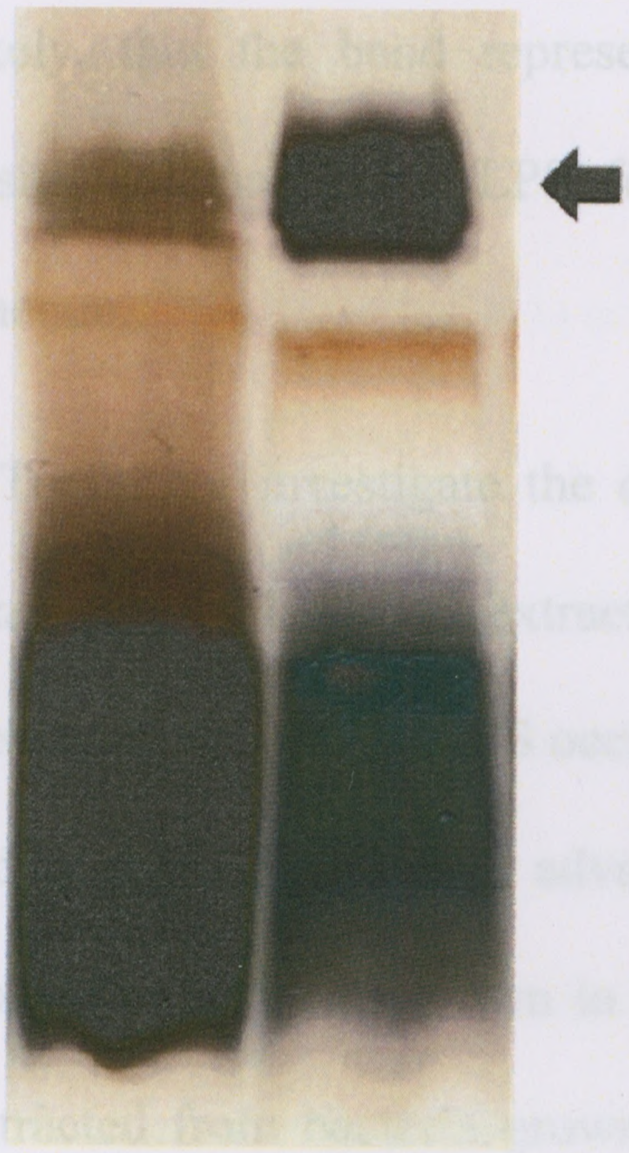

B- Growth in Liquid

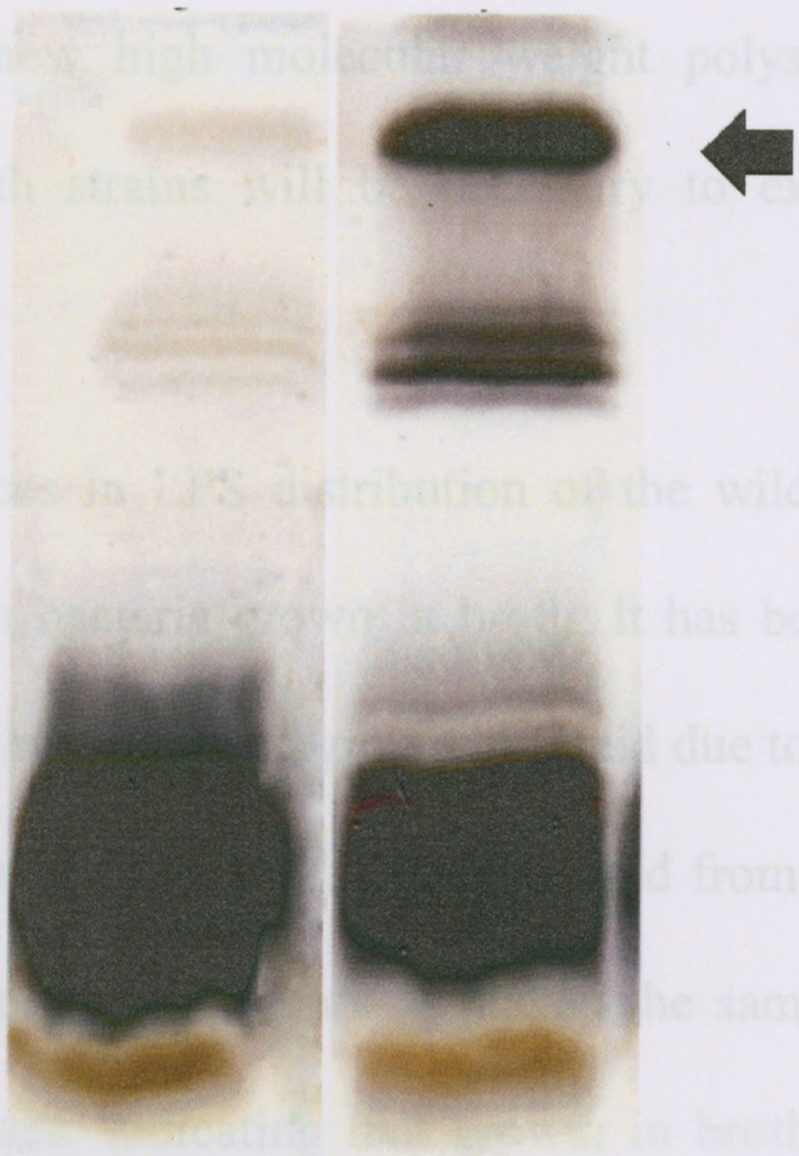

dark region reflects an up-regulation and/or re-distribution of one of the classic *H. pylori* polysaccharides, or the lengthening of its O-antigen chains. It is also possible, although less likely, that the band represents a new high molecular weight polysaccharide. Compositional analysis of LPS from both strains will be necessary to explain this phenomenon.

To further investigate the differences in LPS distribution of the wild-type and *hcpE::kan* strains, LPS was extracted from bacteria grown in broth. It has been shown that alterations to bacterial LPS occur more readily when grown in liquid due to the stress imposed on the bacteria under adverse growth conditions. LPS extracted from wild-type and *hcpE::kan H. pylori* grown in broth culture for 12 hrs displayed the same trend as LPS extracted from bacteria grown on plates, indicating that growth in broth does not impose additional alterations to the LPS profile (Figure 31 A and B). When grown in broth the mutant continues to produce additional LPS compared to the wild-type (Figure 31B, arrow).

3.4.2 Effects of HcpE on the interaction of *H. pylori* with gastric cells

3.4.2.1 HcpE is secreted by wild-type *H. pylori* when infecting AGS cells

To assess the *in vivo* effect of HcpE on infected AGS cells, we had to ensure that the protein was being expressed and secreted under the infection conditions. To promote growth of the AGS cells, infection was not under the ideal microaerophilic conditions that *H. pylori* requires for growth. Since growth under suboptimal conditions could alter the bacterium's normal secretion patterns, its ability to secrete HcpE while infecting AGS monolayers was assessed. Supernatants were collected at 5 and 10 hpi and the presence

of HcpE was assessed by Western blotting with the anti-HcpE antibodies after TCA precipitation of the proteins. HcpE was detected when AGS cells were infected with (a) total cells, and (b) supernatants from overnight growth in broth, as well as in the absence of AGS cells (Figure 32). This indicated that HcpE was secreted under suboptimal conditions and that secretion was not affected by the presence of AGS cells.

Secreted HcpE was stable enough to be detected in this system up to 10 hpi. Moreover, detection of HcpE after infection with *H. pylori* supernatants from the O/N growth in broth media demonstrates the stability of the protein, as all HcpE detected was secreted by the bacteria before infection of the AGS cells. Thus, if HcpE exerts an effect on AGS cells *in vivo*, its effect should be observed in this *in vitro* system as it is secreted and stable within the time frame allotted for this experiment.

3.4.2.2 Inactivation of *hcpE* does not prevent acquisition of hummingbird phenotype

Infection of gastric cells by *H. pylori* has been shown to induce structural changes that correspond to disruption of and/or alterations in basic cell signaling pathways (118). The most prominent alteration observed has been termed the hummingbird phenotype, demonstrated by the extreme elongation of gastric cells. This phenotype has typically been attributed to the presence of the CagA toxin secreted by the *cag*PI, as *cagA*- strains do not induce the same effect (116). As a result, this phenotype has been attributed to increased virulence associated with *H. pylori type I* strains, poorer prognosis and progression to active gastritis (7).

To assess whether our wild-type and *hcpE::kan* strains induce the classic hummingbird phenotype in infected AGS cells, microscopic examination was performed

Figure 32: Detection of HcpE in the supernatants of infected AGS monolayers. To characterize the role of HcpE during infection, wild-type and *hcpE::kan H. pylori* strains were used to infect AGS monolayers. AGS cells were infected with total bacterial cultures or culture supernatants obtained from 12 hrs growth of *H. pylori* in broth. HcpE was detected in the supernatants of AGS cells infected with total cells and culture supernatants at both 5 hpi (Panel A) and 12 hpi (Panel B) by Western blotting with anti-HcpE antibody. HcpE was continuously produced, and secreted by wild-type *H. pylori* in the presence or absence of AGS cells at similar levels (compare total cells +AGS with -AGS). HcpE detected in AGS monolayers infected with culture supernatants reflects the stability of secreted HcpE, as the HcpE detected was secreted during the 12 hr growth in broth, before infection of the AGS monolayers. Uninfected AGS cells and media (F12K media + brucella broth) served as negative controls for non-specific reactivity of the anti-HcpE antibody. Experiment was repeated three times and similar results were obtained in each independent trial.

A- 5hpi

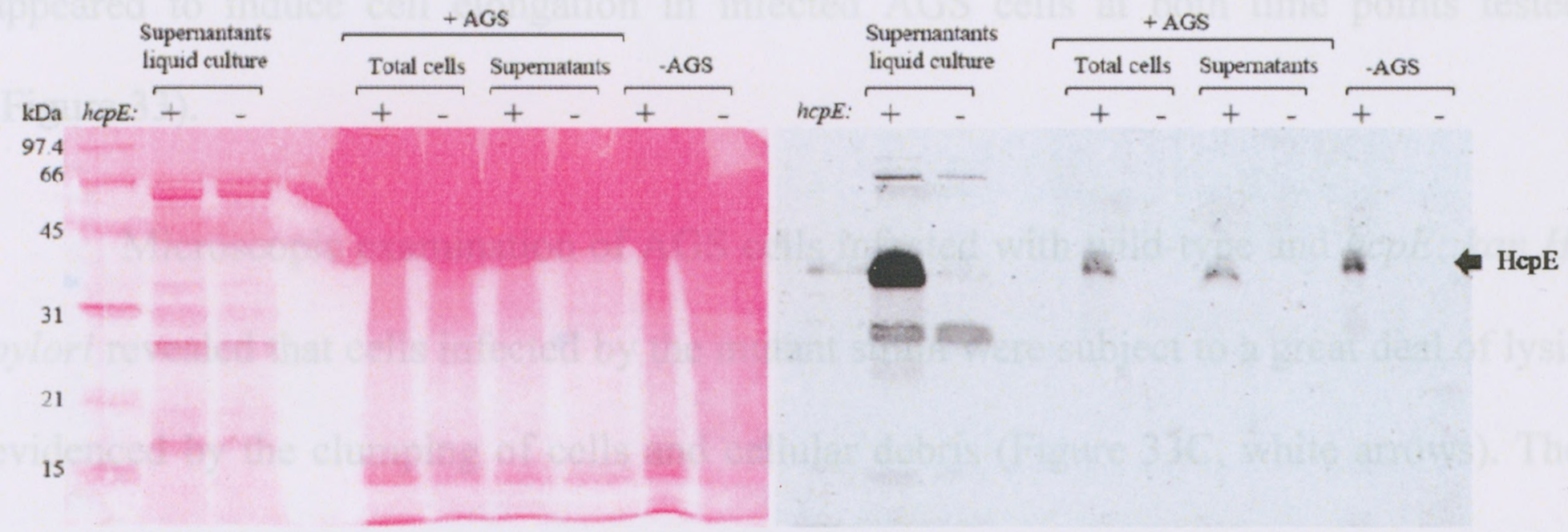

B- 12hpi

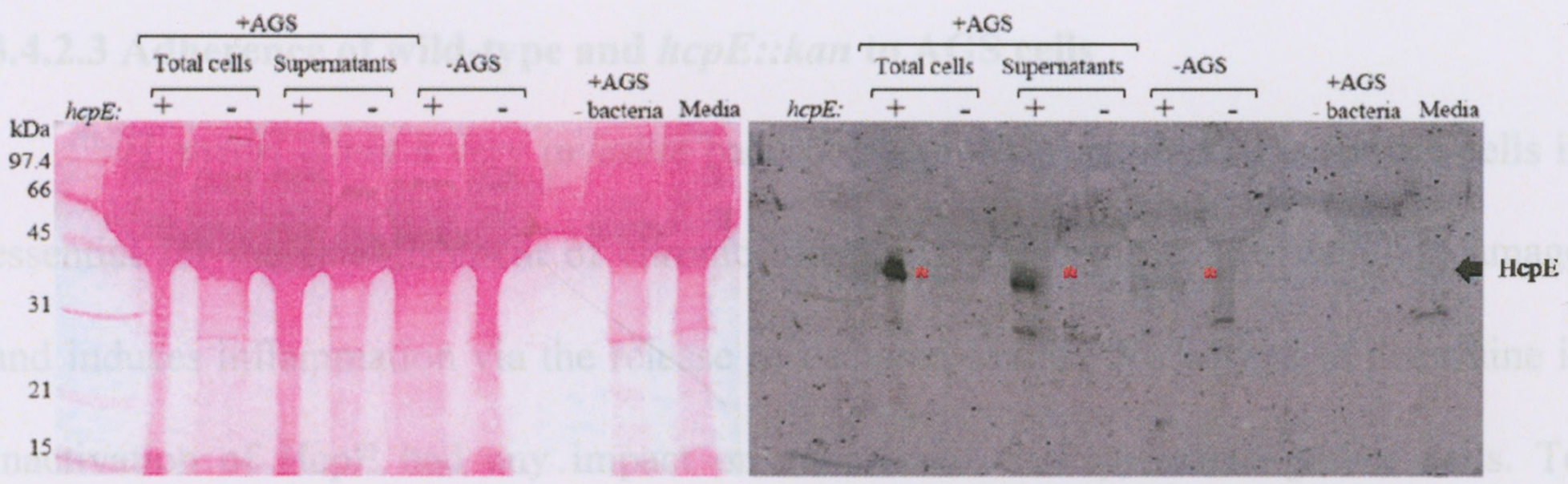

on AGS monolayers that had been infected with *H. pylori* for 5 or 10 hrs. Both strains appeared to induce cell elongation in infected AGS cells at both time points tested (Figure 33).

Microscopic examination of AGS cells infected with wild-type and *hcpE::kan H. pylori* revealed that cells infected by the mutant strain were subject to a great deal of lysis evidenced by the clumping of cells and cellular debris (Figure 33C, white arrows). The source of this phenotype has yet to be determined, but it could be a result of extra LPS released by the mutant which is less viable, and dies under the growth conditions.

3.4.2.3 Adherence of wild-type and *hcpE::kan* to AGS cells

H. pylori is not a very invasive bacterium; however, adherence to gastric cells is essential for the establishment of chronic infections. Adhesion causes cellular damage and induces inflammation via the release of bacterial toxins. We wished to determine if inactivation of HcpE had any impact on adherence of *H. pylori* to gastric cells. To determine the percent of bacteria that adhere to AGS cells after 5 and 10 hrs of infection, the culture supernatants were recovered and the AGS monolayers were washed thoroughly to remove all unbound bacteria. Bacteria that adhered were released via treatment with 0.08% saponin, a mild detergent that is capable of lysing the gastric cells without affecting the viability of the bacteria. The bacteria were enumerated by counting CFUs of the recovered bacteria that were serially diluted and spot plated.

Preliminary qualitative experiments revealed that the knockout mutant was less viable under the tissue culture growth conditions in the absence of gastric cells. Quantitative comparison of viability of wild-type and *hcpE::kan* strains revealed that for

Figure 33: Induction of the hummingbird phenotype in infected AGS cells. Infection of AGS cell monolayers for 5 or 10 hrs with wild-type (B) and *hcpE::kan* (C) *H. pylori* lead to the acquisition of the hummingbird phenotype. This effect reflects changes in cell signaling networks and is characterized by the elongation and spreading of cells compared to uninfected AGS cells that remain unchanged (A). In *hcpE::kan* infected cells, AGS monolayers began to lyse, illustrated by the clumping of cells and an abundance of cellular debris at 5 hpi, which persisted until 10 hpi (white arrows, enlarged). 100X magnification.

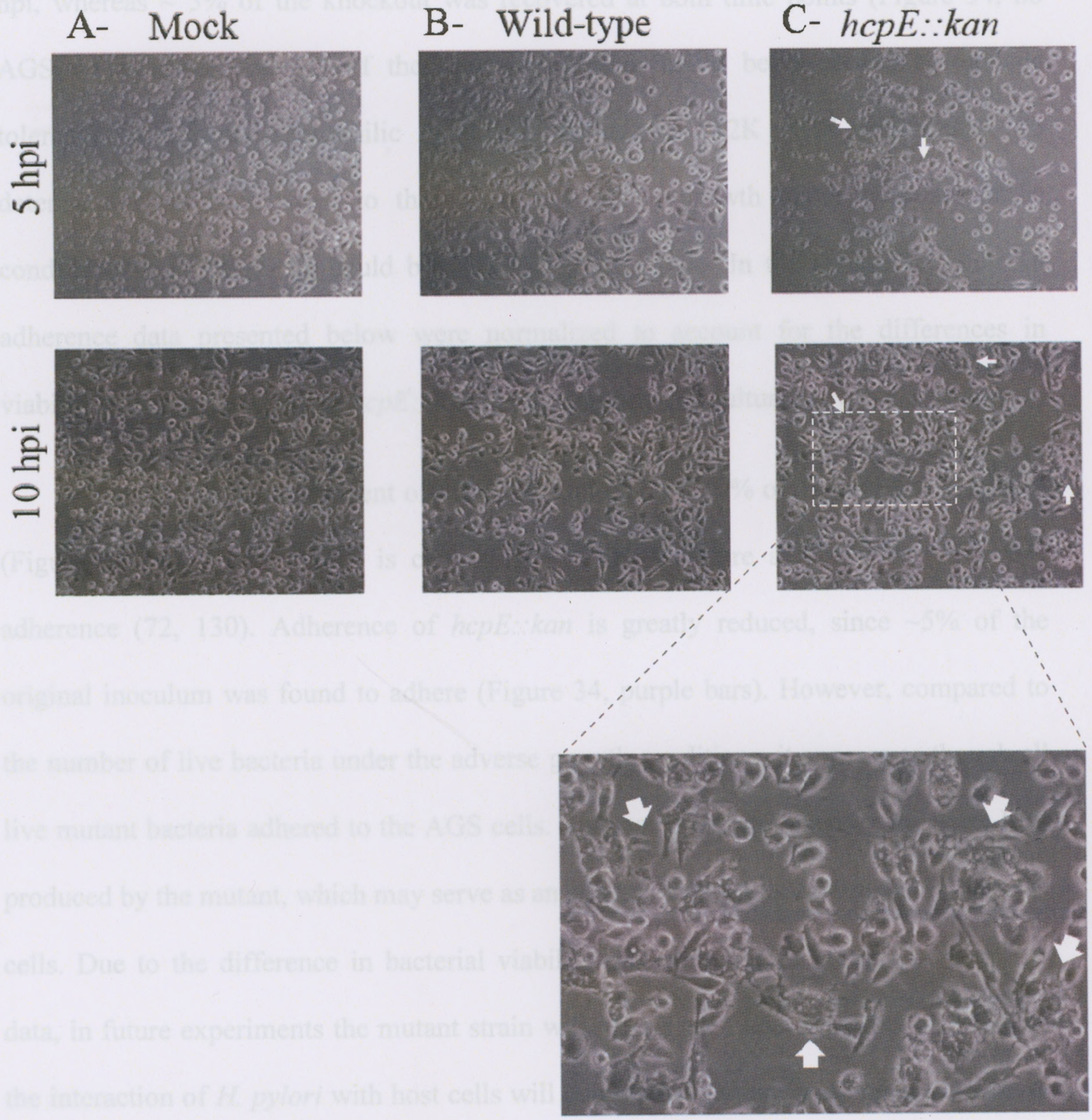
A- Mock
B- Wild-type
C- hcpE::kan
5 hpi
10 hpi

our wild-type *H. pylori*, 20-25% of the initial bacterial input was recovered at 5 and 10 hpi, whereas ~ 5% of the knockout was recovered at both time points (Figure 34, no AGS). The lower viability of the knockout mutant could be attributed to reduced tolerance to non-microaerophilic conditions or to the F12K AGS cell media. To determine what contributed to the reduced viability, growth under microaerophilic conditions in F12K media could be assessed in the future. In the meantime, bacterial adherence data presented below were normalized to account for the differences in viability of our wild-type and *hcpE::kan* strains under tissue culture growth conditions

For wild-type, the percent of adhering bacteria is 9-10% of the original inoculum (Figure 34 blue bars), which is comparable to the literature available for *H. pylori* adherence (72, 130). Adherence of *hcpE::kan* is greatly reduced, since ~5% of the original inoculum was found to adhere (Figure 34, purple bars). However, compared to the number of live bacteria under the adverse growth conditions, it appears as though all live mutant bacteria adhered to the AGS cells. This could be explained by the extra LPS produced by the mutant, which may serve as an adhesin facilitating adherence to the AGS cells. Due to the difference in bacterial viability that complicates interpretation of the data, in future experiments the mutant strain will not be used and the effect of HcpE on the interaction of *H. pylori* with host cells will be assessed via antibody neutralization or via the use of the purified protein.

Figure 34: Bacterial adherence to AGS monolayers. Bacterial adherence to AGS cells was calculated based on the number of CFUs of the original input recovered at 5 and 10 hpi. Wild-type *H. pylori* displayed increased adherence compared to the mutant; however the mutant displayed reduced viability under the non-microaerophilic growth conditions. Bacteria recovered in the absence of AGS cells (marked "no AGS") represent all live bacteria and are presented to compare viability of the wild-type and *hcpE::kan* under tissue culture growth conditions. All data were normalized to the viability of each strain. The graph represents the average of three independent experiments. Blue bars represent the wild-type and purple bars represent *hcpE::kan*.

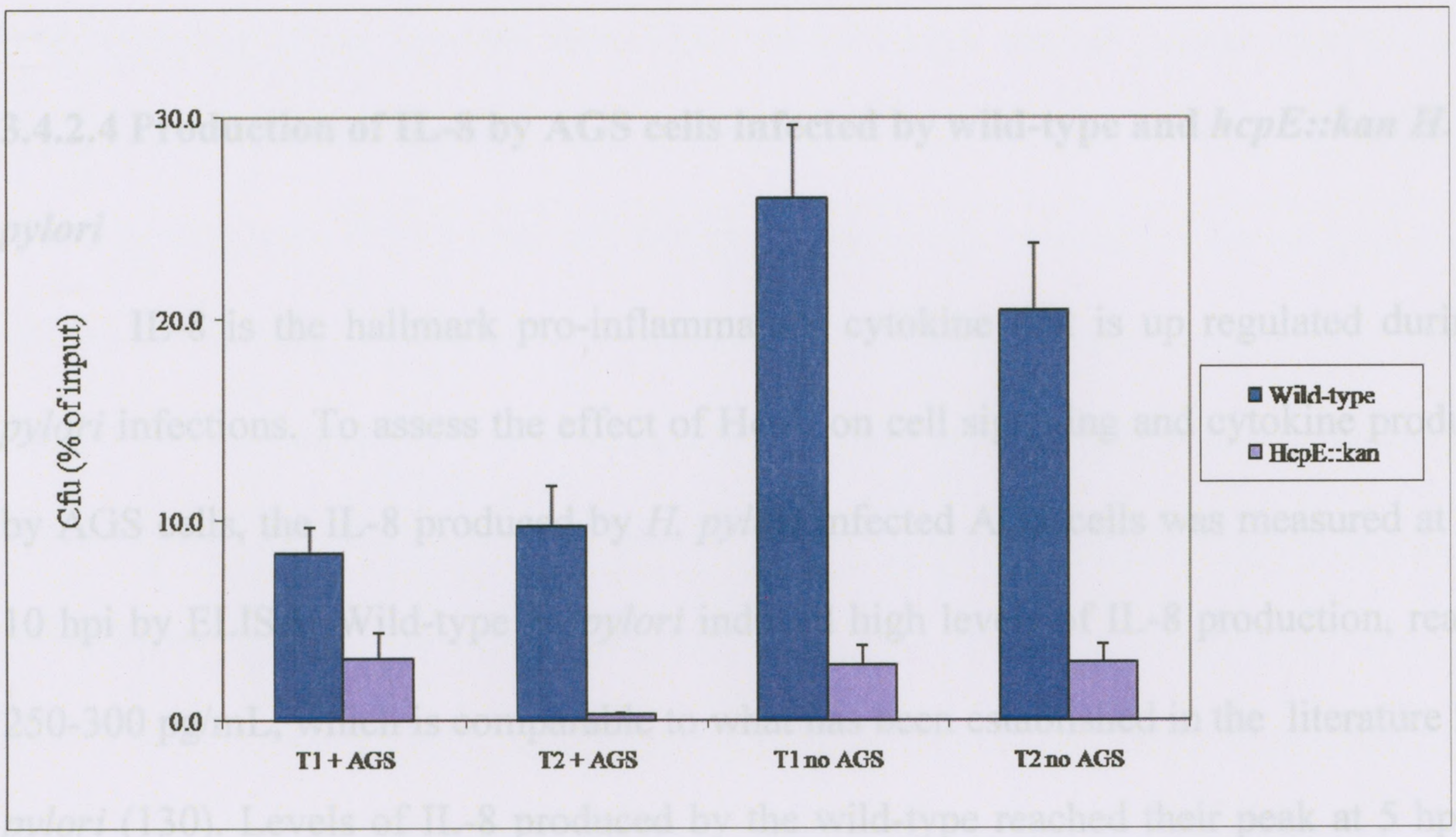
30.0
20.0
10.0
0.0
Cfu (% of input)
T1 + AGS
T2 + AGS
T1 no AGS
T2 no AGS
Wild-type
HcpE::kan

3.4.2.4 Production of IL-8 by AGS cells infected by wild-type and *hcpE::kan H. pylori*

IL-8 is the hallmark pro-inflammatory cytokine that is up regulated during *H. pylori* infections. To assess the effect of HcpE on cell signaling and cytokine production by AGS cells, the IL-8 produced by *H. pylori* infected AGS cells was measured at 5 and 10 hpi by ELISA. Wild-type *H. pylori* induced high levels of IL-8 production, reaching 250-300 pg/mL, which is comparable to what has been established in the literature for *H. pylori* (130). Levels of IL-8 produced by the wild-type reached their peak at 5 hpi, and remain constant until 10 hpi (Figure 35; compare wild-type T1 and T2). The mutant displayed reduced IL-8 production compared to wild-type at 5 hpi, reaching 120 pg/mL. IL-8 production induced by the mutant appeared to be delayed and reached similar levels as the wild-type by 10 hpi. The difference in IL-8 production is correlated with the number of AGS cells that experienced an alteration in signaling as indicated by observation of the hummingbird phenotype by microscopy. For the wild-type 35-40% of AGS cells took on the hummingbird phenotype compared to 12-15% of AGS cells infected by the mutant (Figure 35, panel B and C).

Wild-type and *hcpE::kan* culture supernatants, obtained from the 12 hr growth of *H. pylori* in broth, were not able to induce the acquisition of the hummingbird phenotype, nor the signaling cascade that results in IL-8 production (Figure 35A, E, and F). IL-8 production levels were similar to uninfected and media controls (Figure 35A, D, and G).

The delay in signaling and reduction in the number of live bacteria recovered at 10 hpi could be attributed to the observed death of the AGS cells infected with

Figure 35: Alterations in cell signaling by AGS cells infected with wild-type and *hcpE::kan H. pylori.* Induced IL-8 production and changes in cell morphology characterized by the acquisition of the hummingbird phenotype were measured to assess the effect of HcpE on cellular signaling. AGS cells were infected with total cell pellets from growth of wild-type and *hcpE::kan* in liquid culture and the corresponding culture supernatants (refer to methods 2.23 for details). **Panel A:** IL-8 production was quantified by ELISA. The graph presented represents the trend observed in two independent experiments. AGS refers to uninfected monolayers (no *H. pylori*), and Media + AGS refers to monolayers incubated in mixed media (brucella broth + F12K), used as negative controls for basal levels of IL-8 secretion. T1; 5 hpi and T2; 10 hpi. **Panels B-G**: Microscopy of AGS cells infected with wild-type total bacteria (B), *hcpE::kan* total bacteria (C), wild-type supernatants (D), *hcpE::kan* supernatants (E), uninfected AGS cells (F), or AGS cells incubated with mixed media (brucella broth and F12K; G). Levels of IL-8 produced (pg/mL) correlate with the percentage of cells that display altered signaling patterns by microscopy.

A- IL-8 production

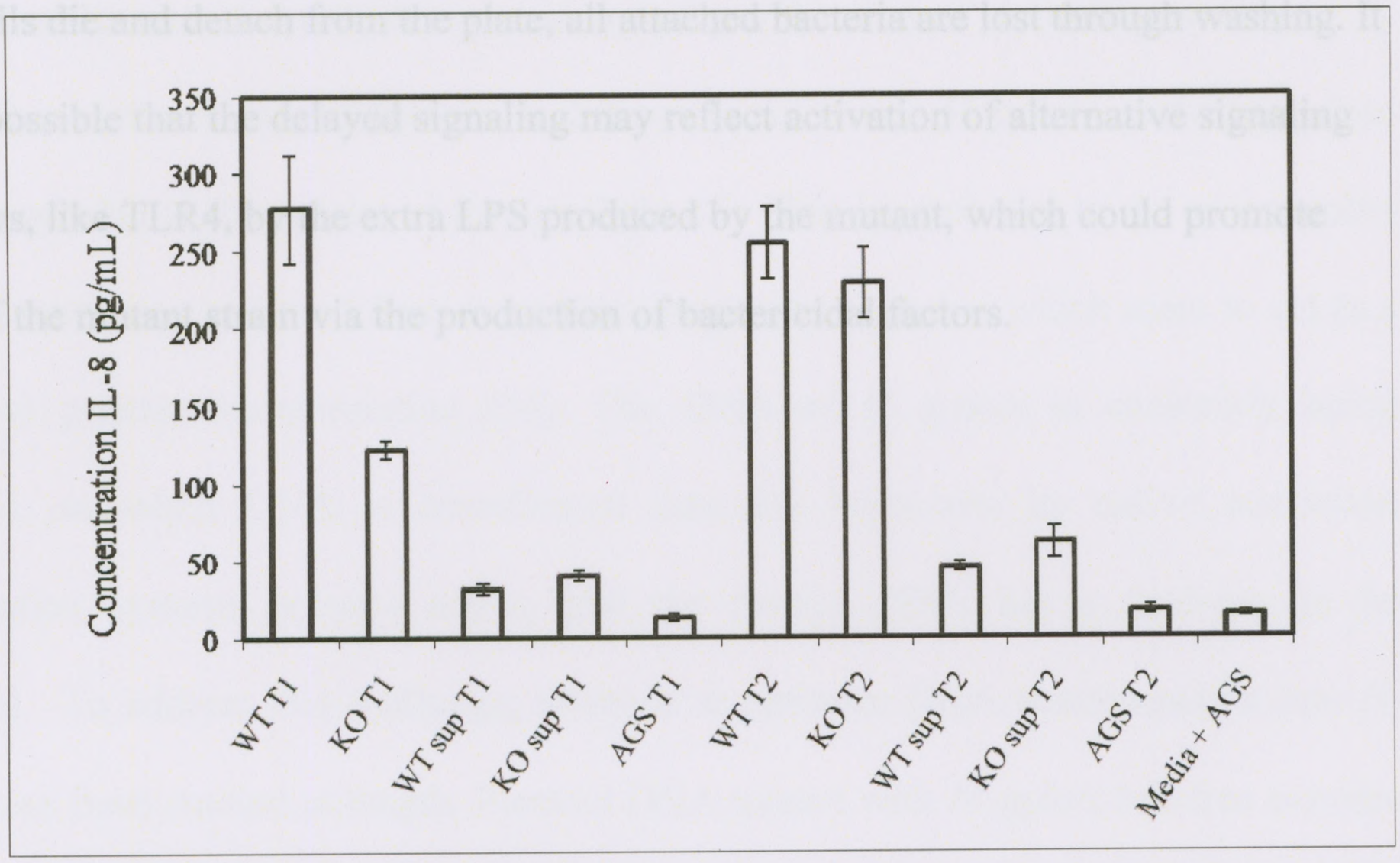

B- Wild-type

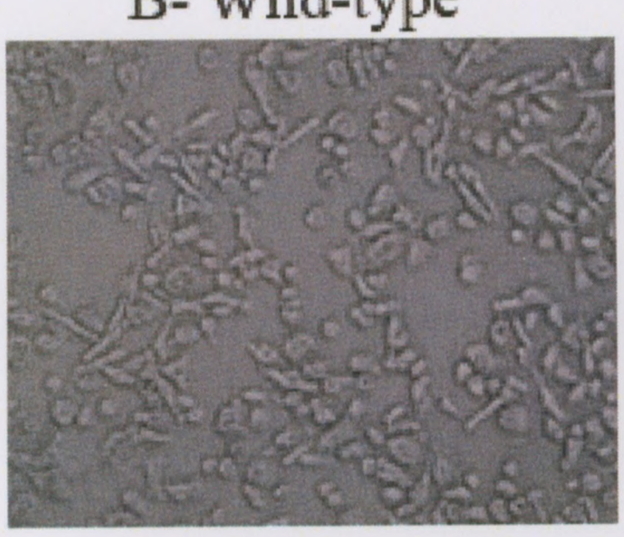

C- *hcpE::kan*

D- AGS (Mock)

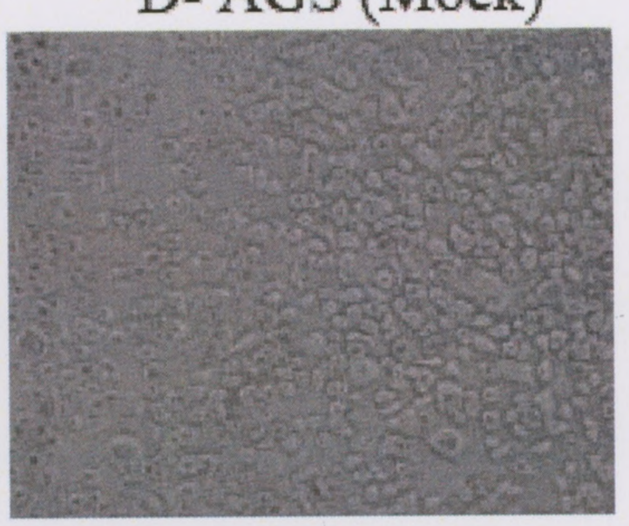

E- Wild-type supernatant

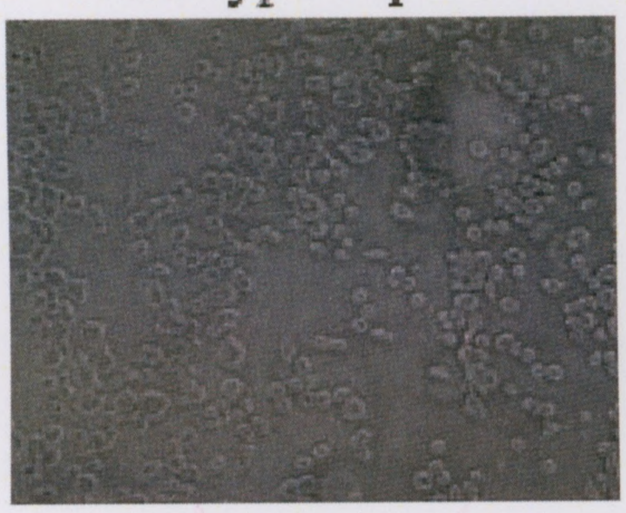

F- *hcpE::kan* supernatant

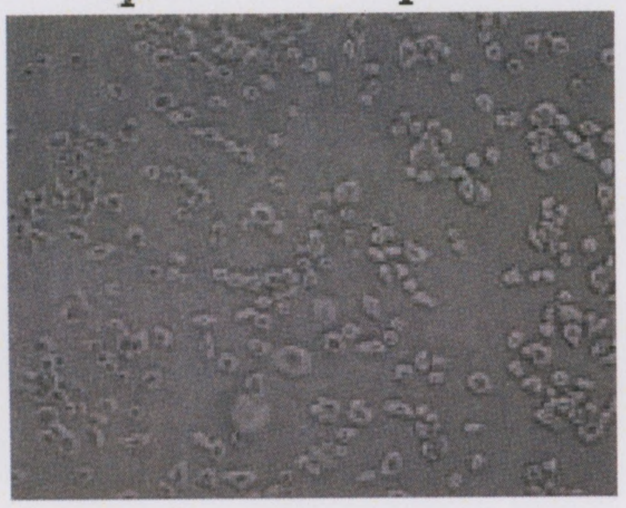

G- Media (Brucella broth +F12K)

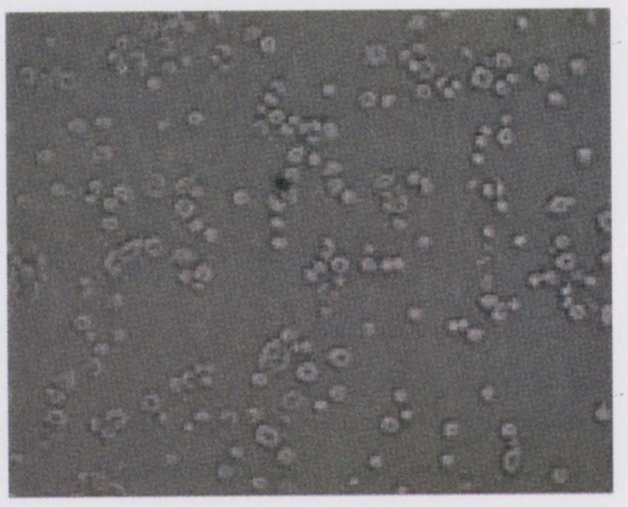

hcpE::kan. When the AGS cells die, fewer live *hcpE::kan* are recovered because as the AGS cells die and detach from the plate, all attached bacteria are lost through washing. It is also possible that the delayed signaling may reflect activation of alternative signaling pathways, like TLR4, by the extra LPS produced by the mutant, which could promote death of the mutant strain via the production of bactericidal factors.

DISCUSSION

4.1 Difficulties associated with expression and purification of recombinant HcpE

Expression of tagged-proteins is difficult to achieve in *H. pylori*, as the bacterium is not hospitable to the uptake of foreign DNA (5). This is attributed to the vast number of DNA restriction and modification systems present in *H. pylori* which seem to act as a barrier to genetic transformation (34). The DNA of *H. pylori* is constantly being modified, so when DNA is transformed into the bacterium its native restriction modification systems become active, and the foreign DNA has a tendency to be degraded. To address this challenge, methods to optimize DNA transformation into *H. pylori* have been studied at length. Plasmid DNA treated with *H. pylori* cell-free extracts in the presence of a methyl donor acquires the same methylation pattern as host genomic DNA. As a result, the restriction barrier to transformation can be overcome by specific DNA methylation *in vitro* increasing transformation efficiency in *H. pylori* (34). The approach of tagging *H. pylori* proteins was nevertheless pursued by a previous member of the Creuzenet and TAP-tagged HcpE was introduced into our wild-type strain (J. Chahal, *unpublished*). However endogenous levels of protein were too low for the assays planned, and the structure of HcpE prevented access of the reagents to cleave the TAP-tagged protein during purification. Therefore, in this thesis, purification of a recombinant histidine-tagged HcpE was utilized to study its biological role, identify specific interactions with other *H. pylori* proteins, and generate knowledge about its role in bacterial virulence.

E. coli is generally used as a model system for the production and over-expression of recombinant *H. pylori* proteins. For this, the *H. pylori* HcpE protein was expressed

using the pET expression system with a C-terminal hexahistidine tag. The pET expression system is a widely used system to mass produce proteins that allows for easy manipulation of how much of the desired protein is expressed and when that expression will occur (129). The system is specific as it uses the T7 promoter which only binds T7 RNA polymerase. The system is controlled through the *lac* promoter and operator. Before the recombinant gene can be transcribed, T7 polymerase must be present. To control T7 expression, the gene on the host cell chromosome is placed under the control of an inducible promoter that is activated by IPTG. When present, this molecule displaces the repressor from the *lac* operator, allowing T7 polymerase to be expressed, and the recombinant protein to be transcribed. For most proteins, this system works seamlessly, resulting in the production of substantial amounts of the recombinant protein. However, for HcpE this system seemed to be less efficient, and difficult to manipulate. Over-expression of HcpE resulted in very low yields of soluble protein (Figure 14A and B). Moreover, this soluble protein was prone to proteolytic degradation into a 30 kDa fragment lacking the C-terminus, and a 10 kDa fragment containing the C-terminal histidine tag. This made purification of HcpE more complex. Conditions maximizing the yield of soluble protein could not be identified by solubility assay (Figure 14). Using the most practical expression conditions (LB media, 24˚C) large volumes (3-4L) of over-expression cultures had to be used to generate nominal amounts of protein.

The difficulties faced in purifying HcpE have been documented for other members of the Hcp family. Purification of HcpC and HcpA was reported to be complicated by the need to re-fold these proteins from inclusion bodies (74, 86) and a complex protocol was designed to solubilize these proteins. Similarly, for HcpE,

purification in the presence on 6M guanidine-hydrochloride was employed to address this issue (see methods 2.11). This technique was successful at increasing the yield of purified HcpE such that enough protein could be produced to generate the anti-HcpE antibody, but the overall yields were still comparatively low.

More recently, it was reported by Dumrese *et al.*, that expression of HcpA and –C as soluble maltose binding protein (MBP)-fusion proteins in the periplasm of *E. coli* facilitated purification and avoided the need to refold the proteins from inclusion bodies (36). MBP fusion proteins are used to increase the solubility of recombinant proteins expressed in *E. coli* as it has been shown that fusion to MBP can promote proper folding of the attached protein into its biologically active conformation (63).

Considering the structural complexity of HcpE, and the other Hcp family proteins, it is not surprising that they mis-fold to form inclusion bodies. Without the proper folding factors to facilitate the formation of disulfide bridges between their many cysteine residues in the periplasm, it is reasonable that the proteins would aggregate into inclusion bodies. However, in the presence of their corresponding periplasmic folding factors, these proteins should achieve their proper conformation facilitating their secretion from cells in a soluble form. To accomplish this, HcpE will be co-expressed with DsbG its proposed folding factor, in the pET over-expression system. Secretion of HcpE into the supernatants of the *E. coli* over-expression system occurred at very low levels (refer to Figure 30); therefore, purification of HcpE from the *E. coli* over-expression pellets corresponded to its most abundant form in these cells.

4.2 Methods employed to assess protein-protein interactions and identify a folding factor for HcpE

It was hypothesized that HcpE remained insoluble due to improper folding in the periplasm in the absence of its native folding factor. In order to obtain soluble recombinant HcpE, its native *H. pylori* folding factor had to be identified. The presence of its many SLR motifs suggests that it may interact with other proteins, after folding, for its function. Identifying these proteins may help infer the function of HcpE. There are many strategies available to detect protein-protein interactions, some of which were outlined in section 1.6. In selecting an appropriate strategy, a number of considerations must be taken into account, as some biological systems are more conducive to certain methods than others. As previously discussed, *H. pylori* is a fastidious organism that is not easy to transform. As a result, methods relying on plasmid transformation are less favorable for this bacterium. An experimental yeast two-hybrid screen was performed in *H. pylori* (108) (Available on http://dpi.nhri.org.tw/protein/hp); however, this screen had its limitations and failed to identify a specific interacting partner for HcpE. The TAP-tag method was disregarded as previous attempts to apply this purification strategy in *H. pylori* by the Creuzenet lab were unsuccessful. With these factors taken into consideration, two methods were selected; (i) an interaction assay based on affinity chromatography, and (ii) affinity blotting of the immobilized substrate. The fundamental difference and rationale for using these two assays is that the former detects interactions between native, folded proteins to infer function, and the latter detects interactions with denatured proteins that relate to folding.

The protein-protein interaction assay based on affinity chromatography (for detailed schematic see Figure 7) was selected as it offered an additional level of specificity as the purified protein, with its affinity-tag could be purified using traditional affinity chromatography, with the addition of a second step to isolate its interacting partner. The first step would facilitate purification of the tagged protein alone, and the second step would allow for re-purification of the tagged protein and its interacting partner following incubation with *H. pylori* proteins. Following elution and resolution of bound proteins, our interacting partner could be identified by MS. This method was specifically designed to identify interactions that occur with mature, folded HcpE, as purified HcpE is secreted by the over-expression system.

Using this technique a protein band was recovered following SDS-PAGE that eluted at the same % imidazole as HcpE that was not present in the corresponding TsaA fraction eluting at the same position. The protein was identified by MS as HP0184. Unfortunately this identification is not helpful in inferring the function of HcpE as its interacting partner is also a hypothetical protein with no known function. The method was also successful at indentifying a specific interacting partner for our negative control protein TsaA, thereby further demonstrating its efficacy. For TsaA, this method recognized the hypothetical protein HP0129, that is believed to be secreted, containing a signal peptide. Since TsaA served as a negative control for these studies, this finding was not pursued.

The second method employed was affinity blotting of the immobilized substrate. This method has the advantage that it specifically identifies interactions between chaperones or folding factors and their unfolded substrate proteins. Substrates are

denatured by SDS-PAGE prior to incubation with cell extracts (for detailed schematic see section 1.6 (e), Figure 8). Using this method, MS identified DsbG (HP0231) to interact with both full-length and truncated HcpE. This finding was encouraging as it supports the structural model proposed for HcpE. Moreover, HcpE (HP0235) is encoded in close proximity to DsbG (HP0231) on the bacterial chromosome. Although both proteins are encoded on opposite strands, this genetic proximity alone suggests that DsbG might be involved in the final folding of HcpE by assisting in the formation of multiple disulfide bonds between the cysteine residues of the 9 SLRs in HcpE, as predicted by our 3D model. *H. pylori* protein-protein interaction maps identified eight interacting partners for DsbG; however, HcpE was not predicted in this screen. Despite this incongruity, the *H. pylori* yeast two-hybrid screens were not confirmed biochemically and the fact that MS identified DsbG to interact with both full length and truncated HcpE strengthens the validity and legitimacy of the interaction. Experimental verification of this interaction was however necessary to validate the MS data and provide more compelling evidence for a functional association between the two proteins.

4.3 Analysis of the alternative methods employed to verify the interaction with DsbG

After MS identified DsbG as an interacting partner of HcpE, the interaction between the two proteins had to be verified biochemically. To confirm this interaction, a number of different methods were employed. Since the folding of HcpE by DsbG is a catalytic process, the validation process should be two-fold in nature, in that it (a) confirms the physical interaction between the two proteins, and (b) demonstrates the

catalytic activity of the interaction, specifically the folding, and consequent solubilization of HcpE.

To test the physical interaction and binding of DsbG to HcpE, a modified version of the affinity blotting methodology was employed. Affinity blotting was the original method that highlighted the HcpE-DsbG interaction. Because of its original success, it was believed that repeating the process with purified or, enriched DsbG would lead to similar results. For purification, DsbG was expressed with a Flag-tag in *E. coli* using the pET expression system. Over-expression of DsbG in our pET system was not very efficient and detection with the anti-Flag antibody was difficult to decipher due to background reactivity with other *E. coli* proteins. Purification was not completely successful and only resulted in the enrichment of DsbG. Nevertheless DsbG is an enzyme, and enzymes are not required in large quantities to process large amounts of substrates. The amount of DsbG obtained was enough to use for the binding assay and refolding assay, but the low concentration made visualization difficult.

According to the model for bond formation by Dsb proteins characterized in *E. coli*, Dsb proteins typically function in pairs: DsbA with DsbB, and DsbC/G with DsbD (85). Consequently, the interaction assays were also done in the presence of wild-type *H. pylori* cell extracts which should provide any partner-Dsb proteins needed for DsbG's activity. According to the prototypical *E. coli* model, after oxidizing free-thiols in the substrate protein, DsbG would be reduced and would need to be re-oxidized to begin a new round of catalytic oxidation. By providing a cell extract, it was thought that if DsbG performed its catalytic activity with a partner protein, the protein would be present and available to oxidize reduced DsbG. However, providing cell extracts made interpretation

more difficult due to non-specific binding of other *H. pylori* proteins to the membrane which resulted in background reactivity on the blots. Moreover, interaction and refolding were observed in our assays without cell extract.

It has become more popular that the *E. coli* paradigm of Dsb bond formation is not conserved in all bacterial species, as some bacteria have extra Dsb proteins, and others are missing key players (37, 122). Recent analysis of *S. aureus* DsbA established that environmental oxidizing agents alone could maintain it in its active oxidized form, eliminating the need for a partner protein to catalyze its oxidation (55). Similar findings are emerging for other bacterial species, supporting the notion that not all Dsb proteins operate in pairs.

It was not surprising that the interaction between HcpE and DsbG was identified both in the presence and absence of wild-type *H. pylori* cell extracts, by Western blot, implying that DsbG does not require a partner protein to recognize its substrate. With this finding, the physical interaction between the two proteins was confirmed; however, its catalytic activity still needed to be assessed.

To assess the catalytic activity of DsbG and its ability to solubilize insoluble HcpE, a refolding assay was designed to quantify the amount of insoluble HcpE that is solubilized in the presence of DsbG. When increasing concentrations of DsbG were added to insoluble HcpE, the amount of HcpE detected in the reaction supernatants increased in a dose-dependent manner. This experiment also provided evidence that *H. pylori* deviates from the Dsb paradigm of *E. coli* since the presence of *H. pylori* cell extracts was not necessary for DsbG to solubilize HcpE. Moreover, in the presence of cell

extracts the effect of DsbG was masked, as endogenous *H. pylori* DsbG was sufficient to solubilize HcpE.

The final method to verify both the interaction and catalysis of disulfide bond formation by DsbG involves co-expression of the two proteins in the same over-expression system. It was previously shown that when over-expressed on its own, HcpE is secreted by *E. coli*, although at very low levels. This was attributed to the presence of a DsbG homologue in *E. coli*. Although the proteins only share 16% identity and 45% similarity, they seem to be similar enough to function on the same substrate, although with a marked reduction in efficiency. Co-expression of the *H. pylori* DsbG in the same construct as HcpE in an inducible system such as the pET expression system should facilitate secretion of large amounts of mature, fully folded HcpE. In addition having such a system would facilitate mass production of recombinant HcpE from *E. coli*.

In future, we will generate our own co-expression strain based on the technology of the commercially available pET Duet vectors. These vectors have T7 promoters for expression of target genes via induction with IPTG, and are designed to co-express two target proteins. In our adaptation of this system, each recombinant protein will have its own ribosome binding site, but transcription will be driven by the same T7 promoter. The original affinity tags on each protein will be maintained to facilitate downstream purifications. With this set-up it is believed that upon induction, both proteins would be generated in stoichiometic amounts. The presence of DsbG will help fold HcpE such that it will become soluble and can be secreted into the supernatants of the *E. coli* cultures. The comparison of the relative yields of the soluble and insoluble HcpE expressed alone

or in conjunction with DsbG will allow us to assess if our hypothesis is correct. Due to time constraints the co-expression construct was not completed.

4.4 Increased LPS production by *hcpE::kan* and its implications in bacterial biology

Bacterial LPS is an important surface component that provides stability to the bacterial outer membrane and contributes to interactions between the bacterial surface and its microbial niche as well as the host environment. LPS thus serves a dual purpose for the bacteria; contributing to its pathogenicity as well as aiding in colonization by providing a surface barrier. The LPS of *H. pylori* is a well characterized bacterial virulence factor (95, 127). Most notably, it aids in evasion of the immune response through molecular mimicry of Lewis blood group antigens. *H. pylori* LPS has been shown to have significantly lower endotoxic and immunological activities compared to that of other enterobacteria.

Initial investigation of the LPS structure of the wild-type and *hcpE::kan* strains was promoted by the unexpected response of the mutant strain to antibiotic exposure. With increasing concentrations of antibiotics, *hcpE::kan* displayed enhanced growth compared to wild-type *H. pylori*. This observation not only contradicted our hypothesis regarding the proposed β-lactamase activity of HcpE, it raised new questions regarding the expression of surface components by the mutant strain.

Extraction and resolution of the bacterial LPS provided some answers by confirming the presence of an extra-high molecular weight polysaccharide in the mutant that was absent in the wild-type strain (Figure 31). The extra surface component appeared to be providing a more resilient external barrier, facilitating growth at higher

concentrations of antibiotic. The appearance of this phenotype made it impossible to assess the β-lactamase activity of HcpE in *H. pylori*, and it raised the question of why the loss of the *hcpE* gene would result in increased LPS production. It is common for bacteria to up regulate the production and expression of cell surface components in the face of stress; however, what prompted such stress in the mutant remains unknown. It is possible that knocking out the *hcpE* gene disrupted a regulatory network involved in LPS biosynthesis.

To investigate this possibility further, qRT-PCR will be useful to compare the relative expression of LPS biosynthesis genes in each strain. HcpE, encoded by ORF HP0235, is located within a cluster of hypothetical genes in the *H. pylori* genome. Its predicted folding factor, DsbG, is encoded in close proximity by the ORF HP0231. Of relevance to LPS biosynthesis, DsbG is located next to a CMP-KDO-synthetase gene, which is involved in activation of KDO, an essential component of the core region of the *H. pylori* LPS molecule. Disruption of a regulatory network involved in LPS biosynthesis could result in over-active genes, which may perhaps increase LPS production in the mutant. To assess gene expression levels, isolation of bacterial mRNA was attempted numerous times, using different methods (84); however, contamination by DNA impeded analysis. To address the presence of a functional regulatory network dependent on HcpE, future work involves studying gene expression levels in the wild-type and *hcpE::kan* strain by qRT-PCR.

At this stage we cannot tell whether the different LPS pattern observed on the gel represents an increase in O-antigen production, or if the O-antigen structure and components are altered. Future work includes performing compositional analysis of the

sugars present in the wild-type and *hcpE::kan* LPS. For compositional analysis the LPS will need to be purified in large quantities from both strains. LPS can then be analyzed in one of two ways. The first method consists of separating the sugars and analyzing them using High Performance Anion Exchange with Pulsed Amperometric Detection (HPAE-PAD) alongside sugar standards. The detailed methods for analyzing sugars using this technology have been well established by the Creuzenet lab. Sugar analysis using HPAE is based on the principle that neutral mono- and oligosaccharides are weak acids. Upon exposure to high pH conditions, charged oxyanions are formed. Combination of HPAE with PAD facilitates detection of these charged sugars. When a potential is applied to the electrode, electrons are transferred to the electrode, and the analytes are oxidized. This process generates a measurable electric current that is detected by the electrode. Under our instrumental set up, PAD is highly specific for carbohydrates. Amino acids should not be oxidized under the high pH conditions, and therefore not be detected. The LPS of *H. pylori* is composed of relatively standard sugars which include glucose, galactose, fucose, N-acetylglucosamine, as well as heptose and its derivatives. These sugars standards can be analyzed in conjunction with the wild-type and *hcpE::kan* LPS, which will allow us to identify the sugars present in the LPS of each strain and highlight the differences. The second method available for compositional analysis involves performing MS and NMR analysis. The Creuzenet lab collaborates with Dr. Knirel (Moscow) to perform these highly specialized experiments.

In addition to characterizing the structural features that lead to differences in LPS composition, the presence of this phenotype can be exploited to study other aspects of bacterial surface component expression. Defects in LPS synthesis have been correlated

with increased sensitivity of bacteria to killing by serum, detergents (SDS and bile salts) (61), or hydrophobic antibiotics, like novobiocin (140), as well as decreased virulence properties in animal models (110, 145). These findings are supported by previous work in the Creuzenet lab which found that LPS mutants displayed significantly higher sensitivity to SDS, and slightly increased sensitivity to novobiocin and bile salts (84). These findings established a direct association between decreased O-antigen production and increased susceptibility to the presence of antibiotics or detergents. When these compounds are given increased access to the outer membrane, in this situation due to decreased O-antigen, the bacterium is more susceptible to their effects. The *hcpE* mutant, that produces more LPS, should exhibit decreased sensitivity, and possibly even protection against detergents, bile salts, and novobiocin treatment, similar to the decreased sensitively observed following challenge with β-lactam antibiotics.

Increased LPS production could also have an effect on the *hcpE* mutant's ability to resist antimicrobial peptides. Antimicrobial cationic peptides are a group of small, naturally occurring positively charged proteins with antimicrobial activities (73). In humans, antimicrobial peptides function as part of the innate immune response to bacterial infections. Their most prominent effect is permeabilizing the bacterial membrane (14), but they have also been shown to inhibit essential microbial processes like protein, cell wall, and nucleic acid synthesis (15, 101). Bacteria have evolved different mechanisms to combat the effects of antimicrobial peptides. Some of these mechanisms are more general, like changing their surface charge, proteolytic degradation, and export by efflux pumps; whereas others are more specific having been attributed to differences in cell surface components like LPS and capsule (17). Different

components of the bacterial LPS molecule have been shown to be important for resistance of Gram-negative organisms to antimicrobial peptides. In some species, it is the O-antigen, while in others it is the outer and inner core that contributes to resistance (73). LPS can also be modified by exposure to antimicrobial peptides, contributing to increased bacterial resistance. With this well documented association between LPS expression and resistance to antimicrobial peptides, it would be interesting to assess the effect of antimicrobial peptides, like polymyxin B, on our wild-type and *hcpE* mutant and determine whether increased LPS production corresponds to increased resistance. The *in vivo* relevance of all findings regarding increased LPS would also need to be established to help assign a role to HcpE during infection.

4.5 Influence of HcpE on human AGS cells

Gastric epithelial cells respond to *H. pylori* infection by activating numerous signal transduction pathways. To date, the responses that are best characterized are those resulting in tyrosine phosphorylation of proteins adjacent to the site of bacterial adherence (118). More specifically, infection has been shown to induce tyrosine phosphorylation of a 145 kDa host protein, the reorganization of host cell actin and associated cellular proteins, and the release of large amounts of IL-8 (119). IL-8 is a neutrophil chemotactic factor that has predominantly been shown to be increased in *H. pylori* infected patients with active gastritis (29). Induction of IL-8 in the more pathogenic, *type I H. pylori* strains *in vitro* has been attributed to the *picB*-gene, which has been compared to the pertussis toxin (136). Other downstream effects include production of TNF-α and IL-6, though at much lower levels than IL-8. Gastric cell synthesis of IL-8 is thought to be important in regulating mucosal neutrophil infiltration

and activation to limit the mucosal damage associated with chronic bacterial infections (29). Taken together, it seems IL-8 production serves two main purposes; (i) induce inflammation of the gastric mucosa, and (ii) perform more of a regulatory function ensuring that inflammation does not escalate to promote persistent infections.

It was previously established that patients infected with *H. pylori* have high antibody titers to Hcp proteins, including HcpE (87). This suggests that the protein is secreted during natural infections, inducing a response by the host. To investigate the role of HcpE *in vivo*, AGS cell monolayers were infected with strains containing, or lacking this protein. Comparison of IL-8 production, bacterial adhesion and AGS cell morphology was employed to assess the effect of HcpE *in vivo*. Interpretation of the findings of these experiments was complicated by a number of factors. Despite normalizing the starting optical density and MOI for both strains such that AGS cells would be infected by the same number of bacteria of each strain, growth of the *hcpE::kan* strain was greatly diminished under tissue culture conditions. To support optimal viability of AGS cells, these experiments were not performed under the ideal microaerophilic growth conditions necessitated by *H. pylori*. The effect of these conditions on bacterial viability was assessed, and it was determined that the mutant was ~20% less viable compared to wild-type *H. pylori*. This effect could not strictly be attributed to the loss of the *hcpE* gene, as microscopy revealed that the AGS cells infected by the mutant strain were also dying. This was evidenced by the clumping of lysed cells at both 5 and 10 hpi (Figure 33). This observation could be a result of the AGS cells dying on account of bacterial infection, releasing their intra-cellular contents, which in turn resulted in toxicity to the bacteria and their subsequent death. It is also possible that the growth

conditions affected the bacteria and contributed to their death, which subsequently had a destructive effect on the AGS cells leading to apoptosis. The trigger of this observation is difficult to decipher. Live/Dead staining could be implemented to quantify the proportion of AGS cells that are killed following infection with the mutant strain. Unfortunately this will not solve the problem of what initiated the cell death; however, it could be valuable to normalize cytokine production by both strains based on the number of live cells present.

Moreover, the mutant strain was identified to be producing more LPS than the wild-type strain. Increased LPS production could be contributing to endotoxicity of the AGS cells. It has been shown that *H. pylori* LPS is not very endotoxic but does effectively activate TLR4 signaling (11, 95, 124). Thus, it is possible that in this infection model, the amount of TLR4 activation is enough to impart a destructive phenotype on the AGS cells.

Both our wild-type and *hcpE::kan* strains induced the hummingbird phenotype in infected AGS cells. However, to conclusively establish a role for HcpE in induction of this phenotype and the alterations in cell signaling associated with its occurrence, this work would have be done in a *cagA* knockout *H. pylori* strain, since the hummingbird has for the most part been attributed to the CagA toxin secreted by the *cag*PI (116). Having a double knockout (*hcpE*- and *cagA*-) would make it possible to study the independent contribution of HcpE to changes in AGS cell morphology.

H. pylori is not a very invasive bacteria. In establishing infection, the bacteria are typically found over mucus-secreting cells, closely associated with the epithelial surface, by not deep within them (7). This close association is essential for pathogenesis and

establishment of persistent infections. Properties of bacterial adhesion have been well studied in *H. pylori*. Numerous adhesins have been classified and characterized (refer to section 1.25). Due to the importance of the ability to adhere to gastric cells, adhesion to AGS cells was quantified in our wild-type and mutant strain to assess the contribution of HcpE to properties of bacterial adhesion. This work established a 5-10% difference in adhesion between the two strains. Due to simultaneous death of *hcpE::kan* under the tissue culture conditions and the induced death of AGS cells mentioned above, it was difficult to compare each strain's ability to adhere to the AGS cells. For interpretation, all adhesion data was normalized to the number of viable cells. As mentioned previously, the addition of live/dead staining could help elucidate this problem and allow adhesion to be quantified normalized to the number of live AGS cells. To alleviate this problem we have two options: (i) use pure HcpE, produced by the co-expression system to infect the AGS cells and perform microscopy and analysis of IL-8 production, or (ii) use our anti-HcpE serum on AGS cells infected with wild-type *H. pylori* and compare to AGS cells infected with wild-type *H. pylori* and an irrelevant antibody to see if neutralizing HcpE will affect IL-8 production.

4.6 Summary and significance

Through this work, we identified two novel interacting partners for HcpE. For unfolded HcpE, we identified DsbG as its periplasmic folding factor and in doing so established that the paradigm for disulfide bond formation established in *E. coli* is not conserved in *H. pylori*. There is currently no known substrate for DsbG, so its interaction with HcpE represents its first recognized substrate. DsbG was not only shown to bind unfolded HcpE, its ability to solubilize insoluble HcpE was demonstrated, thereby

establishing its role in disulfide bond formation. For folded HcpE, we highlighted an interaction with HP0184, a hypothetical protein with no known function to date.

This work also established that HcpE is secreted by *H. pylori* and that its presence outside of cells is not simply a result of cell lysis. We demonstrated a role for HcpE during infection of AGS cells showing that its presence enhanced adherence and elicited increased production of IL-8. Altered LPS expression was identified in our *hcpE::kan* mutant, suggesting the presence of a regulatory network involved in LPS production that is dependent on the presence of HcpE.

Overall, this work contributed to our understanding of interactions between HcpE and other *H. pylori* proteins, as well as laid the groundwork to identify a function for HcpE during *H. pylori* infections. Globally, studying protein interactions within *H. pylori* not only helps characterize individual proteins of biological signification, it contributes to our understanding of the larger interconnected networks of protein interactions that support cell survival and persistence of the bacterium. This knowledge will contribute to our understanding of how *H. pylori* confers pathogenicity in the body and thus how we can prevent, or control *H. pylori* infections in the future.

REFERENCES

1. 2009. World Cancer Report 2008. World Health Organization.
2. **Alm, R. A., L. S. Ling, D. T. Moir, B. L. King, E. D. Brown, P. C. Doig, D. R. Smith, B. Noonan, B. C. Guild, B. L. deJonge, G. Carmel, P. J. Tummino, A. Caruso, M. Uria-Nickelsen, D. M. Mills, C. Ives, R. Gibson, D. Merberg, S. D. Mills, Q. Jiang, D. E. Taylor, G. F. Vovis, and T. J. Trust.** 1999. Genomic-sequence comparison of two unrelated isolates of the human gastric pathogen *Helicobacter pylori*. Nature **397:**176-80.
3. **Amado, M., F. Carneiro, M. Seixas, H. Clausen, and M. Sobrinho-Simoes.** 1998. Dimeric sialyl-Le(x) expression in gastric carcinoma correlates with venous invasion and poor outcome. Gastroenterology **114:**462-470.
4. **Andersen, C. L., A. Matthey-Dupraz, D. Missiakas, and S. Raina.** 1997. A new *Escherichia coli* gene, dsbG, encodes a periplasmic protein involved in disulphide bond formation, required for recycling DsbA/DsbB and DsbC redox proteins. Mol Microbiol **26:**121-132.
5. **Ando, T., Q. Xu, M. Torres, K. Kusugami, D. A. Israel, and M. J. Blaser.** 2000. Restriction-modification system differences in *Helicobacter pylori* are a barrier to interstrain plasmid transfer. Mol Microbiol **37:**1052-65.
6. **Argent, R. H., R. J. Thomas, D. P. Letley, M. G. Rittig, K. R. Hardie, and J. C. Atherton.** 2008. Functional association between the *Helicobacter pylori* virulence factors VacA and CagA. J Med Microbiol **57:**145-150.
7. **Atherton, J. C.** 2006. The pathogenesis of *Helicobacter pylori* induced gastro-duodenal diseases. Ann Rev Pathol **1:**63-96.
8. **Atherton, J. C., P. Cao, R. M. Peek, M. K. R. Tummuru, M. J. Blaser, and T. L. Cover.** 1995. Mosaicism in vacuolating vytotoxin alleles of *Helicobacter pylori*. J Biol Chem **270:**17771-17777.
9. **Aubourg, S. b., N. Boudet, M. Kreis, and A. Lecharny.** 2000. In *Arabidopsis thaliana*, 1% of the genome codes for a novel protein family unique to plants. Plant Molec Biol **42:**603-613.
10. **Backert, S., and T. Meyer.** 2006. Type IV secretion systems and their effectors in bacterial pathogenesis. Curr Opin Microbiol **9:**207 - 217.
11. **Backhed, F., B. Rokbi, E. Torstensson, Y. Zhao, C. Nilsson, D. Seguin, S. Normark, A. M. Buchan, and A. Richter-Dahlfors.** 2003. Gastric mucosal recognition of *Helicobacter pylori* is independent of Toll-like receptor 4. J Infect Dis **187:**829-36.
12. **Baker, L. M., A. Raudonikiene, P. S. Hoffman, and L. B. Poole.** 2001. Essential thioredoxin-dependent peroxiredoxin system from *Helicobacter pylori*: genetic and kinetic characterization. J Bacteriol **183:**1961-73.
13. **Bardwell, J. C. A.** 1994. Building bridges: disulphide bond formation in the cell. Mol Microbiol **14:**199-205.
14. **Blaser, M., and J. Atherton.** 2004. *Helicobacter pylori* persistence: biology and disease. J Clin Invest **113:**321 - 333.
15. **Brotz, H., G. Bierbaum, K. Leopold, P. E. Reynolds, and H.-G. Sahl.** 1998. The lantibiotic mersacidin inhibits peptidoglycan synthesis by targeting lipid II. Antimicrob Agents Chemother **42:**154-160.

16. **Bumann, D., S. Aksu, M. Wendland, K. Janek, U. Zimny-Arndt, N. Sabarth, T. F. Meyer, and P. R. Jungblut.** 2002. Proteome analysis of secreted proteins of the gastric pathogen *Helicobacter pylori*. Infect. Immun. **70:**3396-3403.
17. **Campos, M. A., M. A. Vargas, V. Regueiro, C. M. Llompart, S. Alberti, and J. A. Bengoechea.** 2004. Capsule polysaccharide mediates bacterial resistance to antimicrobial peptides. Infect. Immun. **72:**7107-7114.
18. **Cao, P., M. S. McClain, M. H. Forsyth, and T. L. Cover.** 1998. Extracellular release of antigenic proteins by *Helicobacter pylori*. Infect Immun **66:**2984-6.
19. **Cao, T., and M. Saier.** 2003. The general protein secretory pathway: phylogenetic analyses leading to evolutionary conclusions. Biochim Biophys Acta **1609:**115 - 125.
20. **Carroll, I. M., A. A. Khan, and N. Ahmed.** 2004. Revisiting the pestilence of *Helicobacter pylori*: insights into geographical genomics and pathogen evolution. Infect Genet Evol **4:**81-90.
21. **Cascales, E., and P. J. Christie.** 2003. The versatile bacterial type IV secretion systems. Nat Rev Micro **1:**137-149.
22. **Censini, S., C. Lange, Z. Xiang, J. E. Crabtree, P. Ghiara, M. Borodovsky, R. Rappuoli, and A. Covacci.** 1996. *cag*, a pathogenicity island of *Helicobacter pylori*, encodes type I-specific and disease-associated virulence factors. Proc Natl Acad Sci U S A **93:**14648-53.
23. **Chien, C. T., P L Bartel, R Sternglanz, and S Fields.** 1991. The two-hybrid system: a method to identify and clone genes for proteins that interact with a protein of interest. Proc Natl Acad Sci U S A **88:**9578-9582.
24. **Cianciotto, N.** 2005. Type II secretion: a protein secretion system for all seasons. Trends Microbiol **13:**581 - 588.
25. **Collet, J.-F., and J. C. A. Bardwell.** 2002. Oxidative protein folding in bacteria. Mol Microbiol **44:**1-8.
26. **Corcionivoschi, N., M. Clyne, A. Lyons, A. Elmi, O. Gundogdu, B. W. Wren, N. Dorrell, A. V. Karlyshev, and B. Bourke.** 2009. *Campylobacter jejuni* cocultured with epithelial cells reduces surface capsular polysaccharide expression. Infect. Immun. **77:**1959-1967.
27. **Correa, P., W. Haenszel, C. Cuello, S. Tannenbaum, and M. Archer.** 1975. A model for gastric cancer epidemiology. The Lancet **306:**58-60.
28. **Covacci, A., S. Censini, M. Bugnoli, R. Petracca, D. Burroni, G. Macchia, A. Massone, E. Papini, Z. Xiang, and N. Figura.** 1993. Molecular characterization of the 128-kDa immunodominant antigen of *Helicobacter pylori* associated with cytotoxicity and duodenal ulcer. Proc Natl Acad Sci U S A **90:**5791-5795.
29. **Crabtree, J. E., P. Peichl, J. I. Wyatt, U. Stachl, and I. J. D. Lindey.** 1993. Gastric Interleukin-8 and IgA IL-8 Autoantibodies in *Helicobacter pylori* Infection. Scand J Immunol **37:**65-70.
30. **Das, A. K., P. T. W. Cohen, and D. Barford.** 1998. The structure of the tetratricopeptide repeats of protein phosphatase 5: implications for TPR-mediated protein-protein interactions. EMBO J **17:**1192-1199.
31. **Deml, L., M. Aigner, J. Decker, A. Eckhardt, C. Schutz, P. R. E. Mittl, S. Barabas, S. Denk, G. Knoll, N. Lehn, and W. Schneider-Brachert.** 2005.

Characterization of the *Helicobacter pylori* cysteine-rich protein a as a T-helper cell type 1 polarizing agent. Infect. Immun. **73:**4732-4742.

32. **Dhar, S. K., R. K. Soni, B. K. Das, and G. Mukhopadhyay.** 2003. Molecular mechanism of action of major *Helicobacter pylori* virulence factors. Mol Cell Biochem **253:**207-215.
33. **Di Lallo, G., P. Ghelardini, and L. Paolozzi.** 1999. Two-hybrid assay: construction of an *Escherichia coli* system to quantify homodimerization ability in vivo. Microbiol **145:**1485-1490.
34. **Donahue, J. P., D. A. Israel, R. M. P. Jr, M. J. Blaser, and G. G. Miller.** 2000. Overcoming the restriction barrier to plasmid transformation of *Helicobacter pylori*. Mol Microbiol **37:**1066-1074.
35. **Douraghi, M., S. Saberi Kashani, H. Zeraati, M. Esmaili, A. Oghalaie, and M. Mohammadi.** 2010. Comparative evaluation of three cupplements for *Helicobacter pylori* growth in liquid culture. Curr Microbiol **60:**254-262.
36. **Dumrese, C., L. Slomianka, U. Ziegler, S. S. Choi, A. Kalia, A. Fulurija, W. Lu, D. E. Berg, M. Benghezal, B. Marshall, and P. R. Mittl.** 2009. The secreted Helicobacter cysteine-rich protein A causes adherence of human monocytes and differentiation into a macrophage-like phenotype. FEBS Lett **583:**1637-43.
37. **Dutton, R. J., D. Boyd, M. Berkmen, and J. Beckwith.** 2008. Bacterial species exhibit diversity in their mechanisms and capacity for protein disulfide bond formation. Proc Natl Acad Sci U S A **105:**11933-8.
38. **Eaton, K. A., D. R. Morgan, and S. Krakowka.** 1992. Motility as a factor in the colonisation of gnotobiotic piglets by *Helicobacter pylori*. J Med Microbiol **37:**123-7.
39. **Economou, A.** 1999. Following the leader: bacterial protein export through the Sec pathway. Trend Microbiol **7:**315-320.
40. **Edwards, N. J., M. A. Monteiro, G. Faller, E. J. Walsh, A. P. Moran, I. S. Roberts, and N. J. High.** 2000. Lewis X structures in the O antigen side-chain promote adhesion of *Helicobacter pylori* to the gastric epithelium. Mol Microbiol **35:**1530-1539.
41. **Evans, D. G., T. K. Karjalainen, D. J. Evans, Jr., D. Y. Graham, and C. H. Lee.** 1993. Cloning, nucleotide sequence, and expression of a gene encoding an adhesin subunit protein of *Helicobacter pylori*. J Bacteriol **175:**674-83.
42. **Fitchen, N., P. Williams, and K. R. Hardie.** 2003. Functional complementation of *E. coli* secD and secG mutants by *Helicobacter pylori* homologues. FEMS Microbiol Lett **229:**57-63.
43. **Fomsgaard, A., M. A. Freudenberg, and C. Galanos.** 1990. Modification of the silver staining technique to detect lipopolysaccharide in polyacrylamide gels. J Clin Microbiol **28:**2627-31.
44. **Fraser, G. M., J. C. Bennett, and C. Hughes.** 1999. Substrate-specific binding of hook-associated proteins by FlgN and FliT, putative chaperones for flagellum assembly. Mol Microbiol **32:**569-80.
45. **Geis, G., H. Leying, S. Suerbaum, U. Mai, and W. Opferkuch.** 1989. Ultrastructure and chemical analysis of *Campylobacter pylori* flagella. J. Clin. Microbiol. **27:**436-441.

46. **Gisbert, J. P., and J. M. Pajares.** 2002. *Helicobacter pylori* 'rescue' regimen when proton pump inhibitor-based triple therapies fail. Alim Pharm Ther **16:**1047-1057.
47. **Godlewska, R., A. Dzwonek, M. Mikula, J. Ostrowski, M. Pawlowski, J. M. Bujnicki, and E. K. Jagusztyn-Krynicka.** 2006. *Helicobacter pylori* protein oxidation influences the colonization process. Int J Med Microbiol **296:**321-4.
48. **Goodman, K. J., and P. Correa.** 1995. The transmission of *Helicobacter pylori*. a critical review of the evidence. Int. J. Epidemiol. **24:**875-887.
49. **Goodwin, C. S., R. K. McCulloch, J. A. Armstrong, and S. H. Wee.** 1985. Unusual cellular fatty acids and distinctive ultrastructure in a new spiral bacterium (*Campylobacter Pyloridis*) from the human gastric mucosa. J Med Microbiol **19:**257-267.
50. **Grant, B., and I. Greenwald.** 1996. The *Caenorhabditis elegans sel-1* gene, a negative regulator of lin-12 and glp-1, encodes a predicted extracellular protein. Genetics **143:**237-47.
51. **Guilhot, C., G. Jander, N. L. Martin, and J. Beckwith.** 1995. Evidence that the pathway of disulfide bond formation in *Escherichia coli* involves interactions between the cysteines of DsbB and DsbA. Proc Natl Acad Sci U S A **92:**9895-9899.
52. **Hanahan, D.** 1983. Studies on transformation of *Escherichia coli* with plasmids. J Mol Biol **166:**557-580.
53. **Harris, P. R., H. L. Mobley, G. I. Perez-Perez, M. J. Blaser, and P. D. Smith.** 1996. *Helicobacter pylori* urease is a potent stimulus of mononuclear phagocyte activation and inflammatory cytokine production. Gastroenterol **111:**419-25.
54. **Heneghan, M. A., C. F. McCarthy, and A. P. Moran.** 2000. Relationship of blood group determinants on *Helicobacter pylori* lipopolysaccharide with host lewis phenotype and inflammatory response. Infect. Immun. **68:**937-941.
55. **Heras, B., M. Kurz, R. Jarrott, S. Shouldice, P. Frei, G. Robin, M. Cemazar, L. Thöny-Meyer, R. Glockshuber, and J. Martin.** 2008. *Staphylococcus aureus* DsbA does not have a destabilizing disulfide. J Biol Chem **283:**4261-4271.
56. **Heras, B., S. R. Shouldice, M. Totsika, M. J. Scanlon, M. A. Schembri, and J. L. Martin.** 2009. DSB proteins and bacterial pathogenicity. Nat Rev Microbiol **7:**215-25.
57. **Heuermann, D., and R. Haas.** 1998. A stable shuttle vector system for efficient genetic complementation of *Helicobacter pylori* strains by transformation and conjugation. Mol Gen Genet **257:**519-28.
58. **Hitchcock, P. J., and T. M. Brown.** 1983. Morphological heterogeneity among *Salmonella lipopolysaccharide* chemotypes in silver-stained polyacrylamide gels. J Bacteriol **154:**269-77.
59. **Hu, L. T., and H. L. Mobley.** 1990. Purification and N-terminal analysis of urease from *Helicobacter pylori*. Infect. Immun. **58:**992-998.
60. **Ilver, D., A. Arnqvist, J. Ogren, I. M. Frick, D. Kersulyte, E. T. Incecik, D. E. Berg, A. Covacci, L. Engstrand, and T. Boren.** 1998. *Helicobacter pylori* adhesin binding fucosylated histo-blood group antigens revealed by retagging. Science **279:**373-7.

61. **Itoh, M., K. Wada, S. Tan, Y. Kitano, J. Kai, and I. Makino.** 1999. Antibacterial action of bile acids against *Helicobacter pylori* and changes in its ultrastructural morphology: effect of unconjugated dihydroxy bile acid. J Gastroenterol **34:**571-6.

62. **Josenhans, C., L. Vossebein, S. Friedrich, and S. Suerbaum.** 2002. The *neuA/flmD* gene cluster of *Helicobacter pylori* is involved in flagellar biosynthesis and flagellin glycosylation. FEMS Microbiol Lett **210:**165-72.

63. **Kapust, R. B., and D. S. Waugh.** 1999. *Escherichia coli* maltose-binding protein is uncommonly effective at promoting the solubility of polypeptides to which it is fused. Prot Sci **8:**1668-1674.

64. **Karimova, G., J. Pidoux, A. Ullmann, and D. Ladant.** 1998. A bacterial two-hybrid system based on a reconstituted signal transduction pathway. Proc Natl Acad Sci U S A **95:**5752-5756.

65. **Kim, N., D. L. Weeks, J. M. Shin, D. R. Scott, M. K. Young, and G. Sachs.** 2002. Proteins released by *Helicobacter pylori in vitro*. J Bacteriol **184:**6155-62.

66. **Krishnamurthy, P., M. H. Parlow, J. Schneider, S. Burroughs, C. Wickland, N. B. Vakil, B. E. Dunn, and S. H. Phadnis.** 1999. Identification of a novel penicillin-binding protein from *Helicobacter pylori*. J Bacteriol **181:**5107-10.

67. **Kusters, J. G., A. H. M. van Vliet, and E. J. Kuipers.** 2006. Pathogenesis of *Helicobacter pylori* infection. Clin. Microbiol. Rev. **19:**449-490.

68. **Labigne, A., V. Cussac, and P. Courcoux.** 1991. Shuttle cloning and nucleotide sequences of *Helicobacter pylori* genes responsible for urease activity. J. Bacteriol. **173:**1920-1931.

69. **Ladant, D., and G. Karimova.** 2000. Genetic systems for analyzing protein-protein interactions in bacteria. Resear Microbiol **151:**711-720.

70. **Lasica, A. M., and E. K. Jagusztyn-Krynicka.** 2007. The role of Dsb proteins of Gram-negative bacteria in the process of pathogenesis. FEMS Microbiol Rev **31:**626-36.

71. **Legrain, P., and L. Selig.** 2000. Genome-wide protein interaction maps using two-hybrid systems. FEBS Letters **480:**32-36.

72. **Loh, J. T., V. J. Torres, H. M. S. Algood, M. S. McClain, and T. L. Cover.** 2008. *Helicobacter pylori* HopQ outer membrane protein attenuates bacterial adherence to gastric epithelial cells. FEMS Microbiol Lett **289:**53-58.

73. **Loutet, S. A., R. S. Flannagan, C. Kooi, P. A. Sokol, and M. A. Valvano.** 2006. A complete lipopolysaccharide inner core oligosaccharide is required for resistance of *Burkholderia cenocepacia* to antimicrobial peptides and bacterial survival *in vivo*. J. Bacteriol. **188:**2073-2080.

74. **Luthy, L., M. G. Grutter, and P. R. Mittl.** 2004. The crystal structure of Helicobacter cysteine-rich protein C at 2.0 A resolution: similar peptide-binding sites in TPR and SEL1-like repeat proteins. J Mol Biol **340:**829-41.

75. **Luthy, L., M. G. Grutter, and P. R. Mittl.** 2002. The crystal structure of *Helicobacter pylori* cysteine-rich protein B reveals a novel fold for a penicillin-binding protein. J Biol Chem **277:**10187-93.

76. **Macnab, R. M.** 2003. How bacteria assemble flagella. Ann Rev Microbiol **57:**77-100.

77. **Mahdavi, J., B. Sonden, M. Hurtig, F. O. Olfat, L. Forsberg, N. Roche, J. Angstrom, T. Larsson, S. Teneberg, K. A. Karlsson, S. Altraja, T. Wadstrom, D. Kersulyte, D. E. Berg, A. Dubois, C. Petersson, K. E. Magnusson, T. Norberg, F. Lindh, B. B. Lundskog, A. Arnqvist, L. Hammarstrom, and T. Boren.** 2002. *Helicobacter pylori* SabA adhesin in persistent infection and chronic inflammation. Science **297:**573-8.

78. **Manting, E. H., and A. J. M. Driessen.** 2000. *Escherichia coli* translocase: the unravelling of a molecular machine. Mol Microbiol **37:**226-238.

79. **Marshall, B. J., and J. R. Warren.** 1984. Unidentified curved bacilli in the stomach of patients with gastritis and peptic ulceration. Lancet **1:**1311-5.

80. **Marshall, D. G., W. G. Dundon, S. M. Beesley, and C. J. Smyth.** 1998. *Helicobacter pylori* - a conundrum of genetic diversity. Microbiol **144:**2925-2939.

81. **Massova, I., and S. Mobashery.** 1998. Kinship and diversification of bacterial penicillin-binding proteins and beta-lactamases. Antimicrob. Agents Chemother. **42:**1-17.

82. **Mattapallil, J. J., S. Dandekar, D. R. Canfield, and J. V. Solnick.** 2000. A predominant Th1 type of immune response is induced early during acute *Helicobacter pylori* infection in rhesus macaques. Gastroenterol **118:**307-315.

83. **McGee, D. J., C. A. May, R. M. Garner, J. M. Himpsl, and H. L. Mobley.** 1999. Isolation of *Helicobacter pylori* genes that modulate urease activity. J Bacteriol **181:**2477-84.

84. **Merkx-Jacques, A., R. K. Obhi, G. Bethune, and C. Creuzenet.** 2004. The *Helicobacter pylori flaA1* and *wbpB* genes control lipopolysaccharide and flagellum synthesis and function. J. Bacteriol **186:**2253-2265.

85. **Messens, J., and J.-F. Collet.** 2006. Pathways of disulfide bond formation in *Escherichia coli*. Int J Biochem Cell Bio **38:**1050-1062.

86. **Mittl, P. R., L. Luthy, P. Hunziker, and M. G. Grutter.** 2000. The cysteine-rich protein A from *Helicobacter pylori* is a beta-lactamase. J Biol Chem **275:**17693-9.

87. **Mittl, P. R., L. Luthy, C. Reinhardt, and H. Joller.** 2003. Detection of high titers of antibody against Helicobacter cysteine-rich proteins A, B, C, and E in *Helicobacter pylori*-infected individuals. Clin Diagn Lab Immunol **10:**542-5.

88. **Mittl, P. R., and W. Schneider-Brachert.** 2007. Sel1-like repeat proteins in signal transduction. Cell Signal **19:**20-31.

89. **Montecucco, C., and R. Rappuoli.** 2001. Living dangerously: how *Helicobacter pylori* survives in the human stomach. Nat Rev Mol Cell Biol **2:**457-466.

90. **Moran, A., B. Lindner, and E. Walsh.** 1997. Structural characterization of the lipid A component of *Helicobacter pylori* rough- and smooth-form lipopolysaccharides. J. Bacteriol. **179:**6453-6463.

91. **Moran, A. P.** 2008. Relevance of fucosylation and Lewis antigen expression in the bacterial gastroduodenal pathogen *Helicobacter pylori*. Carb Resear **343:**1952-1965.

92. **Moran, A. P., I. M. Helander, and T. U. Kosunen.** 1992. Compositional analysis of *Helicobacter pylori* rough-form lipopolysaccharides. J Bacteriol **174:**1370-7.

93. **Moran, A. P., and M. M. Prendergast.** 2001. Molecular mimicry in *Campylobacter jejuni* and *Helicobacter pylori* lipopolysaccharides: contribution of gastrointestinal infections to autoimmunity. J Autoimmun **16:**241-56.
94. **Moran, A. P., E. Sturegård, H. Sjunnesson, T. Wadström, and S. O. Hynes.** 2000. The relationship between O-chain expression and colonisation ability of *Helicobacter pylori* in a mouse model. FEMS Immun Med Microbiol **29:**263-270.
95. **Muotiala, A., I. M. Helander, L. Pyhala, T. U. Kosunen, and A. P. Moran.** 1992. Low biological activity of *Helicobacter pylori* lipopolysaccharide. Infect Immun **60:**1714-6.
96. **Newton, D. T., and D. Mangroo.** 1999. Mapping the active site of the *Haemophilus influenzae* methionyl-tRNA formyltransferase: residues important for catalysis and tRNA binding. Biochem J **339 (Pt 1):**63-9.
97. **Odenbreit, S.** 2005. Adherence properties of *Helicobacter pylori*: Impact on pathogenesis and adaptation to the host. Int J Med Microbiol **295:**317-324.
98. **Ogura, M., J. C. Perez, P. R. E. Mittl, H.-K. Lee, G. Dailide, S. Tan, Y. Ito, O. Secka, D. Dailidiene, K. Putty, D. E. Berg, and A. Kalia.** 2007. *Helicobacter pylori* evolution: lineage- specific adaptations in homologs of eukaryotic sel1-like genes. PLoS Comput Biol **3:**e151.
99. **Okamoto, K., T. Nomura, Y. Fujii, and H. Yamanaka.** 1998. Contribution of the disulfide bond of the A subunit to the action of *Escherichia coli* heat-labile enterotoxin. J. Bacteriol. **180:**1368-1374.
100. **Olivieri, R., M. Bugnoli, D. Armellini, S. Bianciardi, R. Rappuoli, P. F. Bayeli, L. Abate, E. Esposito, L. de Gregorio, and J. Aziz.** 1993. Growth of *Helicobacter pylori* in media containing cyclodextrins. J. Clin. Microbiol. **31:**160-162.
101. **Patrzykat, A., C. L. Friedrich, L. Zhang, V. Mendoza, and R. E. W. Hancock.** 2002. Sublethal concentrations of pleurocidin-derived antimicrobial peptides inhibit macromolecular synthesis in *Escherichia coli*. Antimicrob. Agents Chemother. **46:**605-614.
102. **Phadnis, S., M. Parlow, M. Levy, D. Ilver, C. Caulkins, J. Connors, and B. Dunn.** 1996. Surface localization of *Helicobacter pylori* urease and a heat shock protein homolog requires bacterial autolysis. Infect. Immun. **64:**905-912.
103. **Pohl, M. A., J. Romero-Gallo, J. L. Guruge, D. B. Tse, J. I. Gordon, and M. J. Blaser.** 2009. Host-dependent Lewis (Le) antigen expression in *Helicobacter pylori* cells recovered from Leb-transgenic mice. J Exper Med **206:**3061-3072.
104. **Ponting, C. P., L. Aravind, J. Schultz, P. Bork, and E. V. Koonin.** 1999. Eukaryotic signalling domain homologues in archaea and bacteria. ancient ancestry and horizontal gene transfer. J Mol Biol **289:**729-745.
105. **Raetz, C. R. H., C. M. Reynolds, M. S. Trent, and R. E. Bishop.** 2007. Lipid A modification systems in gram-negative bacteria. Ann Rev Biochem **76:**295-329.
106. **Raetz, C. R. H., and C. Whitfield.** 2002. Lipopolysaccharide endotoxins. Ann Rev Biochem **71:**635-700.
107. **Rahme, L. G., M.-W. Tan, L. Le, S. M. Wong, R. G. Tompkins, S. B. Calderwood, and F. M. Ausubel.** 1997. Use of model plant hosts to identify *Pseudomonas aeruginosa* virulence factors. Proc Natl Acad Sci U S A **94:**13245-13250.

108. **Rain, J. C., L. Selig, H. De Reuse, V. Battaglia, C. Reverdy, S. Simon, G. Lenzen, F. Petel, J. Wojcik, V. Schachter, Y. Chemama, A. Labigne, and P. Legrain.** 2001. The protein-protein interaction map of *Helicobacter pylori*. Nature **409:**211-5.
109. **Raina, S., and D. Missiakas.** 1997. Making and breaking disulfide bonds. Ann Rev Microbiol **51:**179-202.
110. **Rioux, S., C. Begin, J. D. Dubreuil, and M. Jacques.** 1997. Isolation and characterization of LPS mutants of *Actinobacillus pleuropneumoniae* serotype 1. Curr Microbiol **35:**139-44.
111. **Rohrer, S., and B. Berger-Bachi.** 2003. Application of a bacterial two-hybrid system for the analysis of protein-protein interactions between FemABX family proteins. Microbiol **149:**2733-2738.
112. **Saier, M.** 2006. Protein Secretion and Membrane Insertion Systems in Gram-Negative Bacteria. Journal of Membrane Biology **214:**75-90.
113. **Saier, M.** 2006. Protein secretion and membrane insertion systems in gram-negative bacteria. J Membr Biol **214:**75 - 90.
114. **Sauvage, E., F. Kerff, M. Terrak, J. A. Ayala, and P. Charlier.** 2008. The penicillin-binding proteins: structure and role in peptidoglycan biosynthesis. FEMS Microbiol Rev **32:**234-58.
115. **Schirm, M., E. C. Soo, A. J. Aubry, J. Austin, P. Thibault, and S. M. Logan.** 2003. Structural, genetic and functional characterization of the flagellin glycosylation process in *Helicobacter pylori*. Mol Microbiol **48:**1579-1592.
116. **Schneider, S., C. Weydig, and S. Wessler.** 2008. Targeting focal adhesions: *Helicobacter pylori*-host communication in cell migration. Cell Comn Signal **6:**2.
117. **Schultz, J., F. Milpetz, P. Bork, and C. P. Ponting.** 1998. SMART, a simple modular architecture research tool: Identification of signaling domains. Proc Natl Acad Sci U S A **95:**5857-5864.
118. **Segal, E. D., J. Cha, J. Lo, S. Falkow, and L. S. Tompkins** 1999. Altered states: Involvement of phosphorylated CagA in the induction of host cellular growth changes by *Helicobacter pylori*. Proc Natl Acad Sci U S A **96:**14559-14564.
119. **Segal, E. D., C. Lange, A. Covacci, L. S. Tompkins, and S. Falkow.** 1997. Induction of host signal transduction pathways by *Helicobacter pylori*. Proc Natl Acad Sci U S A **94:**7595-7599.
120. **Segatori, L., P. J. Paukstelis, H. F. Gilbert, and G. Georgiou.** 2004. Engineered DsbC chimeras catalyze both protein oxidation and disulfide-bond isomerization in *Escherichia coli*: Reconciling two competing pathways. Proc Natl Acad Sci U S A **101:**10018-10023.
121. **Sikorski, R. S., M. S. Boguski, M. Goebl, and P. Hieter.** 1990. A repeating amino acid motif in CDC23 defines a family of proteins and a new relationship among genes required for mitosis and RNA synthesis. Cell **60:**307-317.
122. **Singh, A. K., M. Bhattacharyya-Pakrasi, and H. B. Pakrasi.** 2008. Identification of an atypical membrane protein involved in the formation of protein disulfide bonds in oxygenic photosynthetic organisms. J Biol Chem **283:**15762-15770.

123. **Small, I. D., and N. Peeters.** 2000. The PPR motif - a TPR-related motif prevalent in plant organellar proteins. Trends Biochem Sci **25:**45-47.
124. **Smith, M. F., A. Mitchell, G. Li, S. Ding, A. M. Fitzmaurice, K. Ryan, S. Crowe, and J. B. Goldberg.** 2003. Toll-like receptor (TLR) 2 and TLR5, but not TLR4, are required for *Helicobacter pylori*-induced NF-kB activation and chemokine expression by epithelial cells. J Biol Chem **278:**32552-32560.
125. **Song, S. F. O.-k.** 1989. A novel genetic system to detect protein–protein interactions. Nature **340:**245-246.
126. **Stathopoulos, C., D. R. Hendrixson, D. G. Thanassi, S. J. Hultgren, J. W. St. Geme III, and R. Curtiss III.** 2000. Secretion of virulence determinants by the general secretory pathway in Gram-negative pathogens: an evolving story. Microb Infec **2:**1061-1072.
127. **Stead, C. M., A. Beasley, R. J. Cotter, and M. S. Trent.** 2008. Deciphering the unusual acylation pattern of *Helicobacter pylori* lipid A. J. Bacteriol. **190:**7012-7021.
128. **Stenson, T. H., and A. A. Weiss.** 2002. DsbA and DsbC are required for secretion of pertussis toxin by *Bordetella pertussis*. Infect. Immun. **70:**2297-2303.
129. **Studier, F. W., A. H. Rosenberg, J. J. Dunn, and J. W. Dubendorff.** 1990. Use of T7 RNA polymerase to direct expression of cloned genes. Methods Enzymol **185:**60-89.
130. **Su, B., P. J. M. Ceponis, S. Lebel, H. Huynh, and P. M. Sherman.** 2003. *Helicobacter pylori* activates toll-like receptor 4 expression in gastrointestinal epithelial cells. Infect. Immun. **71:**3496-3502.
131. **Suerbaum, S., C. Josenhans, and A. Labigne.** 1993. Cloning and genetic characterization of the *Helicobacter pylori* and *Helicobacter mustelae* flaB flagellin genes and construction of *H. pylori* flaA- and flaB-negative mutants by electroporation-mediated allelic exchange. J Bacteriol **175:**3278-88.
132. **Suzuki, M., S. Miura, M. Suematsu, D. Fukumura, I. Kurose, H. Suzuki, A. Kai, Y. Kudoh, M. Ohashi, and M. Tsuchiya.** 1992. *Helicobacter pylori*-associated ammonia production enhances neutrophil-dependent gastric mucosal cell injury. Am J Physiol Gastrointest Liver Physiol **263:**G719-725.
133. **Tomb, J. F., O. White, A. R. Kerlavage, R. A. Clayton, G. G. Sutton, R. D. Fleischmann, K. A. Ketchum, H. P. Klenk, S. Gill, B. A. Dougherty, K. Nelson, J. Quackenbush, L. Zhou, E. F. Kirkness, S. Peterson, B. Loftus, D. Richardson, R. Dodson, H. G. Khalak, A. Glodek, K. McKenney, L. M. Fitzegerald, N. Lee, M. D. Adams, J. C. Venter, and et al.** 1997. The complete genome sequence of the gastric pathogen *Helicobacter pylori*. Nature **388:**539-47.
134. **Tsai, C.-M., and C. E. Frasch.** 1982. A sensitive silver stain for detecting lipopolysaccharides in polyacrylamide gels. An Biochem **119:**115-119.
135. **Tseng, T.-T., B. Tyler, and J. Setubal.** 2009. Protein secretion systems in bacterial-host associations, and their description in the gene ontology. BMC Microbiol **9:**S2.
136. **Tummuru, M. K., S. A. Sharma, and M. J. Blaser.** 1995. *Helicobacter pylori* picB, a homologue of the *Bordetella pertussis* toxin secretion protein, is required for induction of IL-8 in gastric epithelial cells. Mol Microbiol **18:**867-76.

137. **Vakil, N., and M. F. Go.** 2000. Treatment of *Helicobacter pylori* infection. Curr Opin Gastroenterol:32-39.
138. **Vanet, A., and A. Labigne.** 1998. Evidence for specific secretion rather than autolysis in the release of some *Helicobacter pylori* proteins. Infect Immun **66:**1023-7.
139. **Wainwright, L. A., and J. B. Kaper.** 1998. EspB and EspD require a specific chaperone for proper secretion from enteropathogenic *Escherichia coli*. Mol Microbiol **27:**1247-60.
140. **Walsh, A. G., M. J. Matewish, L. L. Burrows, M. A. Monteiro, M. B. Perry, and J. S. Lam.** 2000. Lipopolysaccharide core phosphates are required for viability and intrinsic drug resistance in *Pseudomonas aeruginosa*. Mol Microbiol **35:**718-27.
141. **Wattiau, P., B. Bernier, P. Deslee, T. Michiels, and G. R. Cornelis.** 1994. Individual chaperones required for Yop secretion by *Yersinia*. Proc Natl Acad Sci U S A **91:**10493-7.
142. **Weeks, D. L., S. Eskandari, D. R. Scott, and G. Sachs.** 2000. A H+-gated urea channel: the link between *Helicobacter pylori* urease and gastric colonization. Science **287:**482-485.
143. **Woestyn, S., M. P. Sory, A. Boland, O. Lequenne, and G. R. Cornelis.** 1996. The cytosolic SycE and SycH chaperones of *Yersinia* protect the region of YopE and YopH involved in translocation across eukaryotic cell membranes. Mol Microbiol **20:**1261-71.
144. **Yanisch-Perron, C., J. Vieira, and J. Messing.** 1985. Improved M13 phage cloning vectors and host strains: nucleotide sequences of the M13mpl8 and pUC19 vectors. Gene **33:**103-119.
145. **Yethon, J. A., J. S. Gunn, R. K. Ernst, S. I. Miller, L. Laroche, D. Malo, and C. Whitfield.** 2000. *Salmonella enterica* serovar *typhimurium* waaP mutants show increased susceptibility to polymyxin and loss of virulence *In vivo*. Infect Immun **68:**4485-91.
146. **Yu, J., H. Webb, and T. R. Hirst.** 1992. A homologue of the *Escherichia coli* DsbA protein involved in disulphide bond formation is required for enterotoxin biogenesis in *Vibrio cholerae*. Mol Microbiol **6:**1949-1958.